Institut für Nutzpflanzenwissenschaften und Ressourcenschutz (INRES)
Pflanzenkrankheiten und Pflanzenschutz

Application of proximal sensing techniques for epidemiological investigations of *Fusarium* head blight in wheat under field and controlled conditions

Inaugural-Dissertation

zur

Erlangung des Grades

Doktor der Agrarwissenschaften (Dr. agr.)

der Landwirtschaftlichen Fakultät

der Rheinischen Friedrich-Wilhelms-Universität Bonn

vorgelegt von

Ali Al Masri

aus

Talkalakh-Homs-Syrien

Bonn 2018

Referent: Prof. Dr. Heinz Wilhelm Dehne
Koreferent: Prof. Dr. Jens Léon
Prof. Dr. Petr Karlovsky
Angefertigt mit Genehmigung der Landwirtschaftlichen Fakultät der Universität Bonn

Tag der mündlichen Prüfung: 02.02.2018

With a lot of love, dedicated to my mother Walaa and Homeland Syria

Abstracts

Sensors can provide valuable insight into studying the physiological disorder due to plant pathogens. *Fusarium* head blight (FHB) influences the optical properties of wheat (*Triticum aestivum* L.) at canopy and ear levels. This research aimed to investigate these complex disease situations under field as well as controlled conditions with the application of proximal sensing systems.

Observations under field conditions revealed that the presence of foliar diseases is associated with higher *Fusarium* infection in the wheat canopy (cv. Tobak and Pamier), which might be attributed to reduced defence mechanisms. This was reflected in increased FHB incidence visually assessed at growth stage (GS) 83. Fungicides applied against foliar diseases before anthesis reduced FHB presence, which might be not only due to reducing the available inoculum in the canopy but also due to promoting defences against *Fusarium* infection. Furthermore, prediction of FHB through spectral parameters such as blue-green index 2 (BGI2) and photochemical reflection index (PRI) proved to be very promising.

At ear level, development of *Fusarium* infection is dependent on the primary infection site within ears and the prevailing environmental conditions after infection. Such a relationship was verified under controlled conditions after tip, centre and base inoculations, separately, by *F. graminearum* and *F. culmorum* of wheat ears (cv. Passat). Symptom dynamics (FHB index) were slower downwards within ears in comparison to the upward development. In contrast to the symptom appearance, the infection of *Fusarium* species proved to be directed basipetally – a rare development of fungal infections. According to these observations, it could be revealed that higher temperatures accelerated the ripening of ears and allowed these plants to escape the infection within ears. In contrast, at lower temperatures, higher disease severity was observed even for tip infection.

Infrared thermography could predict this primary site of ear infection through temperature span within ears and enabled disease detection before symptoms became visible. The temperature difference between air and ear was negatively correlated to FHB index and allowed disease detection at early senescence stage. Combining the features of thermal measurements and chlorophyll fluorescence images proved to present a high potential in characterising FHB at spikelet level. Discriminating spikelets infected with *F. graminearum* from those infected with *F. culmorum* was enabled with up to 100% accuracy by fusion of sensor data.

This study demonstrated that FHB is influenced by foliar wheat diseases when both have low severities. The control of leaf pathogens by fungicides can play an important part in integrated disease management – also against *Fusarium* infections. It could also be confirmed that primary infection sites within ears and the prevailing environmental conditions after infection are key factors which determine the later development of FHB. Sensors proved to be useful in monitoring and assessing FHB under field conditions – detailed investigations under controlled conditions provided more profound insights in this regard. The findings of this research contribute to a more efficient control of FHB using the concepts of remote sensing to improve precision plant protection and may be applied in selection processes of breeding for FHB resistance as well.

Kurzfassung

Geeignete Sensoren können einen wertvollen Einblick in die physiologischen Verhältnisse in Pflanzen bieten, wenn diese von pathogenen Organismen heimgesucht werden. Die Infektionen von Getreide durch *Fusarium* Arten (*Fusarium* Head Blight = FHB) verändern die optischen Eigenschaften von Wirtspflanzen – vor allem von Weizen (*Triticum aestivum* L.) – sowohl im Getreidebestand als auch auf dem Niveau der einzelnen Ähren. Die vorliegenden Untersuchungen hatten zum Ziel, die näheren Gegebenheiten dieser komplexen Befallssituationen im Freiland und unter kontrollierten Bedingungen durch die Anwendung von zerstörungsfreien Messmethoden zu charakterisieren.

Erhebungen im Feld machten deutlich, dass der Befall mit *Fusarium* Arten durch das Auftreten weiterer Blattkrankheiten im Weizenbestand gefördert wurde. Dies wurde beispielhaft an den Sorten „Tobak“ und „Pamier“ ermittelt und deutet auf eine geringere Widerstandsfähigkeit der Pflanzen gegenüber Fusariosen bei multiplem Befall hin. Dies konnte im Wachstumsstadium 83 (BBCH-Skala) auch makroskopisch festgestellt werden. Fungizidanwendungen, die vor der Blüte durchgeführt wurden, konnten das Auftreten der Fusarien am Weizen reduzieren. Dies war zweifellos auf die Reduktion des verfügbaren Inokulums der *Fusarium*-Arten zurückzuführen. Zugleich kann angenommen werden, dass durch die Gesunderhaltung der Blattfläche auch eine erhöhte Widerstandsfähigkeit der Pflanzen gegenüber Fusariosen hervorgerufen wird. Die Möglichkeit zur Vorhersage von FHB durch spektrale Parameter konnte bestätigt werden. Vor allem der Blue-Green-Index 2 (BGI2) und der photochemische Reflektionsindex (PRI) erwiesen sich als besonders geeignet.

An der Getreideähre ist die Entwicklung der Fusariosen in hohem Maße abhängig von dem primären Infektionsort und den nachfolgenden Umweltbedingungen im Anschluss an die Primärinfektion der Ähre. Dies konnte unter kontrollierten Bedingungen am Weizen der anfälligeren Sorte „Passat“ für Primärinokulationen an der an der Spitze, in der Mitte und an der Basis der Ähren nachgewiesen werden. Es zeigte sich, dass die Symptomentwicklung (FHB Index) in der Ähre deutlich weniger nach unten gerichtet war, als in der Zone oberhalb des Inokulationspunktes. Dies galt sowohl für Infektionen durch *F. graminearum* als auch für *F. culmorum*. Im Gegensatz zur Symptomentwicklung entwickelten sich die Fusariosen vor allem abwärts in der Ähre, ein durchaus eher seltener Prozess für pflanzenpathogene Organismen.

Erhöhte Temperaturen beschleunigen die Reifung der Ähren – obwohl günstig für das Auftreten von Fusariosen ermöglichen diese Bedingungen auch ein „disease escape“ gegenüber *Fusarium*-Arten. Bei niedrigeren Temperaturen führen die Infektionen zu deutlich höheren Infektionsraten, weil mehr Zeit zur Ausbreitung besteht – selbst in den Ährenspitzen. Mit Hilfe der Infrarot-Thermographie gelang es, die Primärinfektionen in der Ähre durch die Temperaturdifferenz zwischen Umwelt und den biologisch relevanten Zonen zu charakterisieren, bevor bereits makroskopisch Symptome erkennbar wurden. Die Gewebetemperaturdifferenzen waren negativ korreliert mit dem FHB Index, erlaubten aber auch eine Bestimmung des Reifestatus der Ähren. Wurden die Infrarotmessungen mit der Messung von Chlorophyll-korrelierten Messungen zerstörungsfrei kombiniert, lies sich damit eine hohe Korrelation identifizieren – insbesondere auf dem Niveau der einzelnen Ährchen. Wurden diese Beziehungen betrachtet, dann ließen sich sogar Unterschiede zwischen *F. graminearum* und *F. culmorum* erkennen.

Die vorliegenden Untersuchungen zeigen, dass das Auftreten von Fusariosen an Getreide auch in besonderem Umfang durch andere Blattkrankheiten gefördert wird – erkennbar allerdings nur bei geringen Befallsintensitäten. Die Förderung der Pflanzengesundheit – auch durch Fungizide – kann zu einer wichtigen Funktion im Integrierten Pflanzenschutz führen, sicher auch zum Schutz vor Ährenfusariosen. Es konnte nachgewiesen und durch Anwendung geeigneter Sensoren genutzt werden, dass die *Fusarium*-Infektionen eine besondere Rolle spielen. Vor allem die Primärinfektionsorte, die sehr umweltabhängig sind haben großen Einfluss auf die Schadwirkung.

Sensoren können offenbar sehr hilfreich bei dem Erkennen und der Befallsbestimmung sein, und das bereits unter Freilandbedingungen. Dies wurde durch Erhebungen unter Feldbedingungen bestätigt durch weitere Untersuchungen unter praktischen Bedingungen ergänzt. Die vorliegenden Ergebnisse und Erkenntnisse können eine effizientere Unterdrückung von FHB ermöglichen. Dabei geht es darum, dass die Elemente des „sensing of diseases“ einerseits in den Integrierten Pflanzenschutz eingebunden werden können und anderseits auch für Selektionsprozesse in der Züchtung zur Vermeidung von FHB genutzt werden können.

List of Abbreviations

ANOVA .....Analysis of Variance
ASD.....Analytic Spectral Device
AUDPC .....Area Under Disease Progress Curve
AUTDC .....Area Under Temperature Difference Curve
BGI2.....Blue-Green Index 2
BR .....Brown Rust
CAN .....Calcium Ammonium Nitrate
CFI.....Chlorophyll Fluorescence Imaging
CLA.....Carnation Leaf Agar
CZID .....Czapek Dox Iprodione Dicloran
DON .....Deoxynivalenol
RD .....Reflectance Difference
EW.....Ears Weight
F.....Fungicide Application against Foliar Diseases
FDF .....Foliar Diseases of Flag Leaf
FHB .....*Fusarium* Head Blight
FIK .....Frequency of Infected Kernels
FIL.....Frequency of Infected Leaves
Fm .....Maximal Fluorescence Yield of PSII
Fus .....Fungicide Application against FHB
Fv/Fm .....Maximal Quantum Yield of PSII
GS.....Growth Stage
GY .....Grain Yield
HSI .....Hyperspectral Imaging
IRT .....Infrared Thermography
K.....Disease Capacity
LDA.....Linear Discriminant Analysis
LSPDA .....Low Strength Potato Dextrose Agar
N.....Nitrogen Level
NDVI.....Normalized Differences Vegetation Index

NIR.....Near Infrared Reflectance
NIV.....Nivalenol
PAM.....Pulse Amplitude Modulated
PDA.....Potato Dextrose Agar
PDB.....Potato Dextrose Broth
PR.....Protein
PRI.....Photochemical Reflection Index
PSII.....Photosynthesis II
PSRI.....Plant Senescence Reflectance Index
PSSR.....Pigment Specific Simple Ratio
r.....Pearson Coefficient
R^2.....Determination Coefficient
RD.....Reflectance Difference
RGB.....Red Green Blue Image
rL.....Slope of Logistic Function
rM.....Slope of Monomolecular Function
RPR.....Raw-Protein Content
RTKW.....Reduction in Thousand Kernel Weight
SLB.....Septoria Leaf Blotch
ST.....Starch
SWIR.....Shortwave Infrared Reflectance
t/y.....Tones/Year
TD.....Temperature Difference
TKW.....Thousand Kernel Weight
TS.....Temperature Span
VIS.....Visible Reflectance
WI.....Water Index
Y[II].....Effective Quantum Yield of PSII
y0.....Initial Disease Value
YR.....Yellow Rust

Contents

1. INTRODUCTION

Food production must be increased by 50% to meet the proposed global demand by 2050 (Chakraborty and Newton 2011). Wheat is one of the three biggest cereal crops with 700 millions t/y since 2013 (FAOSTAT, 2017). It occupies the most important crop in temperate countries for both human and livestock consumptions (Shewry 2009). Wheat production is affected by different diseases which have a potential of yield loss of 32% worldwide (Oerke and Dehne 2004). *Fusarium* head blight (FHB), also known as *Fusarium* ear blight or scab, is one of the most devastating diseases that threaten wheat production in a broad spectrum of ecosystems (Summerell et al. 2010; Dweba et al. 2017).

FHB may cause yield losses up to 50%, making the production of wheat possibly unfeasible. More importantly, *Fusarium* mycotoxins are associated with FHB and endowed with acute and chronic toxicity in humans and animals (Cortinovis et al. 2013). Climate change might increase the risk of FHB epidemics around the world like in central China and possibly in the UK (Madgwick et al. 2011; Zhang et al. 2014). The importance of wheat in global grain production stresses the economic threat of FHB in global food and feed security. Modern formulations of fungicides have contributed to lower the yield loss and raised not only the production but also the quality of crops regarding the contamination with mycotoxins (Ishii 2005). However, the efficiency of the up to date fungicides against FHB is limited (Lienemann 2002; Amarasinghe et al. 2013). Moreover, resistant varieties against this disease cannot be considered as a sole solution because of lack of 100% resistance (Mesterházy et al. 2011). In the light of the aforementioned facts, an effective disease control that considers costs and environment maintenance is of significant interest.

Site-specific application of fungicides following precision agriculture techniques might efficiently contribute against FHB. Precision agriculture integrates sensors, methods of data analysis and pest management systems to optimise agricultural practices according to the spatial and temporal variability in the field (Mahlein 2010). Such a system of modern agriculture might contribute

significantly to the current and future food and feed demands. Innovative sensor systems can provide detailed information and new insights in precision plant protection domain (Mahlein 2016). Integrating such sensors for studying different plant-pathogen interactions, including FHB, under field and controlled conditions was recently often reported (Kuckenberg et al. 2009; Bürling et al. 2011; Bauriegel et al. 2011; Hillnhütter et al. 2011; Wang et al. 2012; Oerke et al. 2014; Leucker et al. 2016; Kuska et al. 2015; Mahlein 2016; Al Masri et al. 2017).

Improved understanding of the epidemiology of FHB in wheat is essential to optimize risk estimations and management strategies to secure wheat production under current and prospective hazards. Current strategies for FHB management can be significantly promoted by integrating sensors. The current study was designed involving Infrared Thermography and Chlorophyll Fluorescence Imaging systems for investigations under controlled conditions and non-imaging hyperspectral system, Analytic Spectral Devices (ASD) FieldSpec, for the investigations under field conditions. Epidemiological aspects related to FHB occurrence were the case in point in the current research:

- The presence of foliar diseases and their control by fungicides.
- The impact of primary infection site on head blight development in ears.
- The impact of environmental conditions after infection.

1.1 *Fusarium* head blight

FHB is a complex disease caused by toxigenic *Fusarium* spp. and non-toxigenic *Microdochium* spp. including at least 17 species (Parry et al. 1995; Waalwijk et al. 2004). Schaffnit (1912) defined *Fusarium nivale* (today is known as *Microdochium nivale*) as the only causal pathogen of FHB. *F. graminearum* Schwabe [teleomorph *Gibberella zeae* (Schwein) Petch] and *F. culmorum* (W.G. Smith) Sacc. (sexual state unknown) are the most common pathogens in the FHB complex infecting wheat (*Triticum aestivum* L.) (Simpson et al. 2001; Bottalico and Perrone 2002; O'Donnell et al. 2004). *F. graminearum* prevails in warmer humid areas worldwide, whereas *F. culmorum* is one of the predominant *Fusarium* species in colder areas such as Europe (Parry et al. 1995; Osborne and Stein 2007).

All over Europe, *Fusarium graminearum, F. avenaceum,* and *F. culmorum* are the most predominant species. *F. poae*, *F. cerealis*, *F. equiseti*, *F. sporotrichioides*, *F. tricinctum* were found to less extent, and *F. acuminatum*, *F. subglutinans*, *F. solani*, *F. oxysporum*, *F. verticillioides*, *F. semitectum* and *F. proliferatum* are the less encountered species with FHB (Bottalico and Perrone 2002; Waalwijk et al. 2004). In northern areas of Europe, such as Scandinavia, Finland and north-western Russia, and in Asia, e.g. Siberia and the Russian Far East, the most dominant pathogens are *F. avenaceum*, *F. arthrosporioides*, *F. tricinctum, F. graminearum*, *F. culmorum, F.* cerealis, *F. poae, F. sporotrichioides* and *F. langsethiae* (Yli-Mattila 2010). In the same region, an increase of *F. graminearum* over *F. culmorum* has been reported by Jennings et al. (2004). In China, the predominant agent causing FHB is *F. graminearum* clade and *F. asiaticum* in wheat and barley, respectively. Additionally, in the upper valleys of the Yangtze River *F. graminearum sensu stricto*, *F. meridionale* and *F. proliferatum* were frequently isolated (Yang et al. 2008). *F. graminearum* is also the predominant pathogen associated with FHB in North America (Shaner 2003).

In conclusion, it seems that the distribution and the predominance of *Fusarium* species is a function of environmental conditions (temperature and humidity, including free moisture) (Infantino et al. 2012; Popovski and Celar 2013). Even within the same area that is subjected to low variation in environmental conditions, high variability in *Fusarium* species profile was confirmed (Schlang 2010). Diverse environmental conditions preference of *Fusarium* species and their heterogeneity in spatial distribution make it difficult to control FHB in wheat plantations.

1.1.1 Disease incidence

Critical time for FHB occurrence is anthesis (Xu et al. 2007; Reis et al. 2016) which starts at the central spikelet of ears and extends up- and downwards (Brown et al. 2010). The combination of optimal environmental conditions for *Fusarium* infection and the variability in temporal and spatial patterns of anthesis within and among ears explain why FHB commonly occurs in few spikelets of single ears. The characteristic symptoms of FHB in wheat are bleached spikelets and ears (Fig. 1.1). However, the infection can take place in other spikelet tissues like the glumes and flower parts or even systemic infection (Guo 2015).

Ears are susceptible to *Fusarium* infection from anthesis until the soft dough age, GS 85 (Wegulo 2012). The infection within ear can then develop, through the entire ear, depending on the primary

site of ear infection (Al Masri et al. 2017). Residuals of maize cultivation have a significant effect on FHB of wheat because they persist for a long time and contribute a high amount of inoculum of *Fusarium* spp. (Blandino et al. 2010).

In infested residues, *F. graminearum* produces asexual spores (macroconidia) which can disperse within wheat canopy by rain-splash and wind. At warm, humid, and wet conditions, the sexual phase of the fungus (*Gibberella zeae*) develops on the infected plant debris. Bluish-black perithecia will be formed on the surface of these residues, and forcibly discharge sexual spores (ascospores) into the air. Infection occurs when the ascospores and macroconidia meet extruded anthers during wheat anthesis, which are thought to be the site of primary infection (Trail 2009; Dweba et al. 2017). The infection develops within the ears depending on the primary site of ear infection (Al Masri et al. 2017).

Figure 1.1 Severe symptoms of *Fusarium* head blight in wheat (cv. Passat by *Fusarium graminearum*).

1.1.2 Mycotoxins

One crucial factor in the occurrence of FHB is the association with *Fusarium*-mycotoxin which contaminates the harvested kernels. Mycotoxins are metabolites essential for the growth of the toxigenic *Fusarium* spp. and play an essential role in the infection process. In cereals, more than

300 mycotoxins could be present. Out of these, a large number can be identified with modern analysis techniques (Zühlke et al. 2008; Herebian et al. 2009; Berthiller et al. 2017). During the last decades, research on the toxicity resulting from FHB infections has identified fumonisins, trichothecenes, and zearalenones as the most dangerous mycotoxins of associated pathogens (Desjardin 2006). Additionally, other toxic secondary metabolites called emergence mycotoxins such as fusaproliferin, beauvericin, enniatins and moniliformin can be detected in combination with the toxins above (Meyer 2006; Jestoi 2008). Beauvericin and enniatins are ionophoric compounds which have the mode of action of transferring mono-and divalent cations through the cell membrane (Steinrauf 1985). However, enniatins were demonstrated in 1947 to possess antibiotic properties (Gäumann 1947).

1.1.2.1 Trichothecenes

Trichothecenes (Fig. 1.2) are a vast group of metabolites that contains an epoxide which is the responsible for their toxicity. They are divided into two groups, A and B, mainly according to the presence of different functional groups in the C-8 positions of the trichothecene (Shank et al. 2011). Diacetoxy- and monoacetoxy-scirpenol (DAS and MAS) and neosolaniol (NEO) are the main toxins of T-2 and HT-2 of the A group. Deoxynivalenol (DON), nivalenol (NIV), 3-AcetylDON, 15-AcetylDON and fusarenone X are the most critical toxins in group B (Desjardin 2006). DON is the most predominant one in the majority of small cereals regions of production across the world (Wegulo 2012). It affects the health of both humans and animals causing acute temporary nausea, vomiting, diarrhoea abdominal pain, headache, dizziness, and fever (Sobrova et al. 2010). The toxicity of trichothecenes is mainly because of protein synthesis inhibition in the eukaryotes. However, the exact mechanism of this inhibition is still unknown yet (Shank et al. 2011). DON contamination has been proven to be a function of the air temperature and average precipitation around the wheat heading time, 4-7 and 7-10 days before and after heading, respectively (Hooker 2002). Visual scoring of FHB proved to be an excellent indication to DON accumulation in kernels (Lemmens et al. 2003). However, there is still no certainty about the effect of environmental conditions like moisture and rainfall on the accumulation of these mycotoxins (Kriss et al. 2010).

1.1.2.2 Zearalenones

Zearalenones (Fig. 1.2) are phenolic resorcylic acid lactones differing in the presence and the reduction state of hydroxyl groups and their acetylation (Desjardin 2006). It has no high accumulation rate in comparison to that of trichothecenes. However, it is of major interest because it is proven to be hepatotoxic, immunotoxic, and carcinogenic to some mammals. Additionally, it showed competition to bind to estrogen receptors and in turn responsibility for hyper-estrogensim and infertility in livestock (Cortinovis et al. 2013).

1.1.2.3 Fumonisins

Fumonisins (Fig. 1.2), a group of polyketide, can be classified into fumonisin A, B, C and P series. It is mainly produced by *F. verticillioides* and *F. proliferatum*. Among described fumonisin groups, FA1, FA2, FB2, FB3 and FB1, only B types have been shown to be toxic (Desjardin 2006). It has been proved that the high consumption of maize contaminated with fumonisin can be associated with disorders in animals and apoptosis as consequences of membrane lipid peroxidation (Caloni and Cortinovis 2010; Garbetta et al. 2015).

Fusarium species associated with FHB in wheat produce different spectrums of mycotoxins. *F. graminearum* and *F. culmorum* produce mycotoxins from trichothecene, zearalenone, and fusarin groups. *F. avenaceum* is known to produce another spectrum like moniliformin and fusarin mycotoxins (Desjardins 2006). Although DON is the most prevalent mycotoxin, however, it is produced by few pathogens associated with FHB, like *F. graminearum* and *F. culmorum*. In contrast, NIV, for example, is produced by a higher number of *Fusarium* spp. which needs to be considered when the risk of FHB is the key of interest (Meier 2003). The stability of mycotoxins in processed feed and food poses a severe extra threat to human and animal health and food safety (Bottalico and Perrone 2002). Maximum limits of various mycotoxins have been already established in many countries to reduce the harmful effects of these metabolites on consumers. The European Commission for example has set lists to explain the thresholds of allowed doses of mycotoxins in different cereals crops and products considering the final purpose of consumption (Ferrigo et al. 2016).

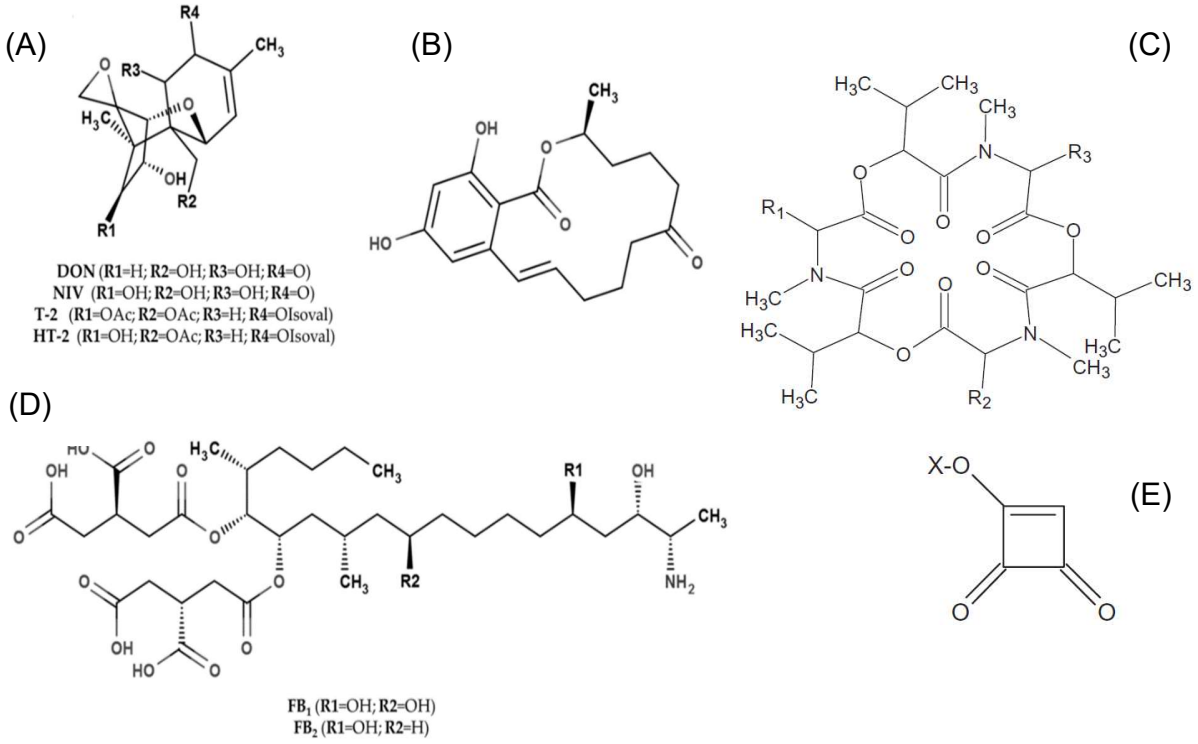

Figure 1.2 Chemical structure of the main *Fusarium* mycotoxins: Trichothecenes (A), Zearalenone (B), Beauvericin and Enniatin (C), Fumonisins (D), and Moniliformin (E). OAc = acetyl function; OIsoval = isovalerate function, X stand for Na^+ or K^+ ions (Jestoi et al. 2004; Ferrigo et al. 2016, both modified).

1.1.3 Disease management

The efficiency of fungicides against FHB is limited (Lienemann 2002; Amarasinghe et al. 2013). Applying chemicals reduces the contamination of cereals with mycotoxins (Mesterházy et al. 2011). Strobilurin fungicide group, for instance, was responsible for reducing the occurrence of FHB because of its effect on *Microdochium nivale*. However, the same group could increase the contamination with DON (Meier 2003). Carbendazim, hexaconazole, mancozeb, benomyl, prochloraz, prothioconazole, tebuconazole, and triadimenol are useful fungicide active ingredients against FHB. However, none of these chemicals resulted in 100% control of FHB (Meier 2003; Amarasinghe et al. 2013; Dweba et al. 2017).

During the last decades, the research efforts have promoted resistance level to FHB in many commercial varieties. Resistant varieties may play an essential role in FHB management, but they cannot be considered as a sole solution because of lack of 100% resistance to FHB in the current

commercial varieties (Mesterházy et al. 2011). Five types of resistance were reported to FHB (Dweba et al. 2017): type I addresses the initial infection by *Fusarium* spp., type II occurs when the host plant prevents the spread of the infection within the ears and type III involves the infection of kernels. Additionally, two types of tolerance were reported: type IV which involves the presence of the infection with no side effect on yield quality and quantity, while type V is the ability of the plant to detoxify the mycotoxins occurring during the infection (Gilbert and Tekauz 2000). However, the acquired resistance is not considered as a sole solution to control FHB (Mesterházy et al. 2011).

Integrated pest management, which involves the use of resistant varieties and fungicides application, might be the best option to control FHB (Wegulo et al. 2011). To increase the efficacy of disease management, several epidemics or mycotoxins risk assessment models have been built (Hooker et al. 2002, van Maanen and Xu 2003; Prandini et al. 2009). The employment of models may be useful for decision-making purposes to prevent/reduce yield losses and hazards for human and animal health based on the correct time for applying chemicals.

1.2 Optical sensor systems

1.2.1 Infrared Thermography

Infrared Thermography (IRT) is an imaging method that transforms the thermal energy of emitted infrared band within the electromagnetic spectrum into false colour images (Mahlein 2016). It is a non-contact, non-intrusive technique to determine the temperature of objects in a relatively short period (Vadivambal and Jayas 2011; Oerke et al. 2014). The spectral range of infrared radiation that can be detected using thermocameras is between 8-12 µm (Mahlein et al. 2012; Oerke et al. 2014; Mahlein 2016). All objects that have a temperature higher than the absolute zero (-273°C) emit infrared radiations as thermal energy from an area of about 2.5×10^{-5} mm² of the object surface. IRT is a function of the surface temperature of the targeted object. Therefore it is considered as data with two dimensions of the objects surfaces and can be applied passively or actively (Meola and Carlomagno 2004). When objects have a temperature similar to the ambient air at measuring time, an external stimulus enables to obtain a temperature different from the ambient air and thus to induce a relevant thermal contrast (Maldague 2002).

Thermal energy detection of a thermocamera is a function of the emissivity coefficient of the object surface under measuring conditions. A blackbody radiates thermal energy with the maximum value at a given temperature with an emissivity of 1. However, this is mostly not the case for real objects like plants, for which a new emissivity value needs to be introduced to get an accurate measurement. The prevailing environmental conditions at measuring are other factors needed to be considered when applying IRT. Parts of the thermal energy might be lost because of the absorption in the atmosphere between object and camera. Emitted infrared radiation from other sources at the ambient might be reflected on the targeted objects and be added to the measured thermal energy (Meola and Carlomagno 2004). These critical factors should be taken into account when setting up the measuring conditions of plant diseases with IRT.

The relative easiness of application, the non-destructive nature of measurement as well as the quick inspection and straightforward interpretation of results make IRT very appropriate for a wide range of applications. However, there are some difficulties specific to IRT like the cost of the equipment, difficulties in obtaining a fast, uniform and highly energetic thermograms over large surface, the effect of thermal added and losses and the emissivity problem as well (Maldague 2002). The first application of IRT was in the World War II for military purposes, and after that, it was used in medicine, agriculture, environment, maintenance, non-destructive evaluation, and thermo-fluid dynamics (Meola and Carlomagno 2004).

In agriculture, IRT is a powerful technique for visualising, diagnosing and quantifying plant stresses resulting from biotic and abiotic factors that modify water status and stomatal behaviour (Jones and Schofield 2008; Jones et al. 2009; Oerke et al. 2014). The method enables the detection of temperature differences at the level of plant organs such as leaves, stems, and ears. It is possible to detect the water status within the entire plant or even within the canopy (Oerke et al. 2006). IRT, for instance, was used to describe the plant water status of grapevine canopies (Jones et al. 2002) and wheat canopy (Lenthe et al. 2007) for large-scale measurements. More specifically, IRT is related to transpiration of the objects for small-scale measurement (Lindenthal et al. 2005; Oerke et al. 2006; Stoll et al. 2008; Wang et al. 2012). Early detection of plant diseases was feasible by thermography in different studies. Downy mildew of cucumber, caused by *Pseudoperonospora cubensis*, was detectable thermographically even before visible symptoms appeared (Lindenthal et al. 2005; Oerke et al. 2006). Also in grapevine, *Plasmopara viticola* infections significantly

reduced leaf temperature before symptoms became visible (Stoll et al. 2008). Early infection stages of *Fusarium oxysporum* f.sp. *cucumerinum* on cucumber roots affected stomata closure in leaves and resulted in increased leaf temperature (Wang et al. 2012). Application of thermal imaging in the field is a promising tool to study spatial patterns of soil-borne pathogens (Hillnhütter et al. 2011). Recently, Al Masri et al. (2017) recommended the application of IRT in studying the phenotyping of wheat resistance to FHB.

1.2.2 Chlorophyll Fluorescence Imaging

Disorders on photosynthetic activities resulting from biotic and abiotic stress factors have been successfully investigated with Chlorophyll Fluorescence Imaging (CFI). Chlorophylls and carotenoids are the initiators of transduction the energy in the process of photosynthesis throughout absorbing photons and transforming it into photochemical energy. Illuminated leaves consume more than 80% in photosynthetic light reaction to build ATP and NADPH which are crucial molecules in the Calvin cycle (Lichtenthaler et al. 2005). In total, there are three processes when the light hits plant: photochemistry, heat, and fluorescence (Fig. 1.3 A) and the latter is a good indicator of biotic and abiotic stress factors that affect the photosynthesis process (Maxwell and Johnson 2000). During the process of energy transformation, a part of the received light is dissipated (1-2%) as heat and red fluorescence light (Maxwell and Johnson, 2000).

When a leaf is kept under dark conditions, the reaction centres of PSII become opened which means that the primary quinone acceptor of PSII, QA, becomes maximally oxidized, in other words, they are ready to perform photochemical reduction of QA (Baker 2008). A beam of weak modulated and non-actinic photosynthetically active photon flux density (PPFD) of about 0.1 μmol m^{-2} s^{-1} will not drive to photosynthesis but will induce a minimal level of fluorescence (F0) (Lichtenthaler et al. 2005). When a short pulse of actinic light characterized by high PPFD of several thousand μmol m^{-2} s^{-1} is usually less than 1 s is applied, maximal fluorescence level Fm is reached because of maximal reduced QA (Govindjee 2004). The difference between F0 and Fm is indicated as variable fluorescence (Fv). The maximal photochemical efficacy of PDII calculated as Fv/Fm is frequently used in fluorescence research. Healthy leaves produce Fv/Fm values in the range of 0.82±0.004 and decrease with stress (Krause and Weis 1991). Further determination of different quenching processes associated with PSII can be obtained by further illumination using actinic light (AL)

source. This AL induces fluorescence yield to a maximum level Fp which is lower than Fm (Fig. 1.3 B) (Lichtenthaler et al. 2005). Within 1 s, different quenching mechanisms are initiated, and the cooperation between the two photosystems is reactivated (Lichtenthaler et al. 2005). These processes result in a decrease of fluorescence yield (over a period of a few minutes) to a low steady state (Ft) (Maxwell and Johnson, 2000). At steady state, the application of saturation pulses will temporarily close all PS II reaction centres and will be associated with maximum fluorescence at illumination (Fm'). The F corresponds to the momentary fluorescence level (Ft) of an illuminated sample measured shortly before application of a Saturation Pulse. The photochemical efficacy of PDII [(Fm'-F)/Fm'] (Genty et al. 1989) at steady state (at which F = Ft) is frequently used in fluorescence research.

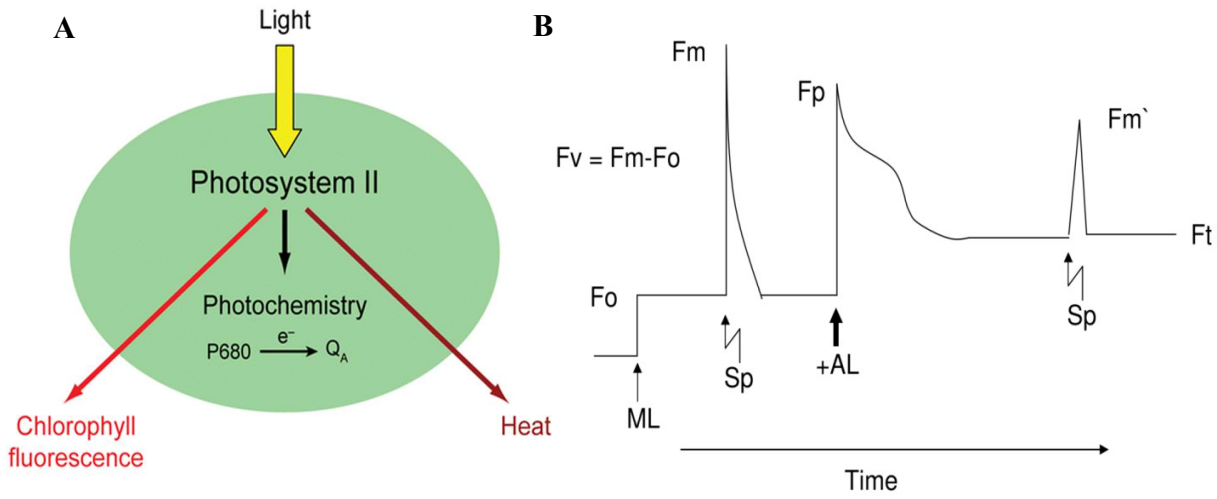

Figure 1.3 A: model of the possible fate of light energy absorbed by photosystem II, B: Typical chlorophyll fluorescence from a dark-adapted leaf using pulse amplitude modulated (PAM) following saturation pulse measuring protocol, ML = weak modulated measuring light; Sp = saturation light pulse; AL = continuous actinic light (van Kooten and Snel 1990; Baker 2008, both modified).

Different approaches can be used to induce and measure chlorophyll fluorescence under laboratory conditions. One procedure is used to evaluate as above described the fluorescence induction kinetic as point or imaging measurements. This approach is called pulse-amplitude-modulated (PAM) chlorophyll fluorescence, and a typical result of a chlorophyll fluorescence quenching analysis is shown in (Fig. 1.3 B). CFI has been implemented successfully in studying plant diseases like leaf rust and powdery mildew of wheat (Kuckenberg et al. 2009; Bürling et al. 2011). It has proved

high capability for assessing plant stress, subjectively and non-destructively. However, it is difficult to reach the full capacity of CFI features in field application because of the dark adaptation needed before running the measurement, high and varying level of light intensity and the time between emission and detection of the measuring beam (Chaerle et al. 2003; Oerke et al. 2014). CFI was used in combination with hyperspectral imaging to study FHB simultaneously, and both sensors proved possible detection after symptoms become visible (Bauriegel et al. 2011).

1.2.3 Spectroscopy

Hyperspectral remote sensing can be defined as the measurement of reflected radiance in the visible range (VIS 400 to 700 nm), the near-infrared range (NIR 700 to 1.100 nm) and the short-wave infrared range (1.100 to 2.500 nm) (Goetz et al. 1985). It can be measured using imaging and non-imaging sensors at microscopic, proximal and remote levels. Contrary to imaging methods which provide spectral and spatial data for the imaged object, non-imaging sensors average the reflectance over a particular area (Mahlein 2016). Leaf pigment content mainly influences the reflectance in the VIS range, the NIR range is a function of leaf structure, internal scattering processes, and of the absorption by leaf water. The reflectance in the SWIR range is influenced by the composition of leaf chemicals and water content (Carter and Knapp 2001; Jacquemoud and Ustin 2001) (Fig. 1.4).

Plant pathogens can cause impairments in the leaf structure and chemical composition during pathogenesis which triggers changes in hyperspectral reflectance (Mahlein 2016). During the last 15 years, a remarkable increase of research and reports that implement hyperspectral technology in studying plant diseases took place. For example, wheat head blight and yellow rust (Huang et al. 2007; Bauriegel et al. 2011), sugar beet Cercospora leaf spot, rust and powdery mildew (Mahlein et al. 2010; Hillnhütter et al. 2011; Mahlein et al. 2012 and 2013) were investigated using Hyperspectral imaging (HSI). HSI proved by studying the interaction between *Cercospora beticola* and different cultivars of sugar beet (Leucker et al. 2016) that the assessment of lesion phenotypes can be a good reporter of cultivar resistance. Kuska et al. (2015) investigated the resistance reaction of different barley genotypes to *Blumeria graminis* f.sp. *hordei* and proved the potential of HSI to characterize this pathosystem based on the level of resistance and susceptibility of the infected barley genotype. The infection of tomatoes by *Phytophthora infestans* (late blight) proved to be

predictable using gradient-descent learning algorithm depending on hyperspectral reflectance signature (Wang et al. 2008). For the field application of HSI, Hillnhütter et al. (2011) recommended using this sensor in combination with geographic information systems (GIS) which can promote the efficacy of detection and mapping of symptoms of beet cyst nematode, *Rhizoctonia* crown, and root rot. All reports agreed on the high potential of applying this technology in characterizing plant diseases more subjectively than the traditional methods. However, these applications are still under establishment, and further improvements are required mainly because of the lack of expertise and the vast files size of recorded data (Bock et al. 2010).

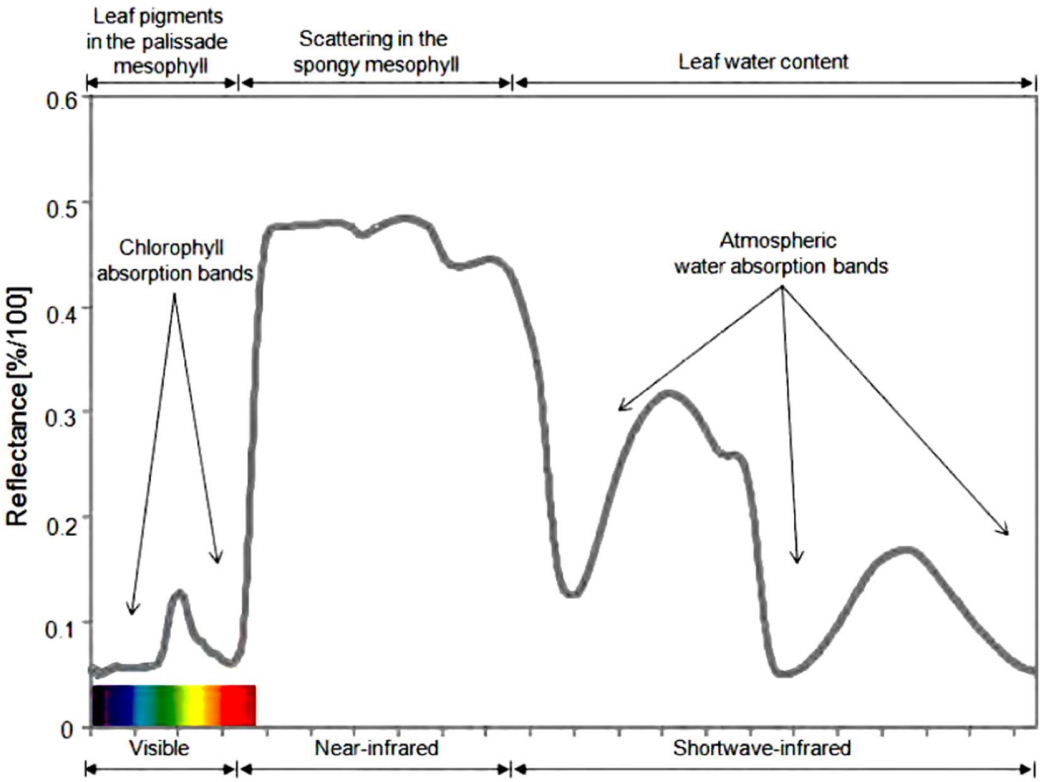

Figure 1.4 Typical reflectance spectra of the leaf (modified from Curran 1989; Jensen 2002; Mahlein, 2011).

Spectral vegetative indices (SVIs) indicate specific parameters of plant functions which reduces the data dimensionality of the entire reflectance spectra and may the computation time as well (Delalieux et al. 2009; Mahlein 2010). However, this method is not capable enough to differentiate between disease or stress factors (Mahlein 2010). Huang et al. (2007) correlated the visual

assessment to the photochemical reflection index (PRI) and proved its potential for quantifying yellow rust in winter wheat. Delalieux et al. (2009) reported that the performance of vegetative indices is dependent on the infection development of apple scab, caused by *Venturia inaequalis*, and the age of apple leaves. The presence of pigments including chlorophyll-a and chlorophyll-b plays a critical role affecting spectral reflection (Moroni et al. 2013). These pigments are controlled by the chemical and the biological activity of host plant (Sims and Gamon 2002). Chlorophyll-a content indicated as pigment simple saturation ratios of chlorophyll-a (PSSRa) was also sensitive to yellow rust in winter wheat and showed a significant correlation with disease severity (Jing et al. 2007). Mahlein et al. (2010) used SVIs to characterise *Cercospora beticola*, *Erysiphe beticola* and *Uromyces betae* on sugar beet and proved the possibility to differentiate among the three diseases using at least two indices in combination. Using indices to extract and interpret hyperspectral data might be promising to develop sensors that can measure specific bands and report the casual stress factor specifically (Mahlein et al. 2010).

1.3 Intention of the current research

The high number of pathogens associated with FHB and their ability to adapt to different environmental conditions even at local climatic conditions make this complex disease of major interest. The accumulation of mycotoxins, which limits food and feed sources, elevates the risks of this disease. The lack of wheat resistance sources and the narrow time window to apply fungicides against FHB are additional challenges. Moreover, up to date registered chemicals against FHB does not provide 100% control efficacy. Many reports highlighted the invasive nature of FHB that might happen because of the global climate change in the future. Accordingly, there is an urgent need to achieve empirical data quantifying the critical epidemiological aspects of FHB under field and controlled conditions. Data collection with the application of sensors might provide new insight into understanding FHB, and later, an effective control strategy might be developed. In other words, reducing the costs and considering the maintenance of environment, for instance by site-specific application of fungicides, might be achieved by integrating the outputs of these sensors.

The case in point in this research is to investigate some epidemiological aspects of FHB under field and controlled conditions with the application of selected proximal sensing methods. The sensing

systems involved in this study were: Infrared Thermography, Chlorophyll Fluorescence Imaging, and Analytical Spectral Device (ASD FieldSpec).

The specific objectives were:

- Canopy: to investigate the influence of foliar wheat diseases and their control by fungicides on FHB under field conditions by applying the ASD device to assess the vitality of wheat canopy.
- Ear: to investigate the impact of primary infection site of *Fusarium* species (*F. graminearum* and *F. culmorum*) on head blight development under different environmental conditions by using Infrared Thermography under greenhouse conditions.
- Spikelet: to investigate the potential fusion of sensor data of Infrared Thermography and Chlorophyll Fluorescence Imaging in characterising FHB caused by *F. graminearum* and *F. culmorum* under controlled conditions.

2. MATERIAL AND METHODS

2.1 Field experiments

Two field trials to study the effect of foliar diseases of wheat and their control with fungicides on FHB were conducted at the Klein-Altendorf research station of the University of Bonn in 2013-2014 (2014 experiment) and 2014-2015 (2015 experiment). Two varieties of winter wheat (*Triticum aestivum* L.) were selected as host plants in both years: Tobak (W.von Borries Echendorf, Leopoldshöhe, Germany), relatively susceptible to FHB, and Pamier (Syngenta Seeds GmbH, Bad Salzuflen, Germany), moderately resistant to FHB (Anonymous 2013).

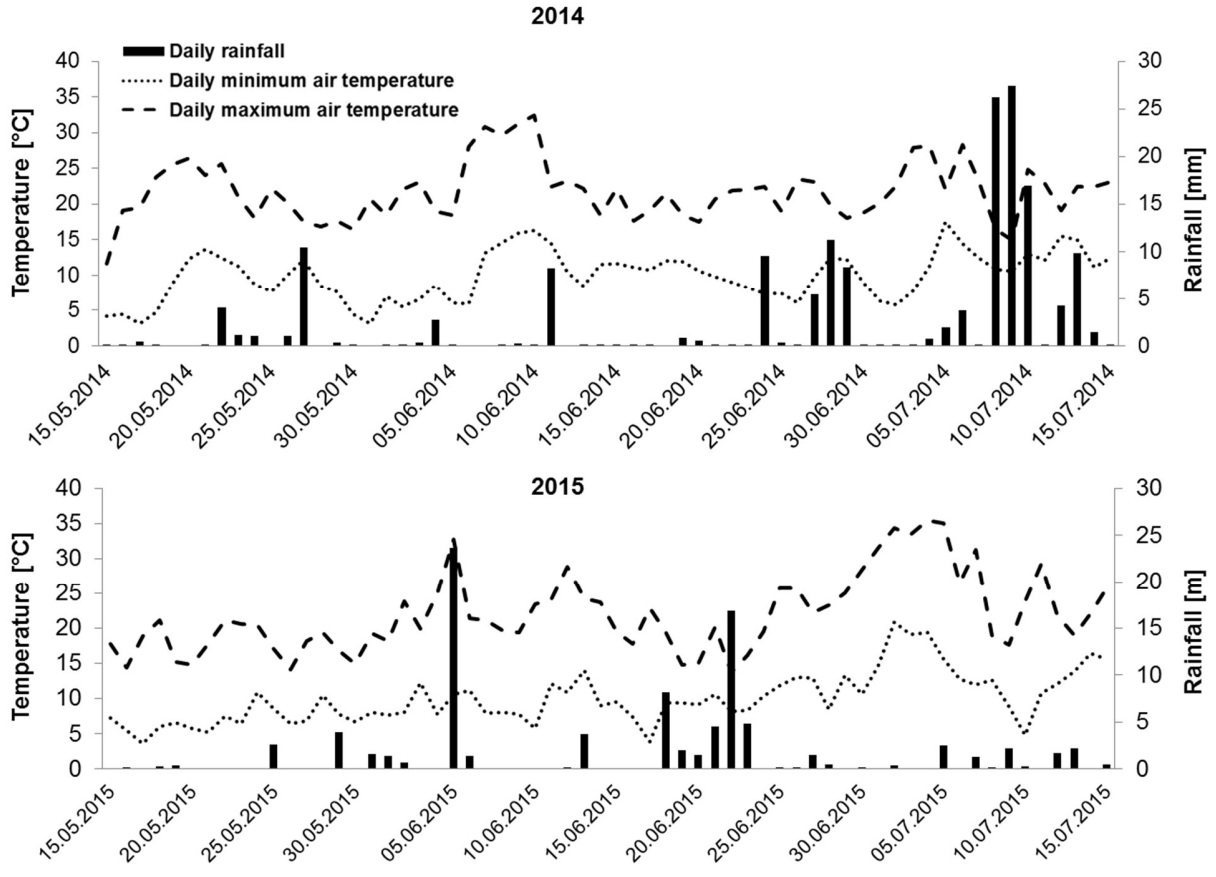

Figure 2.1 Daily meteorological data of rainfall (bars), maximum air temperature (dashed lines) and minimum air temperature (dotted lines) from the 15th of May to the 15th of July of 2014 and 2015. Data source: weather station Campus Klein-Altendorf south, University of Bonn.

In the 2015 experiment, additionally, Sokrates (Saatzucht Engelen Büchling e. K., Oberschneiding, Germany), a variety of winter wheat, was introduced into the experimental design as a marginal variety based on its susceptibility to foliar diseases of wheat (Anonymous 2013) (Tab. 2.1). 24 and 48 plots (in 2014 and 2015, respectively) were designed in a completely randomised design of experiments with a number of replications ≥ 3 for each treatment.

Table 2.1 The characteristics of varieties used in the experiments of 2014 and 2015 under field conditions according to the classification of the Federal Plant Variety Office in Germany (Anonymous, 2013).

Wheat variety	Plant height	Maturity date	Protein content	Susceptibility to wheat fungal diseases				
				Brown rust	Yellow rust	Septoria leaf blotch	Powdery mildew	*Fusarium* head blight
Pamier	5	5	5	3	-	4	2	3
Tobak	4	6	2	7	2	4	2	7
Sokrates	6	5	6	8	-	4	8	3

The description of characters is based on a 1 – 9 scale (BSA scale). A high figure indicates that the variety shows the character to a high degree and a low figure indicates that variety shows the character to a low degree. (-) indicates no available data

Daily rainfall, daily maximum air temperature and daily minimum air temperature were recorded and plotted for two months, from 15 May to 15 July of 2014 and 2015. This time window includes the growth stages (GS) of wheat which are important for FHB epidemics (Hooker 2002), namely from GS 39 when flag leaves are obvious until the maturation (Fig. 2.1).

2.1.1 Experiment set-up in 2014

2.1.1.1 Experimental plants

The winter wheat (*Triticum aestivum* L.) variety Tobak (166.6 kg/ha) and Pamier (120.7 kg/ha) were sown on October 24th of 2013 in plots of 10×1.5 m. Before germination, the herbicide Malibu® (300 g/L Pendimethalin and 60 g/L Flufenacet, application rate 4 L/ha) was applied to avoid weeds. Fertilization with calcium ammonium nitrate (CAN) was applied at GS 24, 30 and 39 with 60 kg/ha each time. At GS 24 the first application of growth regulator Cycocel® known as CCC (Chlorocholine Chloride, application rate 1.0 1/ha) was carried out. The second application was at GS 31/32 with CCC (application rate 0.5 L/ha) and Moddus® (250 g/L trinexapac-ethyl,

application rate 0.3 L/ha). To avoid insects infestation, the insecticide Biscaya® (240 g/L Thiacloprid, application rate 0.3 L/ha) was applied on all experimental plots.

2.1.1.2 Fungicide treatments

The application of fungicides was carried out according to the experimental design to obtain plants infected and non-infected with foliar wheat diseases. The non-fungicide-treated plants, referred to as F-, were grown under natural infection pressure by wheat foliar pathogens. The control plants were obtained by applying fungicides at different growth stages (Tab. 2.2), referred to as F+ treatment. To control FHB at anthesis, the fungicide Orius (Tebuconazole 430 g/L, with the rate of application 1 L/ha) was applied only to treatments (F+). The application of fungicide was made at recommended field rates (Tab. 2.2), products were solved in water 400 L/ha before they were spray-applied on the field.

2.1.2 Experiment set-up in 2015

2.1.2.1 Experimental plants

Tobak (175.1 kg/ha) and Pamier (147.1 kg/ha) were sown on October 20th of 2014 in plots of 11×3 m. The herbicide Malibu® (300 g/L Pendimethalin and 60 g/L Flufenacet, application rate 4 L/ha) was applied to avoid weeds. Additionally, at GS 37 the herbicide MCPA (600 g/L 2-methyl-4-chlorophenoxyacetic acid, esters and organic amines) was applied on all experimental plots. At GS 27 the first application of growth regulator Cycocel® (118 g/L Chlormequat chloride; application rate 1 L/ha) was carried out. The second application was at GS 31 with CCC (application rate 0.3 L/ha) and Moddus® (250 g/L trinexapac-ethyl, application rate 0.5 L/ha). The insecticide Biscaya® (240 g/L Thiacloprid, application rate 0.3 L/ha) was applied on all experimental area (Fig. 2.2).

2.1.2.2 Nitrogen levels

Fertilization (N) with calcium ammonium nitrate (CAN) was applied at GS 23, 30 and 39 with 60 kg/ha each time. At each growth stage, two different doses of the CAN were applied to study the effect of foliar diseases and its control with fungicide under standard nitrogen fertilization (N100 = 60 kg/ha) and under half standard conditions (N50 = 30 kg/ha).

2.1.2.3 Fungicide against foliar diseases

The application of fungicide to control foliar wheat diseases was carried out according to the experimental design at different growth stages of the wheat canopy.

Table 2.2 Rates and appointments of fungicides application during field experiments carried out at the Klein-Altendorf research station of the University of Bonn in 2013/2014 and 2014/2015.

Year	Product	Active ingredients	Application rate (L/ha)	Date of application	Growth stage (GS)
2013/2014	Capalo®	Metrafenone (75 g/L), Epoxiconazol (62.5 g/L), and Fenpropimorph (200 g/L)	2	31 March	30
	Input®	Prothioconazole (160 g/L), and Spiroxamine (300g/L)	1.25	11 April	32/33
	Diamant®	Fenpropimorph (214.3 g/L), Epoxiconazol (42.9g/L), and Pyraclostrobin (114.3 g/L)	1	08 May	39
	Adexar®	Fuxapyroxad (62.5g/L), and epoxiconazole (62.5g/L)	1	08 May	39
	Skyway® Xpro	Prothioconazol (100 g/L), Tebuconazol (100 g/L), and Bixafen (75 g/L)	1	22 May	61
	Orius®	Tebuconazol (430 g/L)	1	22 June	61
2014/2015	Capalo®	Metrafenone (75 g/L), Epoxiconazol (62.5 g/L), and Fenpropimorph (200 g/L)	2	22 April	31
	Input®	Prothioconazole (160 g/L), and Spiroxamine (300g/L)	1.25	07 May	32/33
	Adexar®	Fuxapyroxad (62.5g/L), and epoxiconazole (62.5g/L)	2	27 May	51
	Prosaro®	Prothioconazole (125 g/L), and Tebuconazol (125 g/L)	1	08 June	69

The fungicides that were applied (F+) are shown in (Tab. 2.2). Non-fungicide-treated plants (F-) were grown under natural infection pressure by foliar wheat pathogens.

2.1.2.4 Fungicide against FHB

In the 2015 experiment, fungicide against FHB was applied to the treatment that received fungicides against foliar diseases (F+), as it did in the 2014 experiment, but furthermore also to that without fungicides (F-). In other words, a new factor was introduced in the 2015 experiment to better address the research question about the effect of the fungicide application against foliar diseases on FHB. At GS 69, Prosaro (Prothioconazole and Tebuconazole, with the rate of application of 1 L/ha) was applied (Fus+) or not (Fus-). The application of fungicides was made at recommended field rates (Tab. 2.2). Products were solved in water, 400 L/ha, before they were spray-applied in the field.

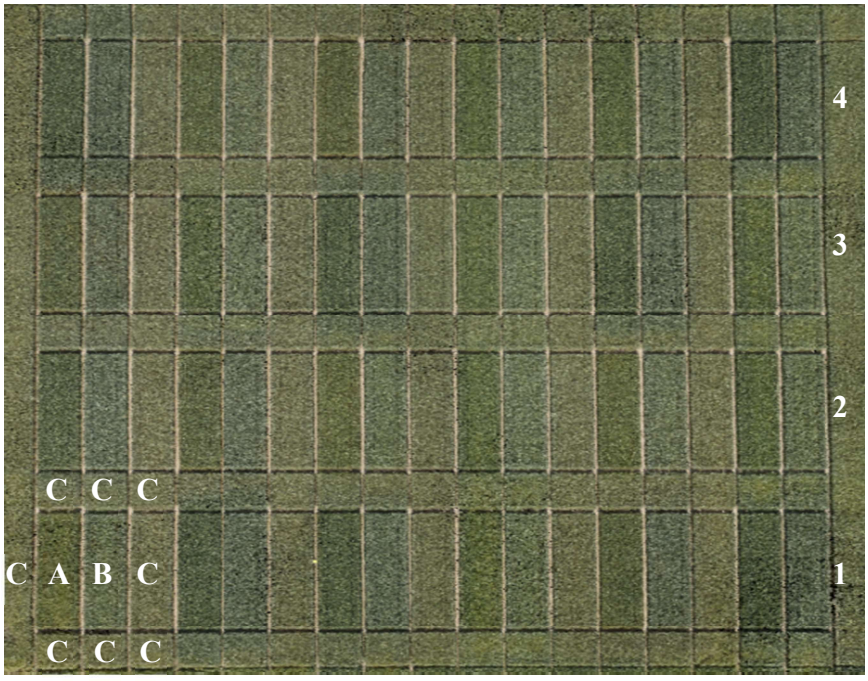

Figure 2.2 Ariel image of the 2015 field experiment, Klein-Altendorf, consisting of four lines of plots in completely randomised design. In each line, plots A (3×11 m) are cultivated with Tobak, plots B (3×11 m) cultivated with Pamier, and plots C (3×11 m) cultivated with Sokrates serving as marginal variety. The other two sides of A, B and C are banded with plots of Sokrates (3×3 m). (Photo made by Wieland, M., Institute of Geodesy and Geoinformation, University of Bonn)

2.1.3 Inoculum and inoculation

In both experiments, the soil was inoculated at GS 31/23 and 27 (in 2014 and 2015 respectively) by manual distribution of maize straws (pieces of 15-20 cm/m^2) which were naturally infected with *Fusarium* species to simulate an increased soil-borne disease pressure. The inoculum was collected in the season before the experiments in both years. The inoculum was collected from the 30-40 cm basal area of maize plants. Pieces were left to dry at room temperature and then cut into pieces of 15-20 cm. The source of inoculum was a selected field experiment (harvested at maturation) at Meßdorfer Feld at the campus of the University of Bonn in which maize plants did not receive fungicide application. In 2014, an appropriate number of plots were left without inoculation (S-), the remaining were inoculated (S+) which was considered as a factor. In contrast, and based on the results of 2014, all plots were inoculated in 2015.

To study the spectrum of *Fusarium* species that naturally colonise the inoculum, 40 pieces of the maize straws were sampled, then three pieces (1 cm length) per sampled maize straw were randomly chosen and placed on Czapek-Dox-Iprodione-Dicloran agar (CZID), the selective medium for *Fusarium* spp. (Abildgren et al. 1987). Fungal isolates of *Fusarium* spp. from CZID were re-cultured on Potato Dextrose Agar (PDA, 39 g/L) and Carnation-leaf agar, CLA. CLA was prepared by placing three sterile leaf pieces (1.5 - 2.5 cm) of young carnation (*Dianthus caryophyllus* L.) in 2% water agar following the method of Nelson et al. (1983) to execute the morphological identification of *Fusarium* species.

2.1.4 Acquisition of canopy parameters before harvest

2.1.4.1 Visual assessment of wheat diseases

Starting after the third application of fungicide against foliar diseases, at GS 55, plots were inspected periodically until GS 83-85. 18 random positions per treatment in 2014 and ≥ 8 in 2015 (≥ 3 replicated plots) were selected to inspect the presence of foliar diseases symptoms on the top three leaves starting from flag leaf (F) until F-2. For each of these locations and leaves, disease severity was averaged over 4-6 plants and scored. At advanced stages of plant development (GS ≥ 79), the inspection included only F and F-1 due to the senescence. Symptoms caused by the main fungal pathogens: *Zymoseptoria tritici* (septoria leaf blotch, SLB), *Puccinia triticina* (brown rust,

BR) and *Puccinia striiformis* (yellow rust, YR) were recorded. Disease severity for each foliar disease was individually estimated following a percentage scale from 0 to 100% (1, 3, 9, 16, 26, 37, 55, 70, 89%) which is recommended for this kind of experiments (Couture 1980). The area under the disease progress curves (AUDPC) for each foliar disease was calculated using the equation 1.

$$\text{AUDPC} = \sum_{i=1}^{n-1}\left(\frac{y_i + y_{i+1}}{2}\right)\left(t_{i+1} - t_i\right) \qquad \text{(Eq. 1)}$$

In which n is the number of assessment times, y_i is the estimated foliar disease at assessment time t_i (Campbell and Madden 1990). AUDPCs of all foliar wheat diseases was then calculated and used to express the total diseases area with foliar diseases. The severities of wheat foliar diseases on flag leaves (FDF), at GS 83, were also assessed and used to express the presence of foliar diseases beside AUDPC. At GS 83, FHB incidence was calculated using equation 2:

$$\text{FHB incidence} = \left(\frac{\text{Number of symptomatic ears}}{\text{Total number of inspected ears}}\right) * 100 \qquad \text{(Eq. 2)}$$

2.1.4.2 Frequency of infected leaves

Shortly before anthesis (GS 55-59), samples of F-2 were collected to study the infection of leaves with *Fusarium* species expressed as the frequency of infected leaves (FIL). Samples were collected from F-2 (≥ 18/treatment) in both years in separate bags for each plot. CZID was used for the reisolation of *Fusarium* spp. after surface sterilization of tip middle and base parts of sampled leaves (each in 1 cm length) with 1.2% sodium hypochlorite for 1.5 minutes followed by rinsing in sterilized water, two times for 2 min. Leaflets were laid in Petri dishes with CZID, three leaflets per Petri dish (one leaf). These samples were incubated for three days under near ultraviolet lights (360-370 nm) before the inspection of the infection of leaves started. The total number of isolates on CZID media was counted and FIL was calculated using equation 3:

$$FIL = \left(\frac{\text{Number of inspected isolates per treatment}}{\text{Total number of inspected isolates from all treatments}}\right) * 100 \qquad \text{(Eq. 3)}$$

The fungal isolates of *Fusarium* spp. from CZID were re-cultured on PDA and CLA following the method of Nelson et al. (1983) to study the morphological identification of *Fusarium* species.

2.1.4.3 ASD FieldSpec

Reflectance spectra were measured with handheld non-imaging ASD FieldSpec 3 Hi-Res [Analytic Spectral Devices (ASD), Boulder, USA]. The spectral range that can be measured by the ASD device is from 350 to 2500 nm. Canopy spectral measurements were done between 12:00 and 15:00 h under bright blue sky conditions. Reflectance values were afterwards interpolated by the RS3 software to 1 nm steps. Spectral jumps between the spectrometer's detectors were removed using the ASD ViewSpecPro software [Analytic Spectral Devices (ASD), Boulder, USA].

The instruments were warmed up for 30 min previous to the measurement to increase the quality and homogeneity of the reflectance spectra. Instrument optimization and reflectance calibration were performed prior to sample acquisition. Each sample scan represented an average of 25 reflectance spectra. In each treatment, reflectance spectra from three points of each plot (equally distanced from one another) were measured. The reflectance of the canopy was measured at GS 73 at a height ~50-55 cm from the canopy with sampled areas between 3.9 and 5.6 dm^2 which equals a circle of 22-27 cm (Fig. 2.3). For normalisation the reflectance spectra, a barium sulphate white reference was fixed on a tripod at the same level of the canopy of each variety. The reluctance spectra were then measured from 0.4×0.4 m BaSO4 calibration panel after 24 measurements of the wheat canopy.

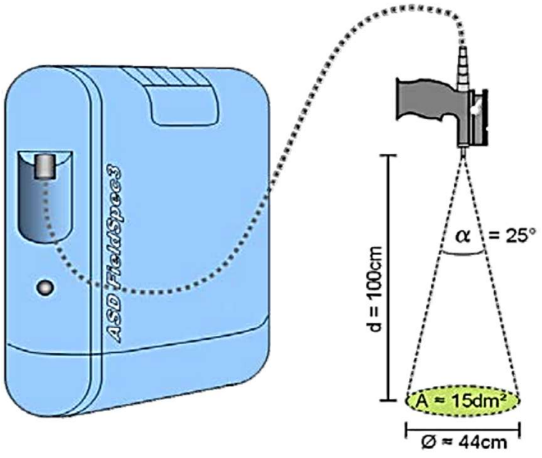

Figure 2.3 Illustration of the technical arrangement of a non-imaging spectrometer, ASD FieldSpec (modified from Danner et al. 2015).

Table 2.3 Summary of spectral indices used in this study derived from ASD measurements (hyperspectral reflectance) of the 2015 experiment.

Index	Equation	Indicator	Reference
Normalized differences vegetation index	NDVI = (R800 - R670)/(R800 + R670)	Biomass and leaf area	Rouse et al. (1974)
Photochemical reflection index	PRI = (R531 - R570)/(R531 + R570)	Epoxidation state xanthophyll's cycle, pigments, and photosynthetic radiation use efficiency	Gamon et al. (1992)
Pigment-specific simple ratios	PSSRa = R800/R680 PSSRb = R800/R635 PSSRc = R800/R470	Chlorophyll a Chlorophyll b Carotenoid c	Blackburn (1998)
Blue-green index 2	BGI2 = R450/R550	Chlorophyll content	Zarco-Tejada et al. (2005)
Plant senescence reflection index	PSRI = (R680 - R500)/R750	Plant senescence	Merzlyak et al. (1999)
Water indices	WI1 = R900/R970	Water content	Peñuelas et al. (1997)
	WI2 = (R1070 - R1200)/(R1070 + R1200)	Related to water	Ustin et al. (2002)
	WI3 = (R860 - R1240)/(R860 + R1240)	Related to water	Gao (1996)
	WI4 = (R819 - R1649)/(R819 + R1649)	Related to water	Hardinsky and Lemas (1983)

Spectral vegetation indices (SVIs) were calculated from the measured reflectance spectra to reduce the dimensionality of data (Tab. 2.3). Normalized differences vegetation index (NDVI), Photochemical reflection index (PRI), Pigment-specific simple ratio of chlorophyll a, b and carotenoid (PSSRa, PSSRb and PSSRc, respectively), Plant senescence reflection index (PSRI), Blue-green index 2 (BGI2) and Water indices (WI1, 2, 3, and 4) were the investigated SVIs.

2.1.5 Acquisition of canopy parameters after harvest

2.1.5.1 Grain yield

Grain yield (GY) of individual plots (t/ha) was determined after reducing the moisture content of harvested kernels to 13-14%. 500 g of each plot were sampled to evaluate thousand kernel weight (TKW), milling quality of wheat kernels and testing for the infection by *Fusarium* spp.

2.1.5.2 Measuring milling quality and thousand kernel weight

To assess the impact of the factors above and their interactions on the quality of harvested kernels in the 2015 experiment, kernels were analysed by using near-infrared reflectance spectroscopy (NIRS) with Diode Array 7250 NIR analyser (Perten Instruments, Inc., USA). According to several reports, NIR sensors are highly usable for the assessment of milling quality of wheat kernels (Blažek et al. 2005, Mutlu et al. 2011, Pojić and Mastilović 2013). Raw-protein content (RPR), protein (PR), and starch (ST) measured as a percentage were chosen among parameters assessed by the instrument.

A sample of 250 kernels was weighted, and the thousand kernel weight (TKW) calculated. The sampling procedure for each treatment was replicated three times, and the mean values of TKW, as well as the corresponding standard error, were calculated for each treatment.

2.1.5.3 Kernel sampling and pathogen re-isolation

To study the infection of kernels with *Fusarium* species, samples from the above mentioned 500 g were sampled (120 kernels from each treatment). The *Fusarium* infection of kernels was investigated using CZID media (Abildgren et al. 1987). Kernels were surface sterilised with 2% sodium hypochlorite for 2 minutes followed by rinsing in sterilised water, two times for 2 min. Six

kernels were placed in each Petri dish and incubated at room temperature (22 ± 3°C) under UV light. After 7-10 days of incubation, the number of total isolates of *Fusarium* spp. from kernels was inspected and the frequency of infected kernels (FIK) was calculated using equation 3. The morphological identification of isolated *Fusarium* species was made following the method of Nelson et al. (1983).

2.1.6 Statistical analysis

Data were analysed statistically using Superior Performing Software System SPSS 24 (SPSS Inc., Chicago, IL, USA). Nonlinear regression analysis of FHB incidence and foliar diseases severities were executed using the software package Sigma Plot (Systat Software Inc. San Jose, CA 95131 USA). FHB incidence was log-transformed to normalise the data distribution before the one-way analysis of variance (ANOVA). Except for the frequency of infected kernels (FIK) and the frequency of infected leaves (FIL), all variables were subjected to a 3-way ANOVA, to study the interactions among fungicide application against foliar diseases (F+ vs. F-), nitrogen levels (N100 vs. N50) and fungicide application against FHB (Fus+ vs. Fus-) in the linear model (2015 experiment). NDVI was log-transformed to normalise the data distribution before running the analyses. Correlation analysis of data from both experiments was tested by Pearson and determination coefficient, r and R^2. Means were compared using Tukey HSD test (significance level $P = 0.05$).

2.2 Experiments under controlled conditions

2.2.1 Plant cultivation

Passat (KWS, LOCHOW, Northeim, Germany), a variety of spring wheat (*Triticum aestivum* L.), moderately resistant to FHB (Anonymous, 2013) was used in all experiments under controlled conditions. Pots of two-litre size (12×12×20 cm) were filled with a mixed substrate (sand, Horizon C, potting substrate consisted of a mixture of organic soil (ED 73, Klasmann-Deilmann, Geeste, Germany) at a 1:3:6 ratio [v/v/v]). Five wheat kernels were sown per pot. After 20 days, two seedlings were left and were supported by sticks and wires to avoid lodging. The plants were cultivated at 20 ± 2°C and 50–70% relative humidity (RH). Supplement artificial light (>300 µmol m^{-2} s^{-1}, Sodium-vapor lamps, Philips SGR 140) was used to obtain a photoperiod of 16/08 h day/night.

2.2.2 Pathogen culture, inoculum preparation, and inoculation

Two *Fusarium* species were used for inoculation: *F. graminearum* isolate S.19, and *F. culmorum* isolate 3.37. Both were isolated from infected wheat kernels at Klein Altendorf, Bonn, Germany, in 2011 and 2004, respectively. The isolates were stored at -80°C in the culture collection of the Institute of Crop Science and Resource Conservation (INRES), University of Bonn. The aggressiveness of the isolates was tested in preliminary experiments in wheat ears and leaves prior to the final experiments.

The inoculum was produced following the method of Moradi (2008). The isolates were cultured in potato dextrose broth (PDB, 24 g/L) in 250 mL Erlenmeyer flasks for 3-4 days on a shaker (170 rpm) at 22°C. Subsequently, 1000 µL suspension was transferred and evenly distributed on the surface of Petri dishes containing LSPDA (low strength potato dextrose agar 12.5 g/L and agar-agar 19.5 g/L) using a sterilised bent-glass rod. Non-sealed Petri dishes were incubated under UV light (near ultraviolet, 360-370 nm) at 22°C. Four days after incubation, conidia were harvested by flooding the plates with distilled water (containing 0.01% of surfactant Tween 20) and brushing the agar surface with a rubber brush. The number of spores in the inoculum suspension was adjusted to 10^5 conidia mL^{-1} using a Fuchs–Rosenthal haemocytometer. The viability of conidia was tested on glass slides to be > 90%.

Four inoculation scenarios were applied for each *Fusarium* species at GS 61-65 (Lancashire et al. 1991). Ears were inoculated by spraying until run off with 10^5 conidia/mL (spray inoculation) or by injecting 10 µL conidial suspension into each of three florets on the ears' top (spikelet level 9 = tip inoculation), centre (spikelet level 5 = centre inoculation), and base (spikelet level 1 = base inoculation), separately. Plants of each inoculation scenario (10 plants) were incubated in separated plastic chambers at optimal conditions for infection, 95% RH and 22-25°C, for 48 hours. Subsequently, plants were grown at 50–70% RH, 16/08 photoperiod, 18/12°C day/night, respectively. Mist-irrigation kept the canopy wet for 1-2 h per day. The same number of non-inoculated control plants was grown under the same conditions.

2.2.3 Histological technique and microscopy

For histological observations, semi-thin sections (0.2 mm^2) were prepared from lemmas and glumes blocks taken from infected spikelets with *F. graminearum* and from the non-inoculated control. The prepared samples were fixed in a Karnosky´s fixative solution (2% paraformaldehyde (SiGMA) and 2% glutaraldehyde (AppliChem)) in a 0.2 M sodium cacodylic acid sodium salt trihydrate buffer pH: 7.2 (Fluka) at room temperature for two hours (Karnovsky, 1965). Material were washed seven times and were put in the cacodylic acid sodium salt trihydrate buffer (pH: 7.2) for 15 minutes, and then in a 2% osmium tetraoxide (ROTH) solution for 1.0 hour. Samples were then washed again in the cacodylic acid sodium salt trihydrate buffer (pH: 7.2). Dehydration process, subsequently, was done in a graded ethanol (AppliChem) water bi-distilled series (15, 30, 50, 70, 90 and 100%), then washing twice (10 minutes each) in propylene oxide 99.5% (ALDRICH) took place.

The method of Spurr (1969) was then followed by the embedding media corresponded to a firm standard ERL medium (8.2 g ERL 4221 Cycloaliphatic epoxide resin), 6 g D.E.R. 736 (Diglycidyl ether of Polypropylene glycol), 11.8 g NSA (Nonenyl succinic anhydride) and 0.2 g DMAE (Dimethylaminoethanol). Samples were embedded then in low viscosity Spurr (SiGMA-ALDRICH) in different propylene oxide pure Spurr ratios: 3:1, 1:1, 1:3 and left overnight at 70°C. Then, the samples were polymerized in 100% Spurr in embedding trays (Agar-Aids) at 70°C for 10 h. Sections were prepared to 500 nm wide with a 45° glass knife using an ultra-microtome (Reichert-Jung Ultramicrotome Ultracut E; Leyca Microsystem, Nussloch, Germany) followed by

staining with 1% toluidine blue for one minute (AppliChem), according to the methodology modified from Gerlach (1977) (0.5 g toluidine, 0.5 g sodium tetraborate, 50 ml bi-distilled water) then rinsing in water. Before observing the infection via microscopy, the sections were mounted and sealed dry overnight. The structures of the pathogen were observed under bright field with a Leitz DMRB photomicroscope. Images were taken with a camera to the Leitz DMRB Leica light microscope using the software Diskus 4.2 (Hilgers, Königswinter, Germany).

2.2.4 Visual assessment of disease dynamics

2.2.4.1 Visual assessment at ear level

Each ear of the treatments (20-25 ears per treatment including the non-inoculated control) was labelled for visual rating. FHB scoring started 5-6 dai by visual rating and calculating the percentage of symptomatic spikelets from the total number of spikelets per ear (FHB index):

$$\text{FHB index} = \left(\frac{\text{Number of symptomatic spikelets per ear}}{\text{Total number of spikelets per ear}} \right) * 100 \qquad \text{(Eq.4)}$$

The visual rating was carried out at intervals of 2-6 days until GS 77-83. At this time the visual rating was not possible anymore because of ear senescence. FHB incidence was calculated in the same intervals by counting the number of symptomatic ears from the total number of inoculated one's from equation 5

$$\text{FHB incidence} = \left(\frac{\text{Number of symptomatic ear per treatment}}{\text{Total number of inoculated ears per treatment}} \right) * 100 \qquad \text{(Eq. 5)}$$

The area under disease progress curve (AUDPC) was calculated for each treatment using equation 1, in which n is the number of assessment times, y_i is the FHB index at assessment time t_i (Campbell and Madden 1990).

2.2.4.2 Modelling of disease dynamics

A monomolecular function (Eq. 6) was fitted to the disease incidence curves after combining observations of the four inoculation scenarios for each *Fusarium* species under each environmental condition.

$$y(t) = K(1 - e^{(-rM*(t-t0))}) \quad \text{(Eq. 6)}$$

Equation 6 has three parameters: *K* is the capacity, *rM* is the rate/slope of the curve, and *t0* is the time at which the first symptoms appear. In addition to the monomolecular function, a logistic function (Eq.7) was fitted to the disease progress curves (FHB index). This was done additionally after combining the observations of the four inoculation scenarios for each *Fusarium* species, under each environmental condition.

$$y(t) = K/(1 + (\left(\frac{K}{y0}\right) - 1)\, e^{(-rL*t)} \quad \text{(Eq. 7)}$$

Equation 7 has three parameters: *K* is the capacity, *rL* is the rate/slope of the curve, and *y0* is the initial value of the disease severity.

Equations 6 and 7 were fitted to the observations using the software package Sigma Plot (Systat Software Inc. San Jose, CA 95131 USA).

2.2.4.3 Visual assessment at spikelet level

The rating system of FHB (Fig. 2.4) was established and used in this study to estimate disease severity within individual spikelet visually.

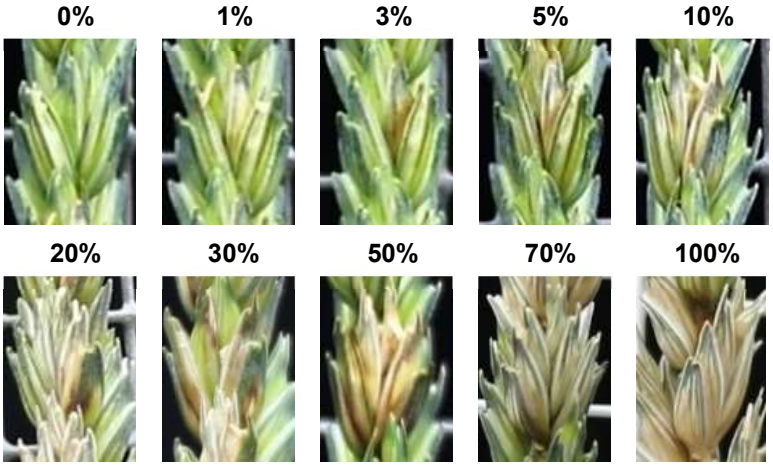

Figure 2.4 Rating system of *Fusarium* head blight severity within single spikelet of wheat.

Disease rates from 1 to 5% represent the early symptoms of FHB namely necrotic lesions on glumes. 10% represents the early bleached symptoms which usually occupy the typical floret, 20,

30 and 50% represent combinations of extended necrotic lesions and bleached florets at different levels. 70% are bleached spikelets but not completely dry and 100% bleached and dry spikelet.

2.2.5 Sensor systems: measuring set-up and data analysis

2.2.5.1 Infrared Thermography

Thermal imaging was performed in a greenhouse under controlled conditions at 50–70% relative humidity (RH) and 17-24°C. Ears were fixed vertically on sheets of metal grids (40×30 cm, holes 12×12 mm) which were already fixed via supporting steaks to the pots of plants, in order to get the best focusing of all ears at measurement. Thermal measurements were performed on 12-13 ears from four plants, as experimental replications for each treatment. 30 minutes before measuring, the system of external artificial supplementary light was shut off to do the thermal measurement passively. Direct sunlight and wind were avoided to stabilise the environmental condition during the measurement in the greenhouse. Thermal images were recorded between 7 and 11 a.m. until 29 dai. The thermocamera was mounted on a tripod placed at 60 cm distance from the plants at the height of ears. A digital thermocamera InfraTec Vario CAM head hr 640 (Jenoptik, Jena, Germany), sensitive to spectral range from 7.5 to 14 μm was used in this study. The camera has a thermal resolution of 0.03 K at 30°C, a geometric resolution of 640 × 480 IR-pixel and 60 Hz IR-image frequency on an external computer. The emissivity was set to 1 at all measuring dates. The thermocamera was controlled by the software IRBIS (InfraTec, Dresden, Germany) installed on an external laptop. The set-up of ears fixed on the sheets of metal grids lasted until the last measuring date, the start of ripening. In parallel, RGB images were taken with a commercial digital camera (Canon, Power Shot Pro 1).

The temporal effect of FHB on ears temperature was investigated by analysing the IR images using the software package IRBIS 3 professional (InfraTec, Dresden, Germany). Maximum, minimum, mean ear temperature and temperature span (TS, the difference between the maximum and minimum temperature) were calculated using lines 5-8 cm long depending on individual ear length. Similar lines were used to calculate the average temperature of ambient air. Two thermal parameters were used to investigate the effect of FHB on ear temperature: (i) TS within ears and (ii) the temperature difference (TD) between the mean ear temperature and ambient air temperature. The area under temperature span curves (AUTSC) and the area under temperature difference curves

(AUTDC) were calculated for each treatment using equation 2 by replacing y_i with the TS_i and TD_i, respectively. The unit for AUTDC and AUTSC is K (Kelvin) × day.

Spatial patterns of FHB after different preliminary site of ear infection were investigated with software written in MATLAB 2011b (The MathWorks Inc., Natick, MA, USA) that analyses the IR-images considering the spatial structure of ears. In this software, IR-images need to be extracted as ASCII and JPEG files congruently from IRBIS then imported into the software. The ASCII files include the temperature data for each pixel of JPEG images in the same sequence of x and y dimensions. JPEG file was extracted using VarioCAM colouring system to show high contrast to the black background of the software window. The software asks first to import the ASCII file, then the corresponding JPEG file. A region of interest, ROI, needs to be drawn using polygon selecting-tools, and then the pixels that belong to the ear within the drawn polygon can be included by giving the order J or excluded by giving the order N. The results are then demonstrated in two-dimensional graphs showing the temperature profile of individual ears as ROI. In these graphs, the y-axis, 1-100%, stands for the ear levels, the base of the ear is at 1%, the very top at 100%. Temperature values shown in the graphs are the mean values of pixels laid in rows of selected ears.

For simultaneous thermal and chlorophyll fluorescence imaging for monitoring of FHB different thermocamera was used. Thermal imaging was performed in a greenhouse under controlled conditions at 50–70% RH and 17-24°C. The artificial supplementary light was reduced at measuring time to 20 ± 2 µmol m^{-2} s^{-1} (Hortilux Schreder, HPS 400W/230V, Holand). Ears were fixed vertically on sheets of metal grids (40×30 cm, holes 12×12 mm) supported by sticks in the pots. A digital thermocamera, VarioCAM® High Definition (Jenoptik, Jena, Germany), sensitive to spectral range from 7.5 to 14 µm with uncooled microbolometer focal plane array was used. The camera has a thermal resolution of 0.03 K at 30°C, a geometric resolution of 1.024 × 768 IR-pixel and 30 Hz IR-image frequency. The emissivity was set to 1 for all measuring dates. The thermocamera was mounted on a tripod flexible to adapt its height in accordance with ears height and placed at 40 cm distance from ears. The thermocamera was controlled using the software package IRBIS 3 professional (InfraTec, Dresden, Germany).

IR images were analysed using the same software package IRBIS 3 professional (InfraTec, Dresden, Germany) by drawing the proper polygons that fit the selected spikelets; the same polygons were moved to a nearby area that did not overlap with ears to get the thermal data of

ambient air. Temperature span (TS) and the average temperature difference between air and spikelets (TD) were calculated (Tab. 2.4).

2.2.5.2 Chlorophyll Fluorescence Imaging

An imaging pulse amplitude modulated chlorophyll fluorometer (PAM) MAXI HEAD (Heinz Walz, Effeltrich, Germany) was used for chlorophyll fluorescence measurements under laboratory conditions. The measurement was done following the protocol of saturation pulse method immediately after plants were dark adapted for 15 ± 2 minutes at room temperature. Standard 18.5 cm distance between ears/leaves and the camera for a 13 cm × 15 cm imagery area was used with a black background.

The CCD camera (1392×1040 pixel) recorded fundamental fluorescence F0 after illumination of the horizontally laid ears with blue light (470 nm) of 0.5 µmol quanta m^{-2} s^{-1} PAR. Maximal chlorophyll fluorescence (Fm) was recorded after a saturation pulse of 2700 µmol quanta m^{-2} s^{-1} PAR for 0.6 seconds. Based on F0 and Fm, the maximal quantum yield of PSII (Fv/Fm) was calculated (Tab. 2.4) indicating the capacity of photosynthesis in the spikelets. Saturation pulses of 396 µmol quanta m^{-2} s^{-1} PAR were produced at intervals of 20 s until the steady state was reached and the effective quantum yield of PSII Y[II] was estimated (based on Fm' Maximal fluorescence at illumination) which indicates the stability of photosynthesis. The CCD camera was controlled via the software package imagingWin professional (Heinz Walz, Effeltrich, Germany). Recorded false colour images of Fm, Fv/Fm and Y[II] were analysed by drawing the proper polygons that fit the selected spikelets.

2.2.5.3 Performing the simultaneous measurement

To investigate the potential of fusion of sensor data, measurements with IRT and CFI were performed on the same day. The thermal imaging was performed under greenhouse conditions before the sunshine hit the cabinet where the experiments took place, from 8:00-9:30 am. Then plants were moved to a laboratory to measure CFI. After measurement, plants were brought back to the greenhouse and fixed again on grids to be ready for the next measurement. Time-series images were performed at 3, 5, 7, 9, 12, 17, 21 and 30 dai. During the data analyses, 6 spikelets were chosen from six ears as experimental replications for each treatment.

Table 2.4 Summary of some indices derived from multi-sensorial monitoring of *Fusarium* head blight in wheat.

Sensor	Index	Equation	Indicator
Infrared Thermography	Temperature span(TS)	TS = maximum – minimum temperature within spikelets	*Fusarium* infection on wheatears at early stage of symptoms development, Al Masri et al. (2017)
	Temperature difference (TD)	TD = average air temperature - average spikelets temperature	*Fusarium* infection on wheatears at early and late stages of symptoms development, Al Masri et al. (2017)
Chlorophyll Fluorescence Imaging	Maximal fluorescence yields (Fm)	Fm (after dark adaptation)	Fast chlorophyll fluorescence kinetics, Kuckenberg et al. (2009)
	Maximal PSII quantum yield (Fv/Fm)	Fv/Fm = (difference between maximum and minimum fluorescence after dark adaptation)/Fm	Maximal photochemical efficacy of photosynthesis II, Kitajima and Butler (1975)
	Effective PSII quantum yield Y [II]	Y [II] = [difference between maximum(Fm') and minimum fluorescence (Ft) after illumination]/(Fm')	Photochemical quantum yields at steady state, Genty et al. (1989)

2.2.5.4 SPAD-meter

For the assessment of chlorophyll content of flag leaves, a Minolta SPAD-502 meter (Minolta Camera Ltd., Osaka, Japan) was used. This instrument is constructed to measure the relative content of chlorophyll by measuring the transmittance of the leaf at 600 to 700 nm and 400 to 500 nm. The measurement was done from tip, centre and base area of leaves and average was then calculated. The measured value by SPAD-meter is unitless and proportional to the amount of chlorophyll.

2.2.6 Kernel sampling and pathogen re-isolation

To study the spatial patterns of *Fusarium* species infection within individual ears, each ear was divided into nine spikelet levels (spikelet level 1 at the ear's base and spikelet level 9 at the ear's tip). For each level, 12 kernels were sampled from 12 ears of the same treatment. The *Fusarium* infection of kernels was investigated on CZID (Abildgren et al. 1987). Kernels were surface sterilised with 2% sodium hypochlorite for 2 minutes followed by rinsing in sterilised water two times for 2 min. Six kernels were placed in each Petri dish. Petri dishes were incubated at room temperature (22±3°C) under UV light. After one week of incubation, the number of kernels infected with *Fusarium* species was counted and the frequency of infected kernels was calculated for each spikelet level.

2.2.7 Modelling of infection gradients

Under the assumption that the frequency of infected kernels of each spikelet level decreases from the inoculation point exponentially upwards and downwards, the following equations were fitted depending on the inoculation site. For the base inoculation (at spikelet level 1) the frequency of infected kernels of the nine spikelet levels x were described by equation 8:

$$f(x) = a\, e^{-b(x-1)} \qquad \text{(Eq. 8)}$$

Parameter a is the incidence at the inoculation site, i.e. at spikelet level 1, and shows the success of the infection. Parameter b denotes the slope of the gradient in an upward direction for spikelet levels x up to 9. For the tip inoculation (at spikelet level 9), the downward gradient was described by equation 9:

$$f(x) = a\, e^{-c(9-x)} \qquad \text{(Eq. 9)}$$

Parameter a is again the incidence at the inoculation site, here at spikelet level 9. Parameter c denotes the slope of the downward gradient for spikelet levels x down to 1. For the centre inoculation (at spikelet level 5), the frequency of infected kernels decreased upwards (to level 9) and downwards (to level 1). Thus equation 10 containing both gradients was applied:

$$f(x) = \begin{cases} a\, e^{-c(5-x)} & \text{for } 1 \le x \le 5 \\ a\, e^{-b(x-5)} & \text{for } 5 < x \le 9 \end{cases} \qquad \text{(Eq. 10)}$$

Like before, parameter *a* is the incidence at the inoculation site, here at spikelet level 5. Parameters *b* and *c* denote the slopes of the downward and upward gradients, respectively. Equation 5 was also applied after spray inoculation to investigate whether gradients exist on these ears or not. The three equations were fitted to the data on the frequency of infected kernels using software package Sigma Plot (Systat Software Inc. San Jose, CA 95131 USA).

2.2.8 Ear weight

To study the effect of primary site of ears infection with both *Fusarium* species on yield loss, the ear weight (EW) was investigated. After harvest at maturity, a total number of ears from each treatment was weighed as the first investigation. Harvested ears were first put in paper bags under room temperature until they homogenously dried. The sampling procedure included all harvested ears from each treatment with replications of 20-25 ears (sample size), and the mean value of EW was calculated with the corresponding standard error for each treatment.

2.2.9 Kernel weight

After sampling at maturity, 20-25 ears from each treatment were threshed separately for thousand kernel weight (TKW). A sample of 100 kernels was weighted, and TKW was calculated. The sampling procedure for each treatment was replicated four times, and the mean value of TKW was calculated with a corresponding standard error for each treatment. The reduction in TKW (RTKW in g) was then calculated by subtracting $TKW_{treatment}$ from $TKW_{non\text{-}inoculated\ control}$ ($TKW_{non\text{-}inoculated\ control} - TKW_{treatment}$).

2.2.10 Statistical analysis

Data were analysed statistically using Superior Performing Software System SPSS 22, 23 and 24 (SPSS Inc., Chicago, IL, USA). Non-linear regression analysis of disease incidence and disease severity (FHB index) were done using the software package Sigma Plot (Systat Software Inc. San Jose, CA 95131 USA). Disease incidences at early and late stages were compared by one-way analysis of variance (ANOVA). RTKW, AUDPC and FIK were subjected to a 3-way ANOVA, including the primary site of ear infection, environmental conditions and *Fusarium* spp., as well as their interactions, in the linear model. FHB index, AUDPCs and FIKs of single infection scenarios

were log-transformed to normalise the data distribution before running the analyses. Pearson's Chi-squared test (χ^2) was used to compare the distribution of infected kernels within ears, *t*-test to compare infection scenarios by both *Fusarium* species. Correlation and regression analysis of AUDPC, FIK and RTKW were tested by Pearson and determination coefficient, *r* and R^2, respectively. Stepwise discriminant analysis and correlation matrix were applied to study the potential of fusion of sensor data (significance level $P = 0.05$). All means were compared using Tukey HSD test (significance level $P = 0.05$).

.

3. RESULTS

The current research focuses mainly on the potential of Infrared Thermography, Chlorophyll Fluorescence Imaging and Hyperspectral Non-Imaging sensors for providing new insight in studying the development of *Fusarium* infection. Under the light of the current problematic situation of FHB and building on the new findings of applying sensors in plant pathology, the present work was designed. An interdisciplinary research that implements sensors for the detection, differentiation and quantification of *Fusarium* head blight of wheat under field and controlled conditions was performed. The present research hypothesised that the foliar wheat diseases and their control by fungicides could influence the available inoculum of *Fusarium* which is a key factor for *Fusarium* infection in ears. After infection occurs in ears, the primary site of ear infection by *Fusarium* species influences the later development of this disease within ears. The present research was focused on the effect environmental conditions on the later development of this disease within ears. Measurement with Infrared Thermography was performed under greenhouse conditions and related to the conventional methods of FHB assessment. In the last step, the potential of fusion of sensor data of Infrared Thermography and Chlorophyll Fluorescence Imaging systems under controlled conditions was investigated.

3.1 Impact of foliar wheat diseases and their control by fungicides on *Fusarium* head blight

3.1.1 Presence of wheat diseases

3.1.1.1 Septoria leaf blotch

In the 2014 experiment, septoria leaf blotch (SLB) reached only very low severities (≤ 2%) even at advanced growth stages of wheat, GS 75-79. The application of fungicide (F+) reduced symptoms in most treatments to levels close to zero. Starting from GS 69, symptoms became visible on Pamier canopy but were earlier visible on Tobak (Fig. 3.1). In the 2015 experiment, the effect of fungicide on SLB was more pronounced because of the higher pressure of disease severity (≤ 12.18%). The progress curves of SLB were not influenced by differences in nitrogen fertilisation (N100 vs. N50) or wheat varieties (Fig. 3.2).

3.1.1.2 Brown rust

In the 2014 experiment, brown rust (BR) had only a low severity (≤ 2%) until GS 73 on both varieties. The sharp increase of BR occurred on Tobak that had not been treated with fungicide (F-) and reached 7.78% (Fig. 3.1). In the 2015 experiment, the application of fungicide (F+) reduced BR severity close to zero. In contrast, higher severities were observed in F+ treatments on both varieties starting from GS 75 and reaching levels similar to that observed in experiment 2014 (Fig. 3.2). Moreover, a low severity of yellow rust (YR) was observed, but only in the 2015 experiment (≤ 1%). Sokrates, the marginal variety, was heavily infected with YR. In total, the severity of foliar diseases on Tobak expressed as the area under disease progress curves of SLB, BR and YR (AUDPC) and foliar diseases severity at GS 83 on flag leaves (FDF) of the 2015 experiment, were significantly affected by the application of fungicides (Tab. 3.5). When AUDPC was considered, a significant interaction between nitrogen levels and fungicide application against foliar diseases was found. Fungicides against foliar diseases and FHB showed interaction regarding foliar diseases expressed as AUDPC and FDF.

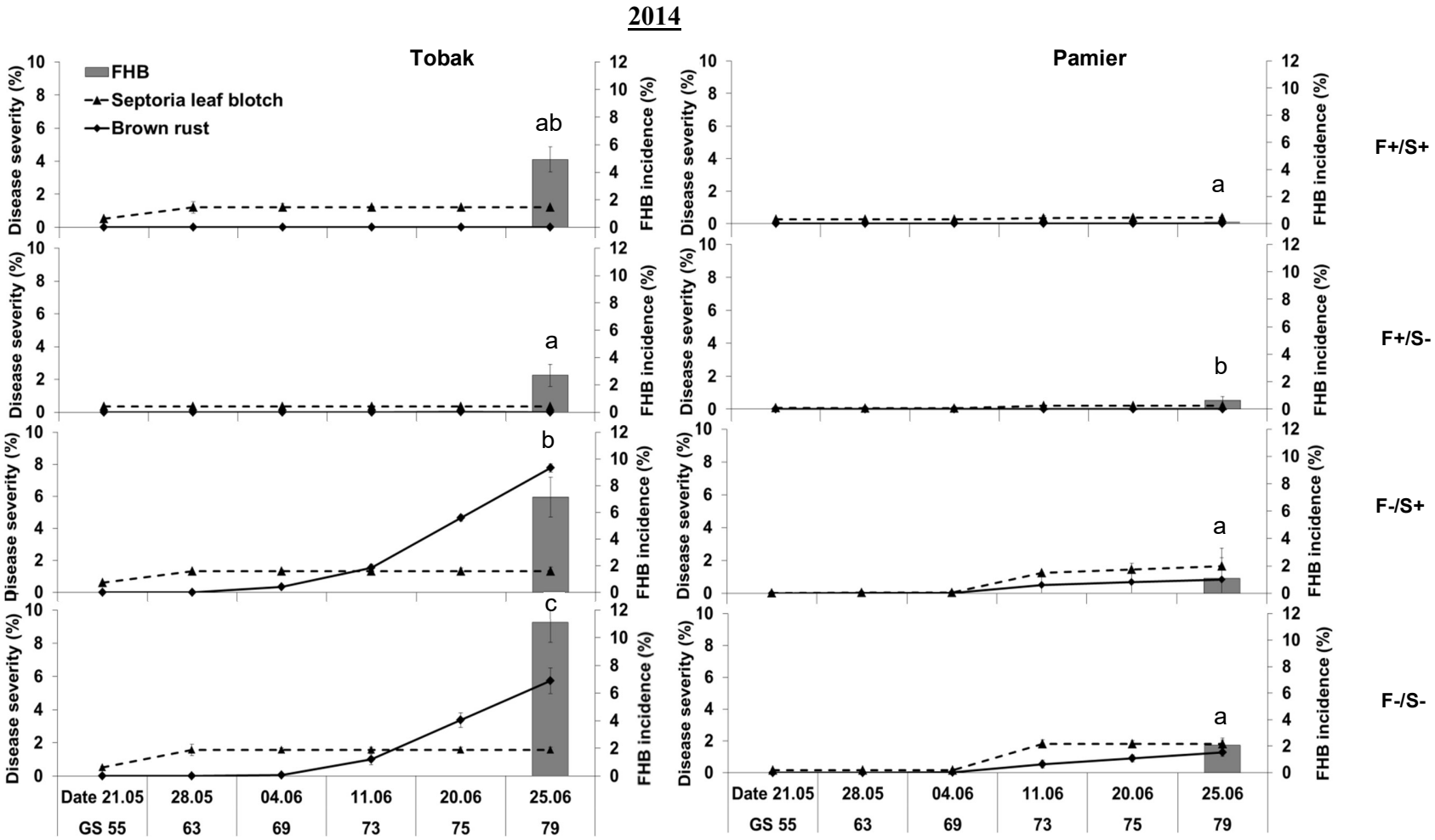

Figure 3.1 The progress of brown rust (solid lines) and septoria leaf blotch severities (dashed lines) on Tobak and Pamier (*Triticum aestivum* L.) treated (F+) or not (F-) with fungicides against foliar wheat diseases and *Fusarium* head blight, (mean ± SE: n = 18). Grey bars indicate *Fusarium* head blight incidence, (mean ± SE: n ≥ 18). Bars with the same letter are not significantly different (Tukey's HSD: $P \leq 0.05$).

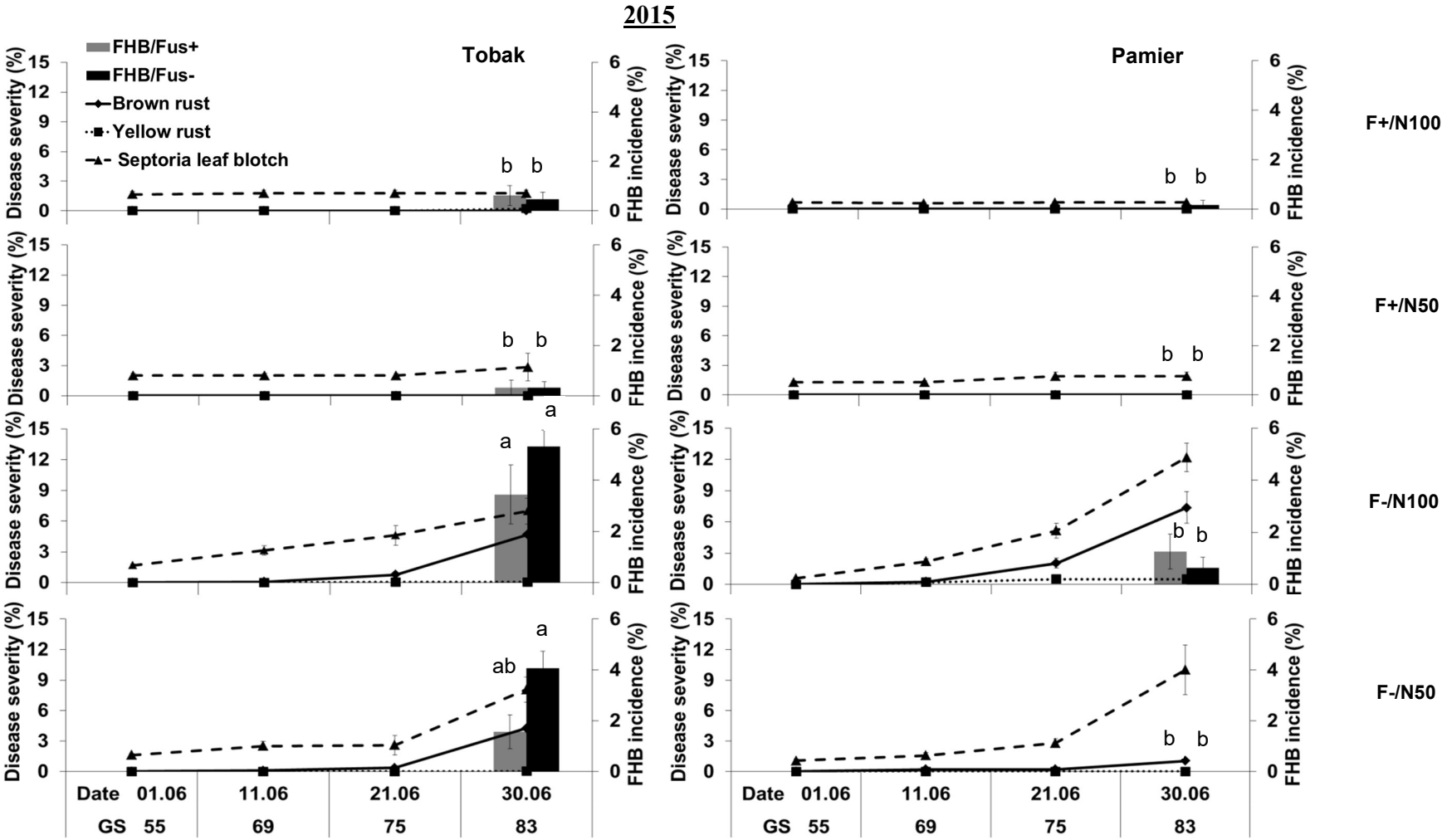

Figure 3.2 Progress of brown rust (solid lines), yellow rust (dotted lines) and septoria leaf blotch severities (dashed lines) on Tobak and Pamier (*Triticum aestivum* L.) treated (F+) or not (F-) with fungicide against foliar diseases and grown at standard nitrogen fertilisation (N100) or half (N50). (mean ± SE: n ≥ 8). Black and grey bars stand for FHB incidence after applying fungicides against *Fusarium* head blight: FHB/Fus+ or not FHB/Fus-, respectively. (mean ± SE: n ≥ 8). Bars (of the same colour) with the same letter are not significantly different (Tukey's HSD: $P \leq 0.05$).

The observations on Pamier regarding AUDPC and FDF were significantly affected by all factors (N, F and Fus). Also, both Fus and N treatments significantly interacted with treatment F regarding both AUDPC and FDF (Tab. 3.6).

3.1.1.3 FHB incidence

FHB was visible at an earlier growth stage (GS 79) in the 2014 experiment compared to that of 2015 (GS 83). Non-fungicide-treated plants showed the highest FHB incidence (11.11%) observed in the 2014 experiment. FHB was significantly reduced after fungicide application on Tobak. In contrast, Pamier exhibited low incidences of less than 2.06% in both treated and non-fungicide-treated plants (Fig. 3.1). In the 2014 experiment, the inoculation with maize straw did not associate with higher FHB incidence (Fig. 3.1).

Higher FHB incidences were observed on Tobak compared to Pamier in the 2015 experiment. The maximum level of FHB in this year was 5.30% on non-fungicide-treated canopy (F-) and ears (Fus-) with fungicide under standard nitrogen fertilization (N100). Nitrogen levels (N50) was associated with lower FHB incidence on both varieties (Fig. 3.2). However, these differences were not significant (Tab. 3.5 and 3.6). The application of fungicide (F+) on Tobak caused a significant reduction in FHB incidence, and interaction was found between the double fungicide applications (F and Fus) (Tab. 3.5).

3.1.2 Relationship between foliar diseases and FHB

Foliar wheat diseases expressed as AUDPC were significantly correlated to FHB incidence in both years (r = 0.63 and 0.53 in the 2014 and 2015 experiments, respectively). Linear regression between AUDPC and FHB incidence was also significant as well (R^2 = 0.40 and 0.28 in the 2014 and 2015 experiments, respectively).

SLB and YR were present with high pressure on Sokrates plots (marginal variety in the 2015 experiment) which did not receive fungicide treatments (11×3 m). Maximum severities were observed at GS 77 (29.25% and 15.96% for YR and SLB, respectively), BR was utterly absent. At GS 85, high FHB incidences were observed in these plots reaching average FHB incidence of 28.33%. Visualised symptoms of FHB were mostly at single spikelet/ear with orange sporodochia (Fig. 3.3).

Plots of Sokrates (3×3 m) that received fungicide application against foliar diseases from the nearby plots of Tobak and Pamier (almost an area of 3×1 m) were additionally inspected to check the presence of foliar diseases and FHB at GS 85, and correlated to each other's (Fig. 3.4). A significant correlation (r = 0.83) and significant linear regression (R^2 = 0.70) was found between FHB incidence and FDF severity of both diseases in Sokrates (Fig. 3.4).

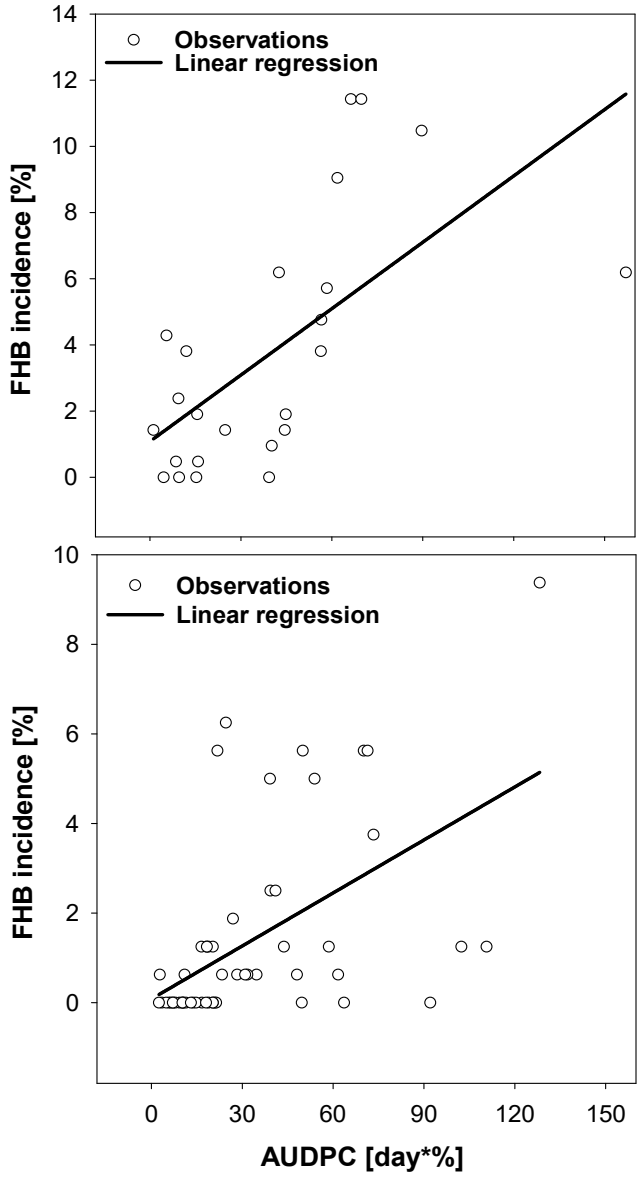

Figure 3.3 Correlation between foliar diseases (caused by *Puccinia triticina* and *Zymoseptoria tritici* in 2014, also by *Puccinia striiformis* in 2015) expressed as area under disease progress curves (AUDPC: 33 days in 2014 and 30 days in 2015) and visualised *Fusarium* head blight symptoms expressed as FHB incidences. Symbols stand for observations and lines are the simulations of linear regressions, (2014: n = 24 pairs, 2015: n = 56 pairs, Pearson method).

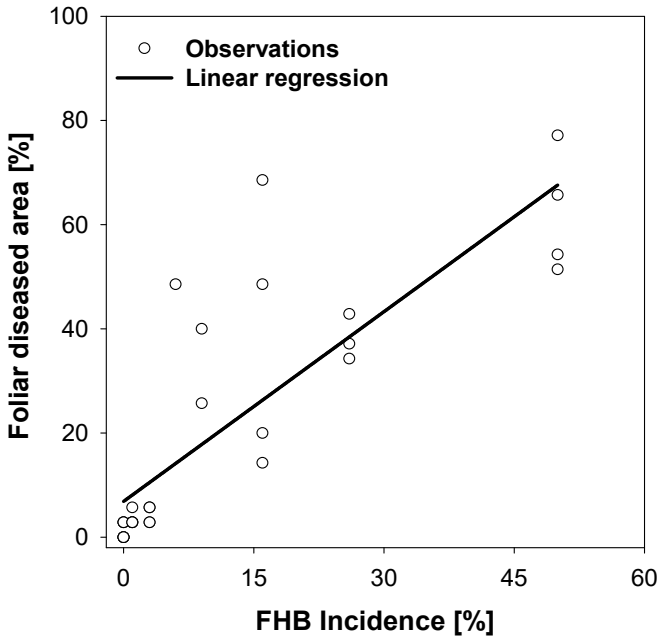

Figure 3.4 Correlation between the diseased area of flag leaves with yellow rust (*Puccinia striiformis*) and septoria leaf blotch (*Zymoseptoria tritici*) and FHB incidence. (n = 30 pairs).

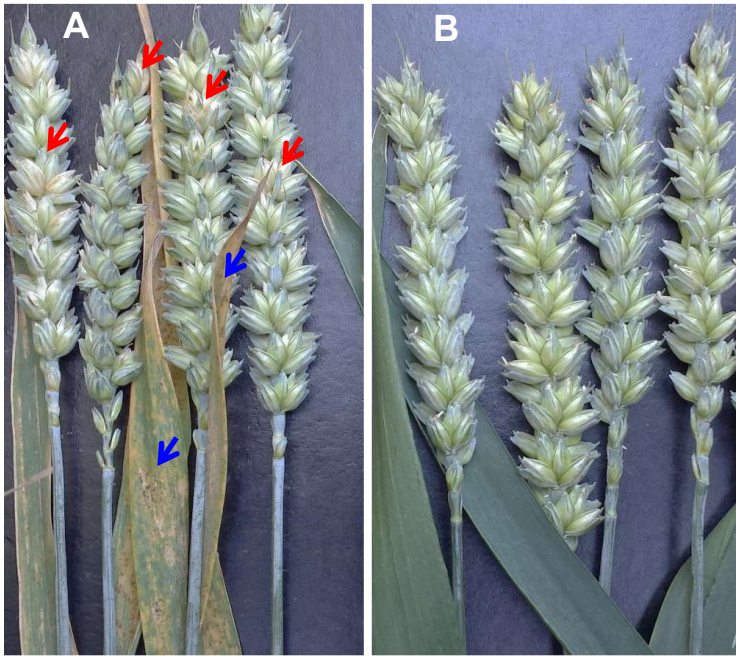

Figure 3.5 Ears showing noticeable symptoms of *Fusarium* head blight of orange sporodochia on spikelets indicated to with red arrows. Infected ears belong to plants with flag leaves heavily infected with foliar diseases indicated to with blue arrows (A), in comparison with the healthy ears with non-symptomatic flag-leaves (B).

3.1.3 Infection of leaves and ears by *Fusarium* spp.

3.1.3.1 Frequency of infected leaves

The frequency of infected leaves (FIL) and kernels (FIK) with *Fusarium* species are shown in (Tab. 3.1). In 2014 experiment, inoculation with maize straw (S+) increased FIL of Pamier from 2.8 to 6.7% and from 11.9 to 22.4% for treated (F+) and non-treated plants (F-) with fungicide, respectively. The variation in FIL of Tobak leaves of different treatments was between 11.6% and 18.1% compared to that of Pamier (Tab. 3.1). Tobak leaves showed higher susceptibility to *Fusarium* infection compared to that of Pamier except plants inoculated (S+) and treated with fungicide (22.4 and 18.1% for Pamier and Tobak, respectively).

Table 3.1 Frequency of infected leaves (FIL) and kernels (FIK) by *Fusarium* spp. due to the influence of: i) Fungicide against foliar diseases (F+, F- with or without treatment, respectively) and the inoculation with maize straw (inoculated with maize straw S+ or not S-) in the 2014 experiment and, ii) Fungicides against foliar diseases, nitrogen levels (N100 vs. N50, standard and half standard, respectively) and fungicide to control FHB at GS 69 (Fus+ and Fus-, with or without fungicide application, respectively) in the 2015 experiment.

	Variety	2014				2015							
						N100				N50			
		S+		S-		F+		F-		F+		F-	
		F+	F-	F+	F-	Fus+	Fus-	Fus+	Fus-	Fus+	Fus-	Fus+	Fus-
FIL	Tobak	11.6	18.1	11.1	15.4	5.6		19.4		5.6		15.3	
	Pamier	6.7	22.4	2.8	11.9	4.2		10.4		3.5		10.4	
FIK	Tobak	14.5	16.4	14.5	14.5	4.5	4.5	5.8	3.9	5.8	5.8	2.6	9.7
	Pamier	3.6	18.9	10.9	7.3	5.8	5.8	3.2	6.5	5.2	4.5	5.2	9.1

n = 126 and 53 for the frequency of infected leaves and kernels, respectively in 2014
n = 72 and 89 for the frequency of infected leaves and kernels, respectively in 2015

In the 2015 experiment, sampling for studying leaf infection was made before the application of fungicide to control FHB (Fus) which means that only two factors influenced FIL (N and F). Fungicide application (F+) reduced the infection of leaves with *Fusarium* species under both N100 (from 10.4 to 19.4%) and N50 (from 3.5 to 5.6%) indicated as FIL.

3.1.3.2 Frequency of infected kernels

In the 2014 experiment, the frequency of infected kernels (FIK) of Tobak from different treatments was within the range 14.5-16.4%. In contrast, substantial variation in FIK was found in Pamier (from 3.6 to 18.9%). The effect of fungicide application on FIK of Pamier was pronounced at S+ plots (18.9 and 3.6% for F+ and F-, respectively). However, the inoculation was not always associated with higher values of FIK. The effect of the inoculum (S+ and S-) on FIK of Pamier was evident at F- (18.9 and 7.3% for S+ and S-, respectively). However, plots with fungicide application showed contradictory results (Tab. 3.1).

The infection of kernels in the 2015 experiment was relatively low. FIK was mostly in a narrow range including all treatments. It was from 2.6 to 5.8% for plants treated with fungicide against FHB (Fus+) and within the range (3.9-9.7%) for plants treated with fungicide to control FHB, (Fus+). In total, Pamier and Tobak had similar FIK with the highest rate obtained when leaves were not treated with fungicide (F-) under N50 (9.7 and 9.1% for Tobak and Pamier, respectively) (Tab. 3.1).

3.1.3.3 Frequency of isolated *Fusarium* spp.

Fusarium species isolated from naturally infected maize straw (inoculum), leaves and kernels are shown in (Fig. 3.6). *Fusarium avenaceum, F. crookwellense, F. culmorum, F. equiseti, F. graminearum, F. poae, F. proliferatum, F. sporotrichioides, F. subglutinans, F. tricinctum* and *F. verticillioides* were morphologically identified in 2014 experiments. In 2014 experiment, *F. equiseti* showed the highest frequency on both inoculums and leaves with a lower presence in kernels. Some species were found on inoculum but were not able to move upward on the canopy like *F. verticillioides*.

Species like *F. avenaceum, F. graminearum, F. sporotrichioides* and *F. proliferatum* showed similar frequency on both inoculum and kernels. *F. culmorum* and *F. tricinctum* showed increased frequency from inoculum upwards. *F. crookwellense, F. subglutinans* and *F. poae* were absent in inoculum but presented in both leaves and kernels (Fig. 3.6). Additional to the above mentioned *Fusarium* species identified in the inoculum, leaves and kernels, *F. semitectum* was identified in the inoculum in the 2015 experiment. *F. graminearum* was most prevalent in the inoculum, but later on, in leaves and kernels, it was with a lower frequency of presence.

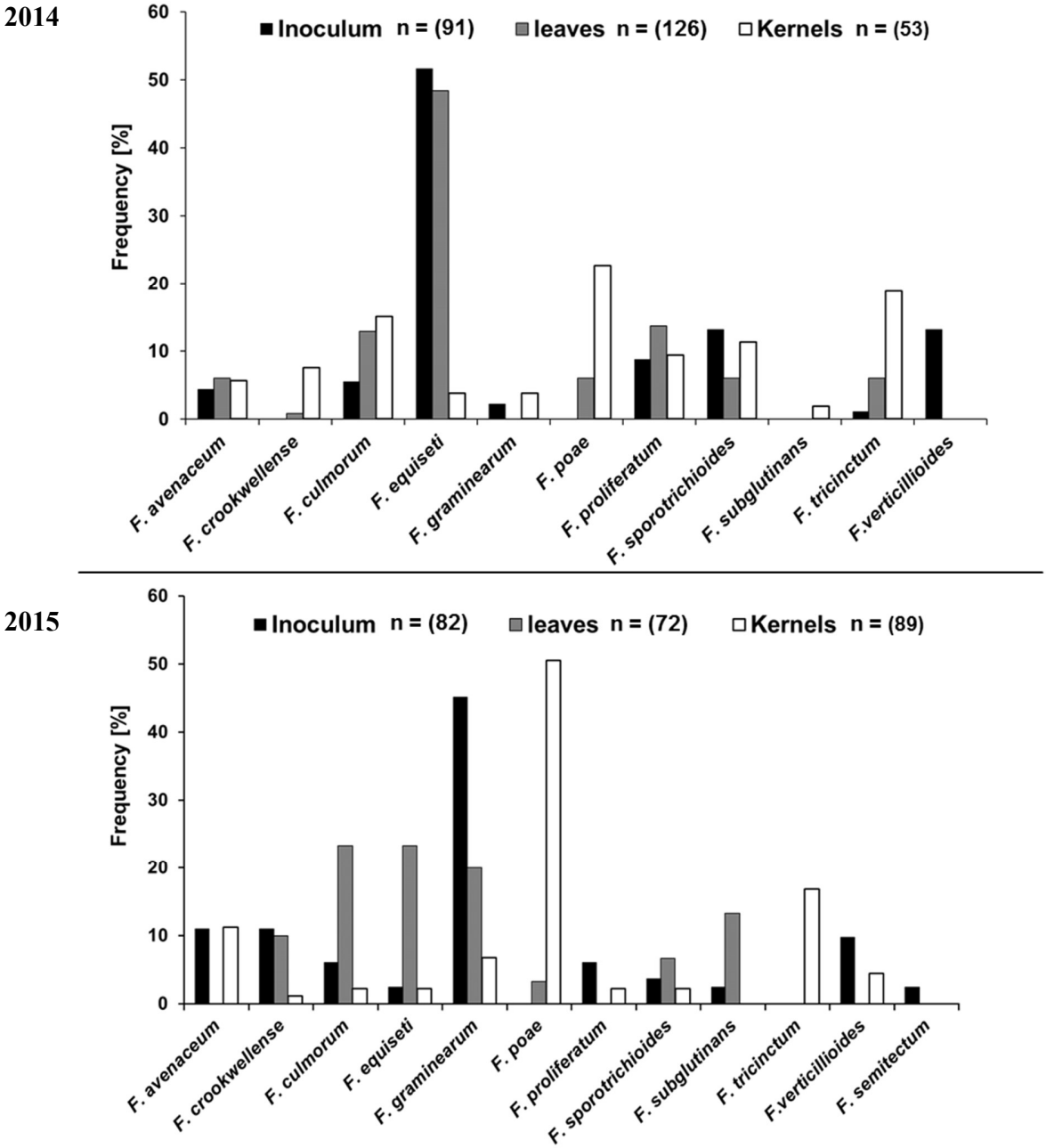

Figure 3.6 Frequency of *Fusarium* species isolated from maize straw (inoculum) before inoculation, leaves (F-2 at GS 55-59) and from kernels at harvest.

F. poae was not present in the inoculum but had the highest frequency in kernels in comparison to the other species. Species like *F. avenaceum, F. culmorum, F. equiseti, F. sporotrichioides, F.*

proliferatum and *F. verticillioides* showed similar frequencies on both inoculum and kernels (Fig. 3.6).

3.1.4 Quantity and quality of kernels

3.1.4.1 Thousand kernels weight

Thousand kernels weight (TKW) of both field trials is shown in (Tab. 3.2). In the 2014 experiment, neither fungicide application nor inoculation affected the TKW of Tobak. In contrast, Pamier was significantly affected by the inoculation (S+) and fungicide application (F+). In the 2015 experiment, TKW of Tobak was significantly affected by all factors (N, F and Fus) with a significant interaction among each other's (N×F×Fus) (Tab. 3.5). TKW of Pamier was significantly affected by only fungicide applications (F and Fus) with a significant interaction between N and F (Tab. 3.6).

Table 3.2 Thousand kernels weight (TKW) and grain yield (GY) as affected by i) the interaction between fungicide application against foliar diseases (F+, F- with or without, respectively) and the inoculation with maize straw (inoculated S+ or not S-) in the 2014 experiment. ii) the interaction among fungicide against foliar diseases, nitrogen levels (N100 standard and N50 half standard) and fungicide application against FHB (Fus+ and Fus-, with or without, respectively) in 2015. (mean, n ≥ 3). Figures with the same letter (within the same row of each year separately) are not significantly different (Tukey's HSD: $P \leq 0.05$).

	Variety	2014				2015							
		S+		S-		N100				N50			
		F+	F-	F+	F-	F+		F-		F+		F-	
						Fus+	Fus-	Fus+	Fus-	Fus+	Fus-	Fus+	Fus-
TKW	Tobak	47.6a	47.3a	48.5a	47.6a	53.2a	52.2a	52.3a	48.8b	53.3a	52.5a	52.9a	52.7a
	Pamier	45.4a	43.1b	44.7ab	43.9ab	49.5a	49.5a	48.7ab	46.7b	49.1ab	49.1ab	50.1a	48.5ab
GY	Tobak	10.7a	10.1a	10.1a	10a	10a	10.1a	9.7ab	9.2bc	8.9cd	8.7cd	8.9cd	8.3de
	Pamier	10.2a	9.7a	10.2a	9.9a	8.4ab	8.7a	8.2ab	7.9b	6.9c	6.8c	6.9c	6.5c

GY of Pamier was significantly affected by N levels and F treatments with a significant interaction between the double fungicide applications (F and Fus) (Tab 3.6). N50 was always associated with

significant reduction in GY compared with standard fertilisation (N100) ($P \leq 0.05$) (Tab 1.2). In total, results revealed that the reduction in kernel quantity of TKW and GY was not within the same trend of influence to the investigated factors.

3.1.4.2 Grain yield

Grain yield (GY) of trials of both years are shown in (Tab. 1.2). In the 2014 experiment, neither fungicide application nor inoculation affected the GY of both varieties. In the 2015 experiment, GY of Tobak was strongly affected by treatments and their interactions. The application of fungicide (F+) has protected GY of Tobak significantly under N100.

3.1.4.3 Protein, Raw-protein and Starch contents

Kernels quality expressed as protein (PR), raw-protein (PRP) and starch (ST) contents of harvested kernels from 2015 experiment is shown in (Tab. 3.3). N100 has significantly increased PR and RPR in harvested kernels of Tobak and Pamier (Tab. 3.5 and 3.6). Similar results were found for the treatment with fungicide (Fus).

Table 3.3 Protein, Raw-protein and Starch as affected by the interaction among fungicide application against foliar diseases (F+, F- with or without, respectively), nitrogen levels (N100 standard and N50 half standard) and treatment with fungicide against FHB (Fus+ and Fus-, with or without, respectively) in 2015. (mean, n ≥ 3). Figures with the same letter within the same row are not significantly different (Tukey's HSD: $P \leq 0.05$).

Variety	Indices (%)	N100				N50			
		F+		F-		F+		F-	
		Fus+	Fus-	Fus+	Fus-	Fus+	Fus-	Fus+	Fus-
Tobak	Protein	11.8a	11.6a	11.6a	11.2a	10.2b	10.05b	10.3b	9.9b
	Raw-protein	13.3a	13.1a	13.1a	12.7a	11.7b	11.55b	11.8b	11.4b
	Starch	73.5ab	73.8ab	73.6ab	74.0a	73.5ab	72.92b	73.6ab	73.2ab
Pamier	Protein	13.4ab	13.4ab	13.6a	12.7b	11.5c	11.7c	11.5c	11.4c
	Row-protein	14.9ab	14.9ab	15.1a	14.2b	13.1c	13.2c	13.0c	12.9c
	Starch	73.1bc	73.2bc	72.4c	73.5ab	73.7ab	73.8ab	74.5a	73.9ab

Only on Pamier, a significant interaction among a different combination of treatments was found

except (N×F) (Tab. 3.6). The application of fungicide against FHB (Fus) on Pamier canopy, cultivated under N100 and F+, increased both PR and PRP (Tab. 3.3). The highest content of ST of Tobak was found in treatments without application of fungicides (F and Fus) (Tab. 3.3). However, no significant effect of any of the investigated factors was observed (Tab. 3.5). Starch content in kernels was more sensitive to treatments in Pamier kernels in comparison to that from Tobak, from 72.4 to 74.5 and from 72.9 to 74 for Pamier and Tobak, respectively (Tab. 3.3). In total, a significant effect of N was found in kernels of Pamier, and a significant interaction was proved between N and Fus (Tab. 3.6).

3.1.5 Hyperspectral reflectance

Reflectance spectra of wheat canopies were characteristic for vital wheat canopy (Fig. 3.7). It was affected by the interaction among treatments of fungicide applications (F and Fus) and nitrogen levels (N100 vs. N5) (Fig. 3.7 and 3.8). The reflectance spectra in shortwave infrared (SWIR) beyond 1750 nm was deleted because of the atmospheric humidity which was associated with high variation in reflectance in that range.

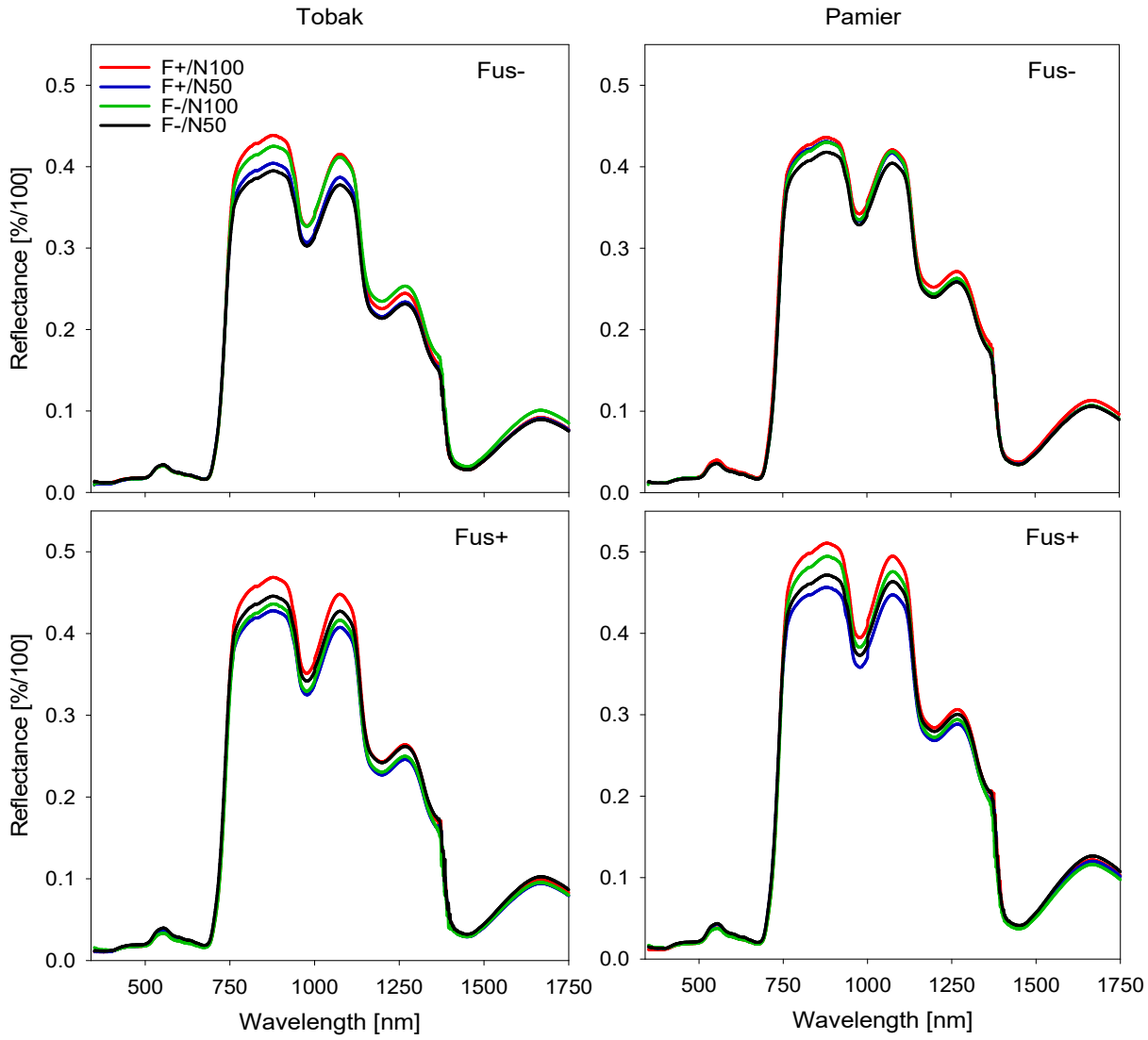

Figure 3.7 Effect of the interaction among fungicide application against foliar diseases (F+, F- with or without, respectively), fungicide application against *Fusarium* head blight (Fus+ and Fus- with or without, respectively) and nitrogen levels (standard nitrogen fertilization, N100 or half, N50) on reflectance spectra of wheat canopy of Tobak and Pamier at growth stages 73. (mean; $n \geq 6$).

In total, the most pronounced differences in reflectance spectra were found beyond the visible range (VIS) starting from 760 nm in the near infrared range (NIR) until 1120 nm in SWIR (Fig. 3.7).

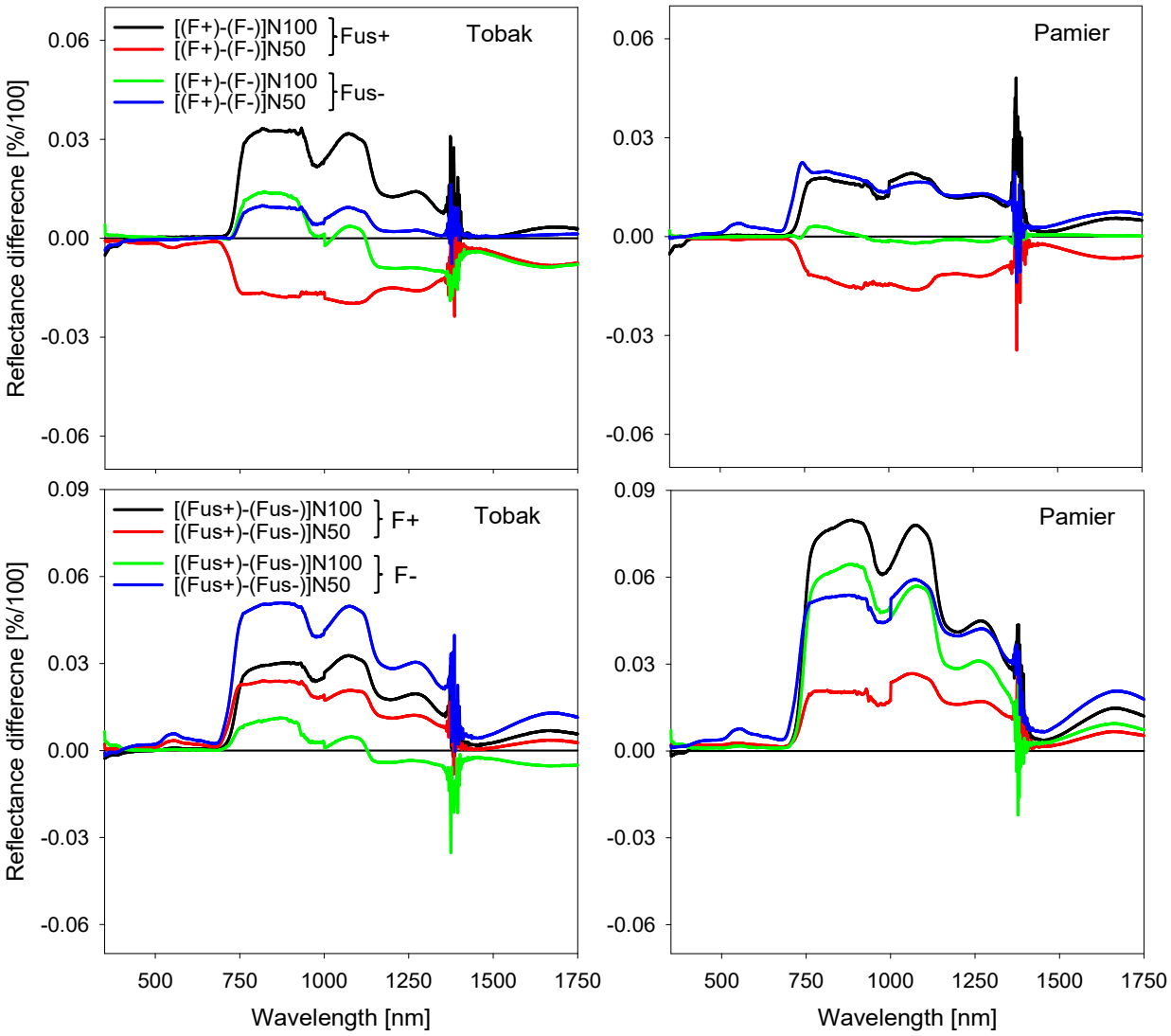

Figure 3.8 Differential reflectance spectra of wheat canopy of Tobak and Pamier varieties treated with fungicide against foliar diseases (F+, F- with or without, respectively) and FHB (Fus+ and Fus- with or without, respectively) under standard nitrogen fertilization (N100) or half (N50), (mean; n ≥ 6). Upper paired: show the effect of Fungicide application against foliar diseases (F), lower paired: show the effect of fungicide to control *Fusarium* head blight (Fus).

Maximum reflectance from different treatments was within the range (0.4-0.5 %/100) in NIR. Canopy with nitrogen level (N50) showed the lowest reflection which was pronounced especially

in the range of 760-920 nm for NIR and 1150-1300 nm for SWIR. Canopies that received fungicide applications (F+) were associated with increased reflection spectra in comparison to non-treated ones (F-), while those that received double fungicide applications (F+/Fus+) showed the highest reflection when the rate of fertilisation was fixed for the comparison (Fig. 3.7).

To better visualise the effect of foliar diseases and their control with fungicides in reflectance spectra of the wheat canopy, reflectance difference (RD) was plotted (Fig. 3.8). Most pronounced changes in RD started from wavelength 750 until 1150. RD showed high variation in measured reflectance in the range 1360-1430 nm. Moreover, it revealed that the application of fungicide (Fus+) was associated with higher reflection over the entire spectrum, except the reflection from Tobak that did not receive the fungicide (F-). The highest RD calculated was from Pamier at standard fertilisation (N100) and fungicide application (Fus+) (Fig. 3.8). In total, reflectance spectra of the wheat canopy were at highest values when it was protected with fungicide (F+ and Fus+) and cultivated under standard fertilisation conditions (N100).

3.1.6 Spectral vegetation indices

Collection of spectral vegetation indices (SVIs) related to various physiological plant parameters was calculated from reflectance spectra of each treatment (Tab. 3.4). NDVI was significantly affected by nitrogen deficiency in canopies of both varieties (Tab. 3.5 and 3.6). The highest values of NDVI was obtained when plants were grown under standard nitrogen conditions (N100) and double fungicide applications (F+ and Fus+). However, lower NDVI values were obtained when the canopy was not properly maintained (N50 and F-/Fus-) (Tab. 3.4).

PRI values were close to zero and were significantly influenced by nitrogen levels, only in Pamier canopies, a significant interaction was found between the two applications of fungicides (F and Fus) (Tab. 3.5 and 3.6). Among indices that assess the chlorophyll content, PSSRa, PSSRb and PSSRc, the standard healthy and fertilised canopy was associated with the highest values of PSSRa, PSSRb and PSSRc (Tab. 3.4). Among investigated factors, only N levels affected these indices significantly in both varieties. Moreover, fungicide application against foliar diseases (F) had a significant impact only in PSSRa and PSSRc on Tobak (Tab. 3.5).

Table 3.4 Effect of the interaction among nitrogen levels (N100 standard and N50 half standard), treatment with fungicide against foliar diseases (F+, F- with or without, respectively) and treatment with fungicide against FHB (Fus+ and Fus-, with or without, respectively) on: normalised difference vegetative index (NDVI), photochemical reflectance index (PRI), pigment specific simple ratio (PSSRa, b and c), plant senescence reflection index (PSRI), blue-green index 2 (BGI2) and water indices (WI1, 2, 3 and 4). The study was run on two winter wheat varieties Tobak and Pamier in 2015. (mean, n ≥ 6). Figures with the same letter within the same line are not significantly different (Tukey's HSD: $P \leq 0.05$).

Variety	Index	N100				N50			
		F+		F-		F+		F-	
		Fus+	Fus-	Fus+	Fus-	Fus+	Fus-	Fus+	Fus-
Tobak	NDVI	0.93a	0.93a	0.93a	0.92a	0.92a	0.91a	0.92a	0.91a
	PRI	-0.03ab	0.00a	0.00a	0.00a	-0.01c	-0.01c	-0.01bc	-0.01bc
	PSSRa	26.17a	26.52a	27.03a	24.87ab	23.01b	21.78b	24.09ab	21.62b
	PSSRb	21.82a	21.04ab	20.76abc	20.14abc	18.07bc	17.39c	17.30c	17.22c
	PSSRc	26.26a	24.65ab	24.82ab	23.23ab	23.61ab	22.57ab	22.62ab	21.47b
	PSRI	0.00a	-0.01a	0.00a	-0.01a	0.00a	0.00a	0.00a	0.00a
	BGI2	0.51abc	0.52a	0.51ab	0.52a	0.47d	0.47cd	0.47d	0.49bcd
	WI1	1.32ab	1.33a	1.31ab	1.30ab	1.30ab	1.29ab	1.29b	1.28b
	WI2	0.65a	0.65a	0.64a	0.62a	0.64a	0.62a	0.62a	0.62a
	WI3	0.29a	0.30a	0.28a	0.27a	0.28a	0.27a	0.27a	0.27a
	WI4	0.30ab	0.30a	0.29ab	0.28ab	0.28ab	0.28ab	0.28ab	0.27b
Pamier	NDVI	0.93a	0.92abc	0.93ab	0.92abc	0.91cb	0.92abc	0.91abc	0.92c
	PRI	-0.01ab	-0.01ab	-0.01ab	0.00a	-0.01ab	-0.01b	-0.01ab	-0.01b
	PSSRa	26.41a	25.57ab	26.92a	24.60ab	21.66b	22.62b	21.97b	22.34b
	PSSRb	20.97a	19.99abc	20.59a	20.19ab	17.07bc	17.49bc	17.08c	17.30bc
	PSSRc	25.98a	24.65ab	25.30ab	24.42ab	22.11b	23.51ab	21.89b	22.61ab
	PSRI	0.00a	0.00a	0.00a	0.00a	0.00a	0.00a	0.00a	0.00a
	BGI2	0.49ab	0.49a	0.49a	0.50a	0.46bcd	0.44d	0.47bc	0.45cd
	WI1	1.28ab	1.29a	1.28ab	1.27abc	1.26bc	1.26bc	1.25c	1.25c
	WI2	0.61ab	0.61ab	0.62a	0.59ab	0.58ab	0.58ab	0.57b	0.58ab
	WI3	0.26ab	0.26a	0.26a	0.24ab	0.23b	0.24ab	0.23b	0.24ab
	WI4	0.27a	0.27a	0.27a	0.26ab	0.25ab	0.25ab	0.25b	0.25b

Table 3.5 Three-way ANOVA showing the effect of the nitrogen levels (N), fungicide against foliar diseases (F) and fungicide against *Fusarium* head blight (Fus) of the variety Tobak. Test was carried out on *Fusarium* head blight visually assessed (FHB), the variables: foliar diseases (expressed as area under disease progress curves AUDPC and foliar diseased area at GS 83 on flag leaves, FDF), indices of kernels quality (raw-protein: RPR, protein: PR and starch ST), thousand kernel weight (TKW), grain yields (GY) and spectral indices: normalised difference vegetative index (NDVI), photochemical reflectance index (PRI), pigment specific simple ratio (PSSRa, b and c), plant senescence index (PSRI), blue-green index 2 (BGI2) and water indices (WI1, 2, 3 and 4). For FHB and NDVI, (data + 1) were log-transformed. F values including the level of significance (* $P \leq 0.5$, ** $P \leq 0.05$) are presented in the remaining columns. (mean, $n \geq 3$).

Variables	**Factors**						
	Nitrogen levels (N)	**Fungicide against foliar diseases (F)**	**Fungicide against FHB (Fus)**	**N× F**	**N× Fus**	**F× Fus**	**N× F× Fus**
FHB	2.57	40.35**	6.83*	1.92	0.10	5.28*	0.01
AUDPC	2.58	8.54*	1.83	0.008**	0.033	8.32*	0.023
FDF	0.26	5.68*	3.46	0.33	0.050	12.7**	1.40
TKW	15.27**	7.01*	11.08*	4.35	4.46	2.60	4.75*
GY	353.94**	91.46**	80.73**	5.92*	26.82*	3.62**	16.18**
PR	160.54**	4.54	17.21**	0.61	0.01	0.11	0.013
RPR	160.54**	4.54	17.21**	0.61	0.01	0.11	0.013
ST	2.03	0.94	0.20	0.20	3.53	0.27	0.00
NDVI	22.33**	0.29	0.01	0.29	0.15	0.01	0.01
PRI	6.28E+32**	0.00	0.00	0.00	0.00	0.00	0.00
PSSRa	21.46**	0.024	9.06*	0.22	0.40	0.26	0.27
PSSRb	30.26**	2.32	3.31	0.41	0.42	1.83	1.00
PSSRc	12.78**	4.32	6.32*	0.53	.21	1.15	0.83
PSRI	1.77	0.44	3.99	0.00	1.77	0.44	0.00
BGI2	38.82**	0.22	5.60*	2.24	0.01	0.22	1.05
WI1	8.33*	7.11*	3.19	0.01	.33	0.27	3
WI2	1.05	2.77	4.74*	0.07	0.07	1.33	2.36
WI3	1.50	4.71*	3.37	0.01	0.20	0.69	2.43
WI4	7.77*	7.28*	8.27*	0.02	0.44	0.71	3.96

Table 3.6 Three-way ANOVA showing the effect of the nitrogen levels (N), fungicide against foliar diseases (F) and fungicide against *Fusarium* head blight at anthesis (Fus) on different parameters of the variety Pamier. *Fusarium* head blight (FHB), foliar diseases (expressed as area under disease progress curves AUDPC and foliar diseased area at GS 83, FDF), indices of kernels quality (raw-protein: RPR, protein: PR and starch ST), thousand kernel weight (TKW), grain yields (Yield) and spectral indices: normalised difference vegetative index (NDVI), photochemical reflectance index (PRI), pigment specific simple ratio (PSSRa, b and c), blue-green index 2 (BGI2) and water indices (WI1, 2, 3 and 4). For FHB and NDVI, (data + 1) were ln-transformed. (- test was not performed; values were 0). F values including the level of significance (* $P \leq 0.5$, ** $P \leq 0.05$) are presented in the remaining columns. (mean, n ≥ 3).

Variables	**Factors**						
	Nitrogen levels (N)	**Fungicide against foliar diseases (F)**	**Fungicide against FHB (Fus)**	**N× F**	**N× Fus**	**F× Fus**	**N× F× Fus**
FHB	2.99	3.42	0.47	2.58	0.196	0.32	0.10
AUDPC	21.72**	115.27**	48.28**	36.50**	1.93	35.30**	1.93
FDF	23.2**	90.71**	46.04**	28.53**	4.03	40.79**	4.03
TKW	2.70	4.86*	5.97*	7.85*	0.07	6.72*	0.07
GY	220.68**	8.74**	1.32	3.45	1.62	5.24*	1.62
PR	244.19**	2.8	4.49*	0.20	6.03*	5.49*	6.0*
RPR	244.19**	2.8	4.49*	0.20	6.03*	5.49*	6.03*
ST	33.34**	0.45	0.96	3.41	6.52*	0.26	6.52*
NDVI	25.41**	0.60	0.00	0.00	0.00	7.37*	0.00
PRI	6.43*	0.71	0.71	0.71	6.43*	0.71	6.43
PSSRa	41.38**	0.08	1.01	0.06	4.17	0.60	4.17
PSSRb	51.17**	0.08	0.19	0.02	1.63	0.09	1.63
PSSRc	21.29**	0.95	0.01	0.01	4.21	0.00	4.21
PSRI	-	-	-	-	-	-	-
BGI2	95.50**	4.67*	2.71	0.04	10.17**	0.09	10.17**
WI1	34.34**	7.14	0.02	0.63	4.21	0.00	4.21
WI2	17.05**	0.68	0.004	0.04	2.13	0.10	2.13
WI3	24.09**	0.92	0.21	0.00	2.46	3.14	2.46
WI4	36.99**	3.05	0.17	0.00	0.44	0.61	0.44

PSRI was not affected by any of investigated treatments (one-way ANOVA, $P \leq 0.05$), but a significant effect of N levels was found (three-way ANOVA, $P \leq 0.05$). The application of fungicide against FHB (Fus+) affected BGI2 on Tobak canopy whereas the application of fungicide against foliar diseases (F+) had a significant effect on Pamier canopy. The canopy of Pamier showed interaction among treatments (N×F and N×F×Fus) regarding BGI2.

Water indices which reveal water content of canopy (WI1, 2, 3 and 4) from Pamier canopy were significantly affected by only nitrogen levels. On Tobak canopy, WI1 and WI2 were significantly affected by N levels. Water indices of Tobak canopy showed higher variations in comparison to that of Pamier (Tab. 3.5).

3.1.7 Correlation matrix

Correlation matrix among the FHB incidence, foliar wheat diseases, the frequency of infected kernels and leaves, indices of kernels quality and quantity and spectral vegetative indices (SVIs) are presented in (Tab. 3.7). Visually assessed FHB was significantly correlated to foliar wheat diseases (AUDPC and FDF, r = 0.6 and 0.5), leaf infection (expressed as FIL, r = 0.4) and it was correlated as well to grain yield (r = 0.3). Among investigated SVIs, PRI and BGI2 were positively correlated to FHB (r = 0.4).

Foliar diseases (AUDPC) were associated with a higher infection of leaves by *Fusarium* spp. The infection of flag leaves with foliar pathogens was negatively correlated with TKW (r = -0.4). The only significant correlation to infected kernels rate (FIK) was to PSSRa (r = -0.3). The water content of canopy was according to water indices significantly correlated to TKW (r = 0.5) in addition to Protein content indices (r = 0.6).

Grain yield was significantly correlated to all investigated SVIs but has no relationship to any of the other parameters. Protein indices were significantly correlated with pigment specific simple ratios ($r \geq 0.6$). In total, all SVIs were significantly correlated with each other with exception to PSRI which showed lower significant correlations to the others (Tab. 3.7).

Table 3.7 Correlation matrix expressed as (r) among *Fusarium* head blight visually assessed (FHB), the severity of foliar diseases (expressed as area under disease progress curves AUDPC and foliar diseased area at GS 83 on flag leaves, FDF), frequency of infected kernels and leaves (FIK and FIL, respectively), indices of kernels quality (raw-protein: RPR, protein: PR and starch: ST), thousand kernel weight (TKW), grain yields (GY) and spectral indices: normalised difference vegetative index (NDVI), photochemical reflectance index (PRI), pigment specific simple ratio (PSSRa, b and c), plant senescence reflection index (PSRI), blue-green index 2 (BGI2) and water indices (WI1, 2, 3 and 4). Data are a combination of all observations from two wheat varieties (Tobak and Pamier). (field experiment 2015, n = 56 pairs, Pearson method).

Correlation is significant at the 0.01 level (2-tailed)

	FHB	AUDPC	FDF	FIL	FIK	TKW	GY	RPR	PR	ST	NDVI	PRI	PSSRa	PSSRb	PSSRc	PSRI	BGI2	WI1	WI2	WI3	WI4
FHB	1.0																				
AUDPC	.6	1.0																			
FDF	.5	.9	1.0																		
FIL	.4	.4	.3	1.0																	
FIK	.1	.2	.2	.1	1.0																
TKW	0	-.2	-.4	-.1	-.1	1.0															
GY	.3	0	-.1	0	-.1	.5	1.0														
RPR	-.2	-.2	0	-.1	-.1	-.6	0	1.0													
PR	-.2	-.2	0	-.1	-.2	-.6	0	1	1.0												
ST	-.1	.2	0	.1	.2	-.1	-.2	-.2	-.2	1.0											
NDVI	.1	.1	.1	.1	-.1	-.2	.4	.6	.6	-.1	1.0										
PRI	.4	.3	.2	.2	-.1	-.1	.5	.2	.2	.1	.5	1.0									
PSSRa	.1	0	0	.1	-.3	-.1	.5	.6	.6	-.1	.7	.5	1.0								
PSSRb	.1	.1	.1	.1	-.1	-.1	.6	.9	.6	-.2	.9	.6	.8	1.0							
PSSRc	-.1	0	0	0	-.1	-.2	.4	.6	.6	-.2	.9	.3	.7	.9	1.0						
PSRI	-.3	-.1	0	-.1	.1	-.1	-.4	.1	.1	-.2	-.1	-.4	-.2	-.2	0	1.0					
BGI2	.4	.2	.2	.2	-.1	.1	.7	.2	.2	-.1	.4	.8	.6	.6	.2	-.6	1.0				
WI1	.1	-.1	-.2	0	-.1	.5	.9	0	0	-.2	.5	.5	.6	.6	.5	-.4	.6	1.0			
WI2	.2	0	0	.1	-.1	.5	.8	-.1	-.1	-.2	.5	.4	.5	.6	.5	-.3	.5	.9	1.0		
WI3	.2	0	-.1	0	-.1	.5	.8	-.1	-.1	-.2	.4	.4	.4	.6	.5	-.3	.6	.9	1	1.0	
WI4	.2	0	-.1	0	-.1	.5	.9	0	0	-.2	.5	.5	.6	.7	.5	-.3	.6	1	1	1	1.0

3.2 Impact of primary infection site of *Fusarium* species on head blight development

3.2.1 Infection development on glumes

The infected spikelets tissues (glume and lemma) were investigated microscopically 10 dai (Fig. 3.9). The infection was proved under a light microscope, and the hyphae of *F. graminearum* were visible intercellular and on the surface of lemma to the inner side of florets where kernels develop at 10 dai. Before necrotic lesions become visible in the infected glume (5-10 mm distance from the visible necrotic lesion in the same glume), the section in this area showed the destruction of cell walls (Fig. 3.9 P).

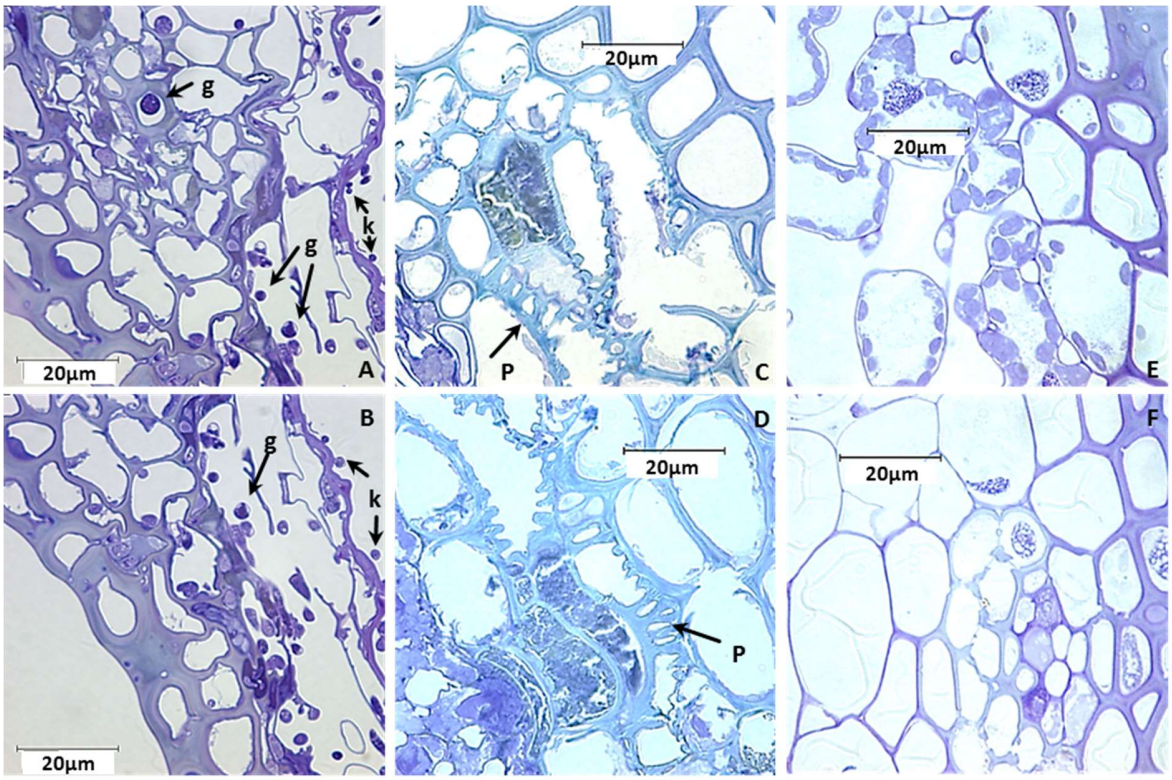

Figure 3.9 Sections of spikelet tissues infected with *F. graminearum* (lemma A and B; glume C and D) and non-infected ones (glume E and F) observed by bright light microscopy 10 dai. g, hyphae developed in the intercellular of lemma; k Hyphae on the surface of lemma to the inner side of florets where kernels develop. p; destruction of cell walls of glume infected with *F. graminearum* before necrosis become visible in the position of the section. Ears were inoculated at GS 61-65.

3.2.2 Disease incidence

FHB incidence, the percentage of symptomatic ears observed 6 dai of cv. Passat was 62.03% for inoculated ears with *F. graminearum* after combining the four inoculation scenarios. Inoculated ears with *F. culmorum* showed 74.12% FHB incidence with no significant difference at that assessment date between *Fusarium* spp. (Fig. 3.10). Disease incidence increased sharply after inoculation by *Fusarium* spp. until 11-13 dai, at this time range almost the asymptotic stage of disease incidence was reached and no further symptomatic infected ears were observed. The average number of infected ears with *Fusarium graminearum* was higher than that of *F. culmorum*, at 30 dai 98.21% versus 94.67%, with no significant difference between *Fusarium* spp. Over time, the development of disease incidence increased significantly when FHB incidence at 6 dai was compared to that at the asymptotic stage (Fig. 3.10).

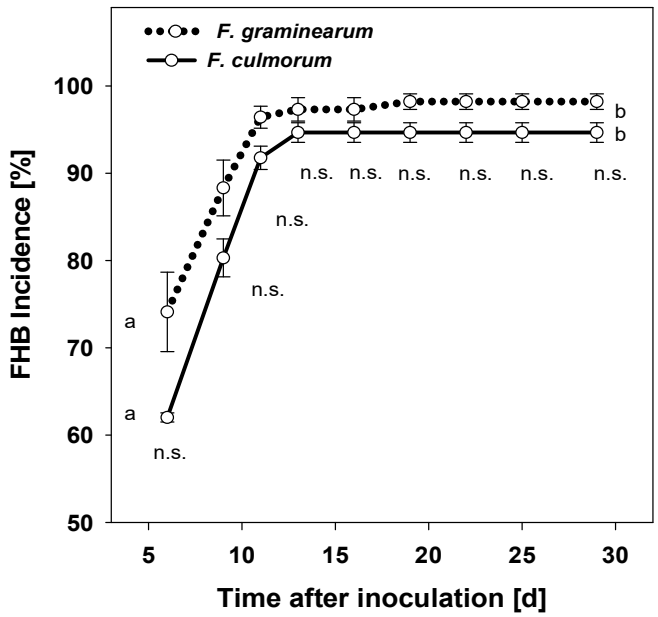

Figure 3.10 Progress curves of *Fusarium* head blight incidence due to *F. graminearum* (dotted line) and *F. culmorum* (solid line) measured as the average proportion of symptomatic ears out of inoculated ones following spray, tip, centre and base inoculation combined for each *Fusarium* spp. Ears were inoculated at GS 61-65. Different letters at the same line differ significantly according to Tukey's HSD, n.s., not significantly different, $P \leq 0.05$ (mean ± SE: $n \geq 108$).

3.2.3 Disease severity

The disease severity of FHB (FHB index) of both *Fusarium* species under 18/12°C developed in curves similar to those from the monomolecular functions of monocyclic diseases (Fig. 3.11).

The FHB indices calculated over all inoculation scenarios were very similar for both species with no significant differences in the assessment dates. At the last assessment date (34 dai, GS 83-85), the maximum disease severity was 68.08% and 72.56% for the infection with *F. graminearum* and *F. culmorum*, respectively (Fig. 3.11).

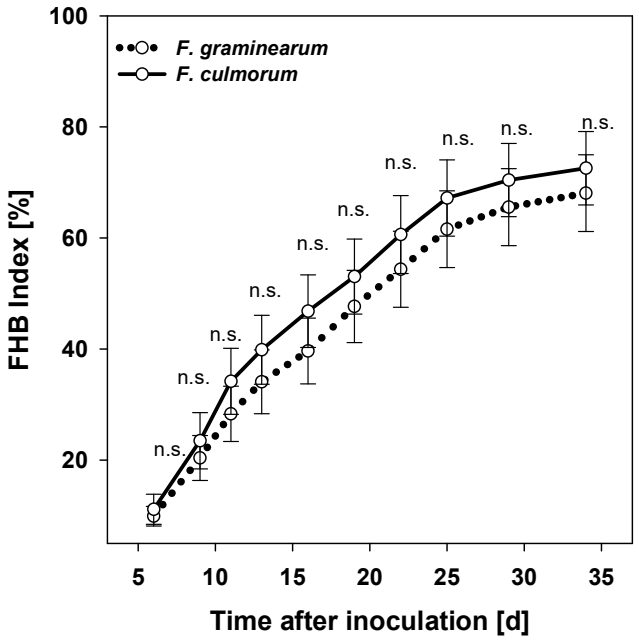

Figure 3.11 Progress curves of *Fusarium* head blight incidence due to *F. graminearum* (dotted line) and *F. culmorum* (solid line) measured as the average proportion of symptomatic spikelets per ear (FHB index) following spray, tip, centre and base inoculation combined for each *Fusarium* spp. Ears were inoculated at GS 61-65. Different letters at the same line differ significantly according to Tukey's HSD, n.s., not significantly different, $P \leq 0.05$ (mean ± SE: $n \geq 80$).

Disease severity of FHB depending on the primary site of ear infection showed differences between *Fusarium* species (Fig. 3.12) which were absent after combining the inoculation scenarios and considering only the *Fusarium* spp. (Fig. 3.12). These differences were most pronounced after inoculation with *F. culmorum* starting at 11 dai. Tip inoculation resulted in the lowest disease severity compared to the others. Spray inoculation resulted in the highest disease severity, significantly higher than that after tip inoculation when AUDPC was considered (Tab. 3.8). Centre and base inoculations led to the middle class of diseases severity in most of the assessment dates. Spray inoculation with both *Fusarium* species caused the maximum disease severity 77.30% and 90.68% for *F. graminearum* and *F. culmorum*, respectively.

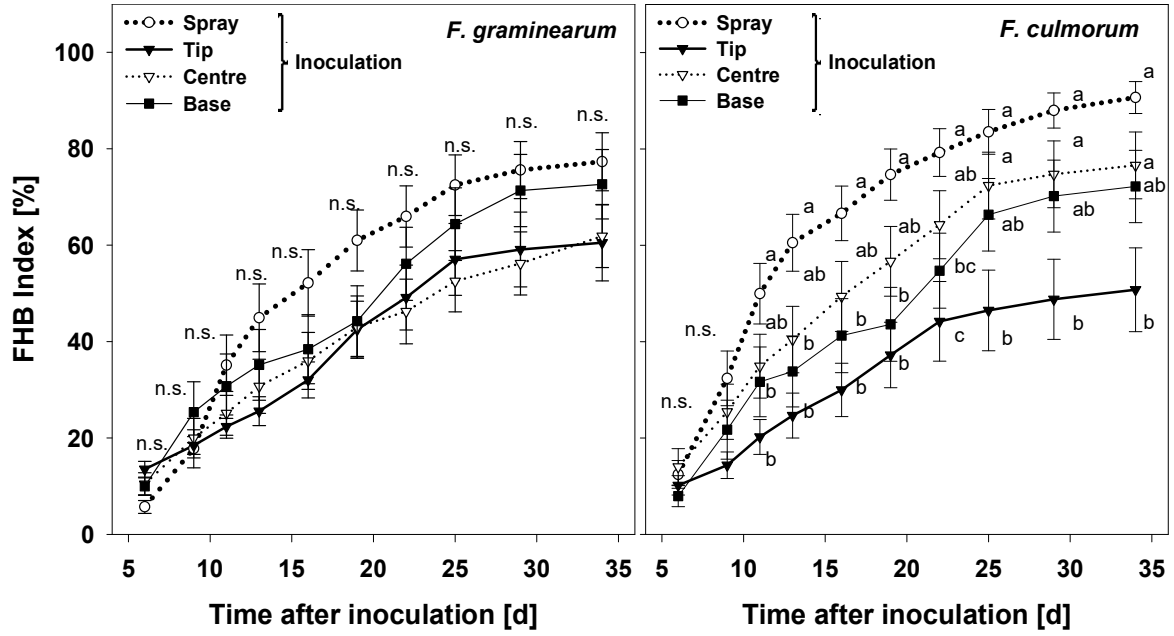

Figure 3.12 Progress curves of *Fusarium* head blight due to *F. graminearum* (left) and *F. culmorum* (right) in wheat ears after spray, tip, centre and base inoculation of ears measured as the average proportion of symptomatic spikelets per ear (FHB index). Ears were inoculated at GS 61-65. Different letters at the same date differ significantly according to Tukey's HSD, n.s., not significantly different. $P \leq 0.05$ (mean ± SE: n = 11-13).

Table 3.8 Effect of spray, tip, centre and base inoculation of individual wheat ears with *Fusarium graminearum* and *F. culmorum* on the area under disease progress curve of FHB (AUDPC 28 days, % days, n = 11-13). Ears were inoculated at GS 61-65.

***Fusarium* species**	**Inoculation scenario**			
	Spray	**Tip**	**Centre**	**Base**
F. graminearum	1559.52	1162.90	1159.57	1371.96
F. culmorum	1927.53*	996.79	1547.62*	1361.54
Overall mean	1743.53 a	1079.85b	1353.60b	1366.75b

* Significant difference between *Fusarium* species within infection scenario (*t*-test; $P \leq 0.05$).
ab Figures with the same letter are not significantly different (Tukey's HSD; $P \leq 0.05$).

Base and centre inoculations caused AUDPCs not significantly different from that after tip and spray inoculation. AUDPC values demonstrated that the aggressiveness of *F. culmorum* was higher than that of *F. graminearum* after centre inoculation (Tab. 3.8).

3.2.4 *Fusarium* infection on flag leaves

The infection of *F. graminearum* on ears developed to stems and flag leaves in different degrees according to the primary site of ears infection. This colonisation was observed at minimal for tip infection, the only infection scenario that did not reduce chlorophyll content of flag leaves compared to control at 24 dai. At this time point of assessment, the flag leaves of ears after spray- and base-inoculation were thoroughly dried.

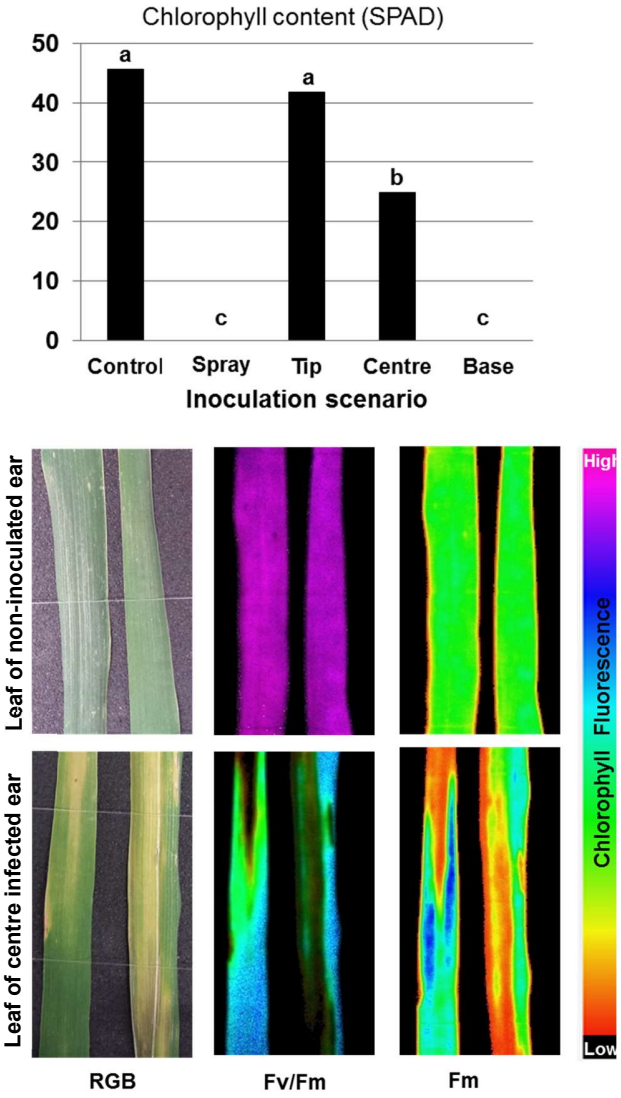

Figure 3.13 Effect of primary site of *F. graminearum* infection of wheat ears on chlorophyll content (up) after spray, tip, centre and base inoculation and on chlorophyll fluorescence (down) of flag leaves after centre inoculation at 24 dai. Fv/Fm: the maximum quantum yield of photosystem II and Fm: maximum chlorophyll fluorescence. Ears were inoculated at GS 61-65. Columns with the same letter are not significantly different (Tukey HSD test, $P \leq 0.05$).

The effect of *Fusarium* infection development downward was better visualised using the Chlorophyll Fluorescence Imaging (Fig. 3.13). The false-color images of Fv/Fm, maximum quantum yield of photosystem II, and Fm, maximum chlorophyll fluorescence, showed very clearly the reduction in the photosynthesis activities of infected leaves compared to that of non-inoculated control. The extended growth stages of wheat at 18/12°C allowed *Fusarium* species to grow downward and to infect leaves.

3.2.5 Distribution of *Fusarium*-infected kernels within ears

The distribution of infected kernels after spray inoculation revealed the tendency of *Fusarium* infection to move downward better than upward (Fig. 3.14).

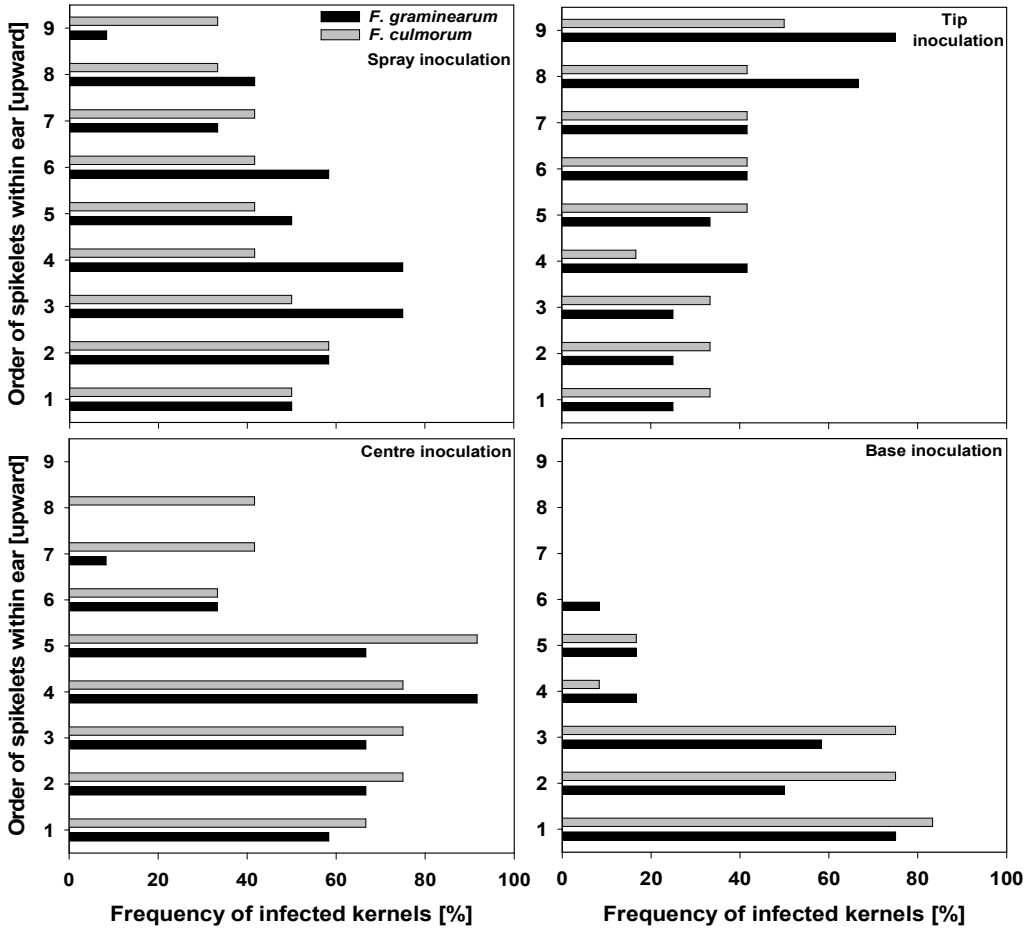

Figure 3.14 Effect of the primary site of *Fusarium* infection of wheat ears and *Fusarium* species on the spatial distribution of infected kernels at harvest. Ears had been inoculated with *F. graminearum* and *F. culmorum*, respectively, by spraying, tip only, centre only, and base only at GS 61-65 (n = 12).

Re-isolation of the pathogens at harvest from different spikelet levels (labelled from 1 to 9 upwards) of infected ears showed gradients of infected kernels across single ears (Fig. 3.14). After base inoculation, the frequency of infected kernels from the spikelets above decreased sharply, and no pathogen was detected at the uppermost three spikelet levels of the ear. After tip inoculation, in contrast, the re-isolation rate decreased rather slowly on the lower spikelet levels resulting in more than 25% infected kernels on the lowest spikelet level at the ear's base.

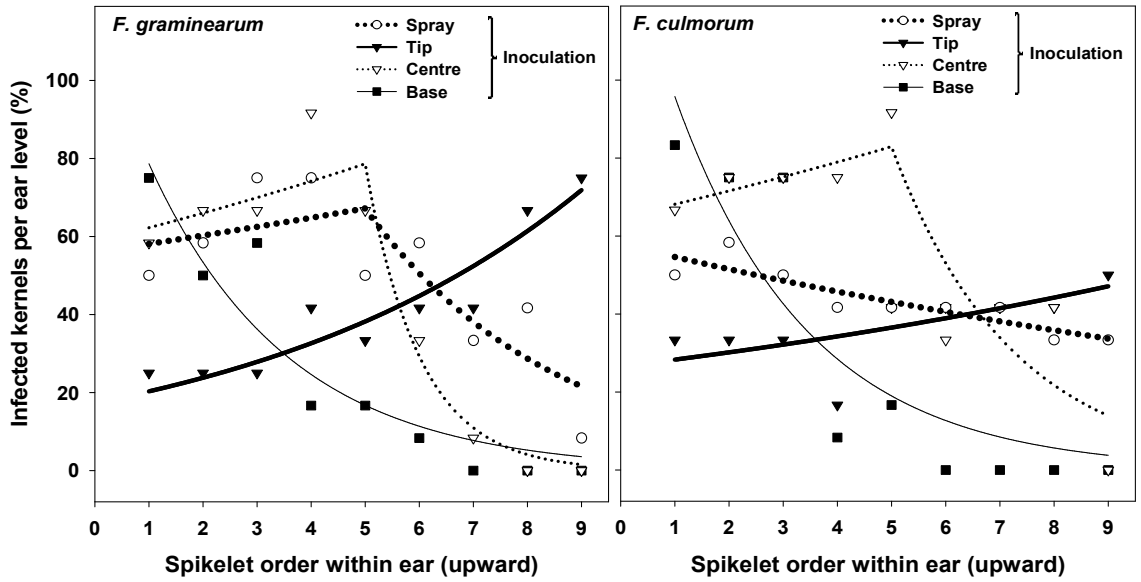

Figure 3.15 Effect of the primary site of *Fusarium* inoculation of wheat ears and *Fusarium* species on the gradients of infected kernels within ears at harvest. Ears had been inoculated with *F. graminearum* and *F. culmorum*, respectively, by spraying, tip only, centre only, and base only at GS 61-65. Dotes stand for the observations, Lines represent the estimation following equations 8, 9 and 10 for the base, tip and centre inoculations, respectively. Equations 10 was fitted to the observation of spray inoculation as well, (n = 12).

Both *Fusarium* spp. were able to spread within ears downwards better than upwards. This effect became evident also after centre inoculation. The frequency of infected kernels from spikelets 4 to 1 was only slightly lower than at the point of inoculation (spikelet 5), but re-isolations decreased considerably from spikelet levels 5 to 9, especially for *F. graminearum.*

After spray inoculation, the frequency of infected kernels at the top was lower than that at the ear base. Only this treatment demonstrated a significant difference between *Fusarium* species; *F. graminearum* resulted in a higher frequency of infected kernels (Fig. 3.14). Centre and spray

inoculation resulted in higher frequencies of infected kernels compared to the base and tip inoculations with no significant difference within these pairs.

Table 3.9 Estimated parameter values of the exponential model (equations 8, 9 and 10) simulating the gradients of the frequency of infected kernels within single ears following spray, tip, centre and base inoculation with *F. graminearum* and *F. culmorum*. Parameter *a* simulates the frequency of infected kernels at the point of inoculation. *b* and *c* describe the slopes of the gradients in up- and downward direction from the inoculation point. (n = 12).

	Parameter	Inoculation scenario			
		Spray	**Tip**	**Centre**	**Base**
F. graminearum	*a*	67.2 ± 9.7**	71.9 ± 5.0	78.6 ± 7.4	78.7 ± 8.8
	b	0.28 ± 0.11	-	0.98 ± 0.25	0.39 ± 0.07
	c	0.04 ± 0.06*	0.16 ± 0.02	0.06 ± 0.04*	-
	R^2	0.70	0.89	0.94	0.89
F. culmorum	*a*	43.1 ± 2.8	47.1 ± 5.1	82.9 ± 10.6	95.9 ± 15.3
	b	0.06 ± 0.03*	-	0.45 ± 0.13	0.41 ± 0.11
	c	-0.06 ± 0.03*	0.06 ± 0.03	0.05 ± 0.06*	-
	R^2	0.79	0.44	0.82	0.82

* Value not significantly different from 0.
** Estimated parameter value ± standard error

The gradients of infected kernels rate following different primary site of ear inoculation with *F. graminearum* and *F. culmorum* is shown in Fig. 3.15. The base inoculation resulted in steep upward gradients which could be reasonably described by equation 8 for both *Fusarium* species (R^2 = 0.89 and 0.82 for *F. graminearum* and *F. culmorum*, respectively) with very similar values for slope *b* (0.39 and 0.41, respectively) (Tab. 3.9). After tip inoculation, the gradients were shallower. Equation 9 showed a high goodness of fit to the frequency of infected kernels for *F. graminearum* (R^2 = 0.89 compared to 0.44 for *F. culmorum*). The values of slope parameter *c* (in downward direction) were 0.16 and 0.06, respectively, distinctly lower than those for upward direction. After centre inoculation, the pathogens spread upwards and downwards from the point of inoculation, but with a bias downwards for both *Fusarium* species. According to the simulation of equation 10, the gradients upwards (*b* values) were considerably steeper (0.98 and 0.45) than

downwards (c values, 0.06 and 0.05) for *F. graminearum* and *F. culmorum*, respectively. The c-values were not significantly different from 0 indicating that the frequency of infected kernels of the lower levels was constant. The application of equation 10 to the infection rates after spray inoculation also revealed that only the slope of the upward gradient for *F. graminearum* was significantly different from 0. In all other cases, the frequency of infected kernels could be considered as constant.

3.2.6 Effect of FHB on ear weight

Both *Fusarium* species caused a significant reduction in ears weight (EW) as an indicator of grain loss due to FHB in comparison to non-inoculated control ears (Fig. 3.16).

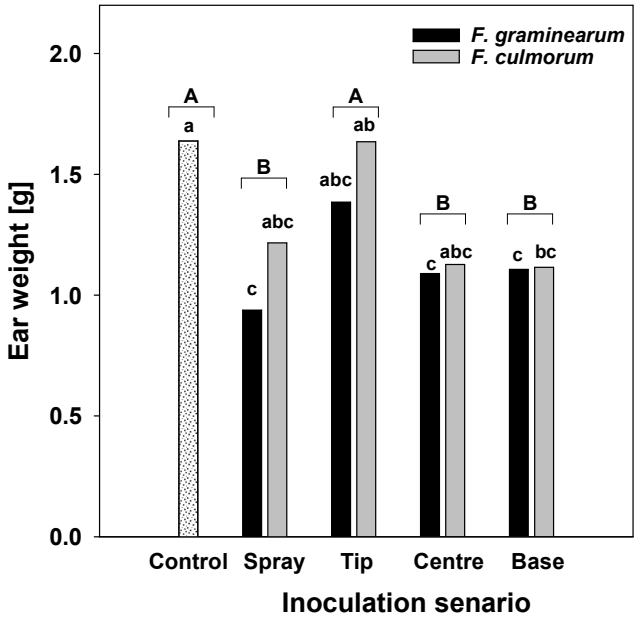

Figure 3.16 Effect of the primary site of *Fusarium* infection of wheat ears on the ears weight as an indicator of grain mass loss at harvest. Ears had been inoculated with *F. graminearum* and *F. culmorum*, respectively, by spraying, tip only, centre only, and base only at GS 61-65 in comparison to non-inoculated control. Different small letters show significant differences according to Tukey's HSD (One-way ANOVA), different capital letters according to Tukey's HSD (univariate test) $P \leq 0.05$, (n = 23).

Fusarium graminearum caused a higher reduction in EW compared to that of *F. culmorum* with no interaction between *Fusarium* spp. and inoculation methods. However, no significant difference between *Fusarium* species in reducing EW was found. FHB after tip inoculation was the only

scenario that did not reduce EW in comparison to non-inoculated control when both pathogens were considered (Fig. 3.16).

3.2.7 Effect of FHB on kernel weight

Both *Fusarium* species caused a significant reduction in thousand kernel weight as compared to non-inoculated control ears. Spray inoculation with *F. graminearum* caused the highest reduction in TKW (43.4%), (Tab. 3.10). *F. graminearum* was more aggressive than *F. culmorum* after the spray and tip inoculation and reduced TKW significantly stronger. Tip inoculation was the only scenario that did not reduce TKW. After spray inoculation, FHB caused significant higher TKW reductions compared to centre inoculation but was not significantly different from that after base inoculation.

Table 3.10 Effect of spray, tip, centre and base inoculation of wheat ears with *F. graminearum* and *F. culmorum* on thousand kernel weight in g (n = 4). Ears were inoculated at GS 61-65.

***Fusarium* species**	**Non-inoculated control**	**Inoculation scenarios**			
		Spray	**Tip**	**Centre**	**Base**
F. graminearum		21.3	36.0	27.1	26.3
F. culmorum		24.7*	39.3*	26.1	24.8
Overall mean	38.0 a	23.0 c	37.6 a	26.6 b	25.5 bc

* Significant difference between *Fusarium* species within infection scenario (*t*-test; $P \leq 0.05$).
abc Figures with the same letter are not significantly different (Tukey's HSD; $P \leq 0.05$).

3.3 Characterising the impact of environmental conditions on *Fusarium* head blight development within ears

3.3.1 Incidence curves

The disease incidence depended on both, the different environmental conditions and the *Fusarium* species, *F. graminearum* and *F. culmorum* (Fig. 3.17). Observations, which are a combination of all FHB incidences after spray, tip, centre and base inoculations, developed sharply until around 10 dai before reaching the asymptotic stage. 37-74% of inoculated ears showed symptoms on 6 dai at 18/12°C, showing a higher rate if developed under wet conditions. This rate was lower, 16-68%, on ears developed under higher temperatures, 24/18°C, 5-6 dai. At the asymptotic stage, *Fusarium* spp. caused incidences from 70-87%.

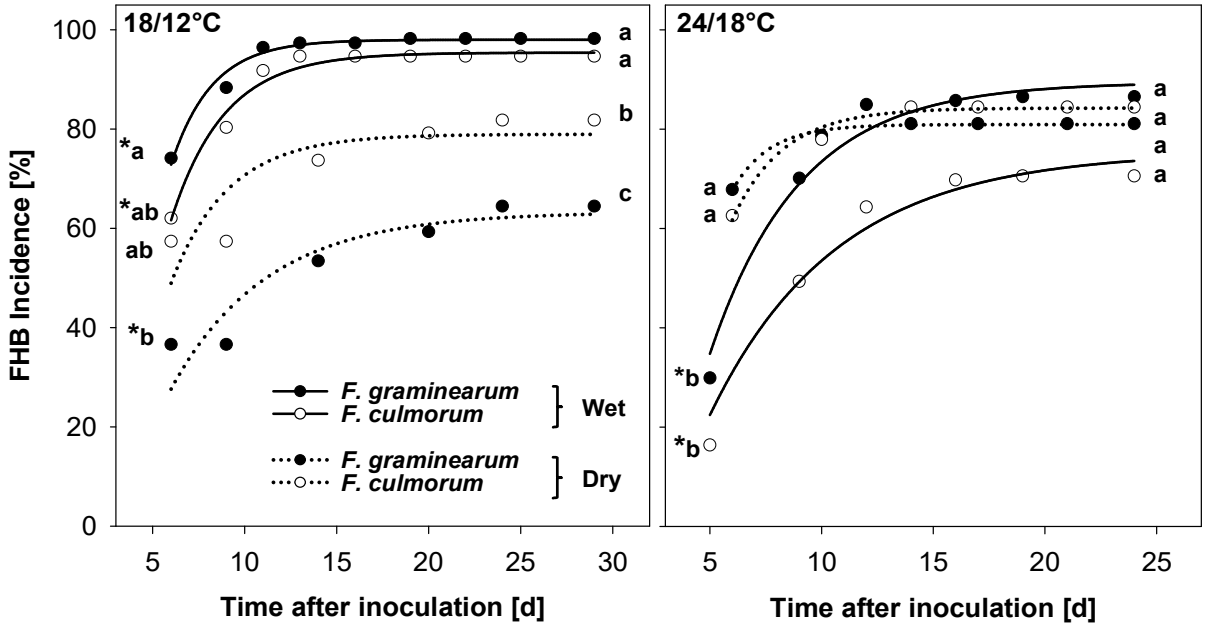

Figure 3.17 Progression of *Fusarium* head blight (FHB) incidence due to *F. graminearum* and *F. culmorum* infection in wheat ears after combining observation from spray, tip, centre and base inoculations for each *Fusarium* spp. Dots stand for observations and lines are simulations based on the monomolecular model (equation 6). Infections were developed at two temperature regimes (18/12 vs. 24/18°C day/night) with or without short-term spells of moisture (wet or dry, respectively). The same letter denotes no significant difference at the same time point of assessment (Tukey HSD test, $P \leq 0.05$). Asterisk denotes significant difference between the first and last incidence rate of the same curve (*t*-test, $P \leq 0.05$). Ears were inoculated at GS 61-65, ($n \geq 90$).

These were not significantly different from each other, whether or not short-term spells of moisture were applied at 24/18°C. However, the differences were more pronounced at 18/12°C, with 64-98%, whereas the wet conditions were associated with the highest disease incidence observed, for both *F. graminearum* and *F. culmorum*. Under both temperature regimes, short-term spells of moisture increased the FHB incidence significantly. Differences in disease incidences between *Fusarium* spp. were most pronounced at 18/12°C, at dry conditions, whereas *F. culmorum* caused significantly higher incidences than *F. graminearum* (Fig. 3.17).

Table 3.11 Estimated parameter values of the monomolecular model (equation 6) describing the incidence of *Fusarium* head blight after combining observations from spray, tip, centre and base inoculations with *F. graminearum* and *F. culmorum*, separately at GS 61-65. Parameter *K* is the capacity of disease incidence, *rM* the slope of the curve, *t0* was fixed at 3 days. FHB incidence was observed in two temperature regimes (18/12 and 24/18°C day/night) with or without short-term spells of moisture (wet or dry, respectively), (n ≥ 90)

	Parameter	Environmental conditions			
		18/12°C wet	**18/12°C dry**	**24/18°C wet**	**24/18°C dry**
F. graminearum	*K*	97.99 ± 0.56 **	78.94 ± 3.81	89.44 ± 2.70	80.92 ± 0.26
	rM	0.45 ± 0.02	0.32 ± 0.07	0.25 ± 0.03	0.60 ± 0.01
	F	263.80	9.43	165.21	452.70
	R^2	0.97	0.70	0.98	0.99
F. culmorum	*K*	95.39 ± 0.78	63.28 ± 4.04	75.46 ± 3.9	84.24 ± 0.69
	rM	0.35 ± 0.02	0.19 ± 0.04	0.18 ± 0.03	0.44 ± 0.02
	F	308.77	20.18	130.75	198.26
	R^2	0.98	0.83	0.97	0.98

* Value not significantly different from 0

** Estimated parameter value ± standard error

The estimated parameter of disease progress curves of infected ears following different primary site of inoculation with *F. graminearum* and *F. culmorum,* under different environmental conditions, are shown in Tab. 3.11. The progression of FHB incidence could be reasonably described by the monomolecular function (equation 6) for both *Fusarium* species under different environmental conditions ($R^2 \geq 0.70$ and ≥ 0.83 for *F. graminearum* and *F. culmorum*,

respectively). The best fit of equation 6, to observations as *F* values reveals, was at 24/18°C dry, for the infection with *F. graminearum,* and at 18/12°C wet, for the infection with *F. culmorum*. All estimated parameters were significantly different from 0 when *t0* was given a fixed value, *t0* = 3. The highest estimated capacity of disease incidence was obtained at 18/12°C wet (97.99 and 95.39 for *F. graminearum* and *F. culmorum* respectively). In contrast, the lowest was obtained at the same temperature under dry conditions (78.94 and 63.28 for *F. graminearum* and *F. culmorum* respectively). Irrespective of the *Fusarium* species and environmental conditions, the dynamics of disease incidence was steeper as *rM* revealed (between 0.19 and 0.60). Furthermore, *F. graminearum* showed steeper dynamics of disease incidence development compared to *F. culmorum* (Tab. 3.11).

Table 3.12 The average percentage of *Fusarium* incidences in wheat ears at the asymptotic stage of incidence development after spray, tip, centre and base inoculations with *F. graminearum* and *F. culmorum*, separately at GS 61-65. After incubation, FHB was observed in two temperature regimes (18/12 vs. 24/18°C day/night) with or without short-term spells of moisture (wet or dry, respectively), ($n \geq 22$).

	Inoculation scenarios	**Environmental conditions**			
		18/12°C wet	**18/12°C dry**	**24/18°C wet**	**24/18°C dry**
F. graminearum	Spray	92.86	74.19	100.00	73.91
	Tip	100.00	63.33	84.38	91.67
	Centre	100.00	66.67	93.94	82.61
	Base	100.00	53.57	67.74	76.19
F. culmorum	Spray	89.66	81.48	93.94	77.27
	Tip	100.00	81.48	77.42	95.65
	Centre	96.43	87.50	62.50	90.91
	Base	92.59	76.67	48.39	73.91

FHB incidences following different primary site of ear inoculations with *F. graminearum* and *F. culmorum* under different environmental conditions, at asymptotic stages, are shown in (Tab. 3.12). In few cases, the incidence was 100% (all inoculated ears showed symptoms). At 18/12°C wet, almost all inoculated ears showed symptoms (≥ 92.86%). At 18/12°C dry, the incidence was

lower, between 53.56% and 87.50%. At higher temperatures, however, this trend of higher incidence rate under wet conditions was only valid in the case of spray inoculation (Tab. 3.12).

3.3.2 Severity curves

3.3.2.1 FHB index in total

Observed and simulated dynamics of disease severity (FHB index) depending on the two pathogens, *F. graminearum* and *F. culmorum*, in the four environmental regimes, are shown in Fig. 3.18. The development of *Fusarium* infection was recognisable until 34-35 dai when the asymptotic stage was reached at 18/12°C wet and dry. In contrast, at 24/12°C at 24 dai the visual assessment was not possible anymore, and a lower calculated disease severity was obtained. The asymptotic stages were reached faster under wet conditions in both temperature regimes with the highest FHB index of 72.56% for *F. culmorum* at 18/12°C wet. At lower temperatures, *F. culmorum* showed higher disease severity compared to that of *F. graminearum* which was opposite at 24/18°C.

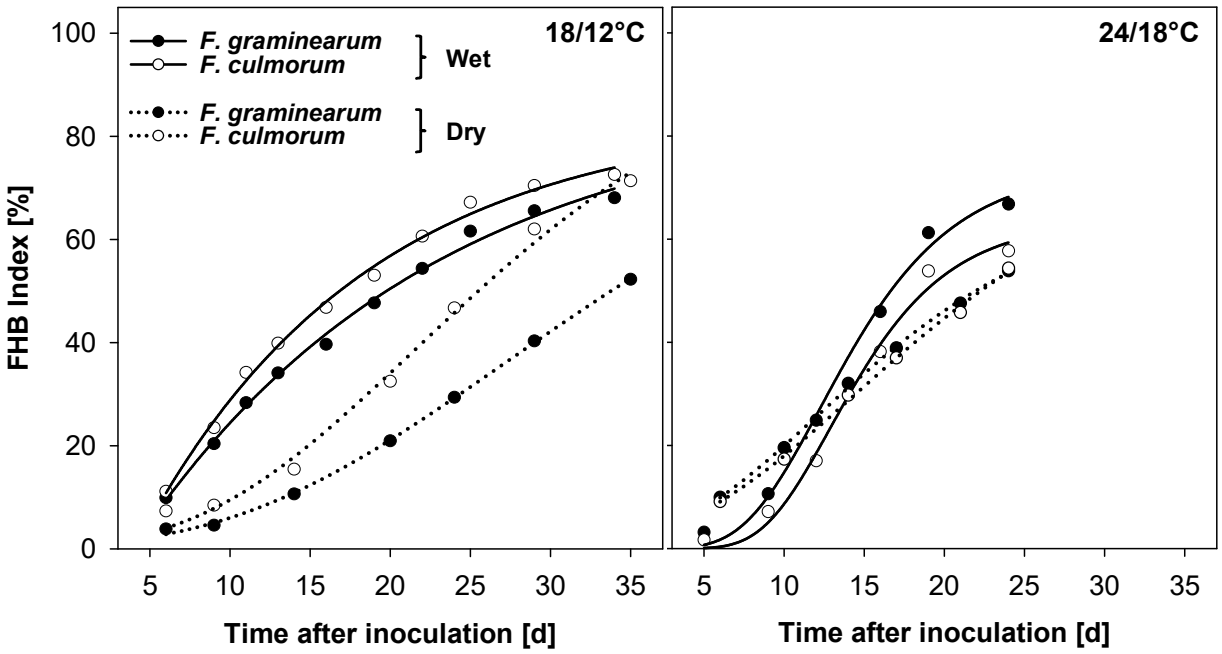

Figure 3.18 Progression of *Fusarium* head blight severity (FHB index) due to *F. graminearum* and *F. culmorum* infection in wheat ears after combining observations from spray, tip, centre and base inoculations for each *Fusarium* spp. Infection developed in two temperature regimes (18/12 and 24/18 °C day/night) with or without short-term spells of moisture (wet or dry, respectively). Dots stand for observations and lines are simulations from the monomolecular model (equation 6, only at 18/12°C wet) and the logistic model (equation 7). Ears were inoculated at GS 61-65, ($n \geq 75$).

Table 3.13 Effect of environmental conditions and *Fusarium* spp. on the area under disease progress curve (AUDPC in %: 18/12°C wet 28 days; 18/12°C dry 30 days; 24/18°C wet 19 days; 24/18°C dry 19 days) of *Fusarium* head blight after combining observations from spray, tip, centre and base inoculations for each pathogen. FHB was observed in two temperature regimes (18/12 and 24/18 °C day/night) with or without short-term spells of moisture (wet or dry, respectively). Ears were inoculated with *F. graminearum* and *F. culmorum* at GS 61-65. ($n \geq 75$).

***Fusarium* species**	**Environmental conditions**			
	18/12°C wet	**18/12°C dry**	**24/18°C wet**	**24/18°C dry**
F. graminearum	1310.33	744.08*	730.33*	587.03
F. culmorum	1537.63	1050.82	611.10	553.85
Overall mean	1414.98a	907.68b	677.20c	570.33c

* Significant difference between *Fusarium* species (*t*-test; $P \leq 0.05$).
abc Figures with the same letter are not significantly different (Tukey's HSD; $P \leq 0.05$).

The development of *FHB* was significantly affected by environmental conditions and the *Fusarium* species, as AUDPC revealed (Tab. 3.13). At 18/12°C dry, *F. culmorum* was more aggressive than *F. graminearum,* and a significant difference in AUDPC was found. At higher temperatures on the contrary *F. graminearum* was more aggressive. 18/12°C wet were the optimal conditions for disease severity, considering the combination of both *Fusarium* species. Furthermore, short-term spells of moisture increased the disease severity significantly at 18/12°C (Tab. 3.13). In contrast, at higher temperatures (24/18°C) lower disease severity was obtained, and no significant effect was found, neither at wet nor at dry conditions.

The monomolecular and logistic models (equation 6 and 7) showed high goodness of fit to the dynamics of the FHB index (Tab. 3.14) when R^2 was considered ($R^2 \geq 95$). However, the values of *F* are showing different degrees of the goodness of fit. The higher the *F* value, the better the goodness of the model. At 18/12°C wet, *F* values estimated by the logistic function were low in comparison to *F* values at the other environmental conditions (369.23 and 241.97 for *F. graminearum* and *F. culmorum,* respectively). This was the opposite of the estimated *F* values calculated by the monomolecular function (759.66 and 811.86 for *F. graminearum* and *F. culmorum,* respectively). Considering both R^2 and *F* values, the logistic function represented the disease severity dynamics better in most environmental scenarios. The only exception was at 18/12°C wet, under this condition the monomolecular function was better to describe FHB index.

Table 3.14 Estimated parameter values of the monomolecular and logistic models (equation 6 and 7, respectively) describing the dynamics of disease severity (FHB index) of *Fusarium* head blight after combining observations from spray, tip, centre and base inoculations for each *Fusarium* spp. Parameter *K* is the capacity of the disease progress curves, *y0* the initial disease level, *t0* the time at which the first symptoms become visible and *rM* and *rL* are the rate parameters of the monomolecular and logistic models, respectively. HLB was observed in two temperature regimes (18/12 vs. 24/18 °C day/night) with or without short-term spells of moisture (wet or dry, respectively). Ears were inoculated with *F. graminearum* and *F. culmorum* at GS 61-65, (n ≥ 75).

Parameter			Environmental conditions			
			18/12°C wet	**18/12°C dry**	**24/18°C wet**	**24/18°C dry**
Logistic function	*F. graminearum*	*K*	69.93 ± 2.37**	64.66 ± 2.34	69.31 ± 1.70	59.71 ± 2.74
		y0	5.50 ± 1.03	1.58 ± 0.18	0.55 ± 0.15	3.63 ± 0.66
		rL	0.17 ± 0.02	0.14 ± 0.006	0.34 ± 0.02	0.20 ± 0.02
		F	369.23	2658.38	929.72	548.36
		R^2	0.99	0.999	0.998	0.997
	F. culmorum	*K*	72.96 ± 8.57	80.49 ± 3.04	59.98 ± 1.82	63.66 ± 5.19
		y0	5.85 ±1.39	1.98 ± 0.38	0.20 ± 0.09*	3.58 ± 0.87
		rL	0.19 ± 0.02	0.16 ± 0.01	0.40 ± 0.03	0.18 ± 0.02
		F	241.97	1007.54	589.50	324.34
		R^2	0.99	0.998	0.997	0.995
Monomolecular function	*F. graminearum*	*K****	87.23 ± 5.35	100 ± 103.49*	100 ± 108.55*	100 ± 24.42
		t0	3.86 ± 0.42	6.63 ± 1.78	5.55 ± 1.13	3.54 ± 0.59
		rM	0.05 ± 0.007	0.02 ± 0.03*	0.06 ± 0.05*	0.04 ± 0.01*
		F	759.66	35.71	26.48	402.53
		R^2	0.99	0.95	0.95	0.99
	F. culmorum	*K****	84.11 ± 3.31	100 ± 63.45*	100 ± 84.05*	100 ± 46.08*
		t0	4.05 ± 0.35	6.155 ± 1.89	5.99 ± 1.30	4.02 ± 0.1
		rM	0.07 ± 0.007	0.03 ± 0.04*	0.04 ± 0.06*	0.04 ± 0.02*
		F	811.86	27.42	20.08	121.15
		R^2	0.99	0.97	0.93	0.99

* Value not significantly different from 0

** Estimated parameter value ± standard error

*** *K* values were restricted to ≤ 100

Regarding the estimated capacity of disease severity, the logistic function showed a better estimation than that of monomolecular function, when they were compared in the asymptotic stages. The estimation of *K* values following the monomolecular function was in most cases equal

to 100 and not significantly different from 0, except the dynamics at 18/12°C wet. The estimated value was even higher than 100 when the model was fitted without restricting the *K* values to be equal or less than 100.

The estimation of *y0,* following the logistic function, was significantly different from 0 under all environmental conditions for both *Fusarium* species, except 24/18°C wet ($y0 \geq 0.20$ and ≤ 5.85 dai). The disease progress curves of FHB, described by logistic functions, had similar rate values in different environmental conditions (*rL* between 0.14 - 0.20 per day). The only exception was at 24/18°C wet, where *rL* was 0.34 and 0.40 for the disease development of the infection with *F. graminearum* and *F. culmorum*, respectively. When *t0* was fixed to 3 days in the monomolecular function, like in the case of disease incidence, the model could only fit to the disease severity at 18/12°C wet. Therefore, *t0* was not fixed but estimated from the data. Except for 18/12°C wet, the estimated *K* values exceeded the top capacity 100%, which cannot happen in reality.

Consequently, the capacity was restricted at 100%. However, when the capacity parameter was restricted, the values of the rate parameter *rM* were not significantly different from 0. Thus the monomolecular model was not useful in these cases. Only at 18/12°C wet, the rate parameter was significantly different from 0 (*rM* = 0.05 and 0.07 per day for the infection with *F. graminearum* and *F. culmorum*, respectively) (Tab. 3.14).

3.3.2.2 FHB index at 18/12°C

At 18/12°C, the growth stages GS 83-85, at which no visual assessment was possible anymore, were reached at 34-35 dai while these GS were reached at 24 dai at 24/18°C. Under wet conditions, the disease development was stronger compared to dry conditions and reached the asymptotic stage earlier at both temperature regimes.

Overall, at the asymptotic stage of disease development, the spray and centre inoculations caused the highest disease severity (Fig. 3.19 and 3.20). Only at 18/12°C wet, the FHB indices caused by

F. graminearum after spray, tip, and centre and base inoculations were not significantly different to each other, in the asymptotic stage (Fig. 3.19).

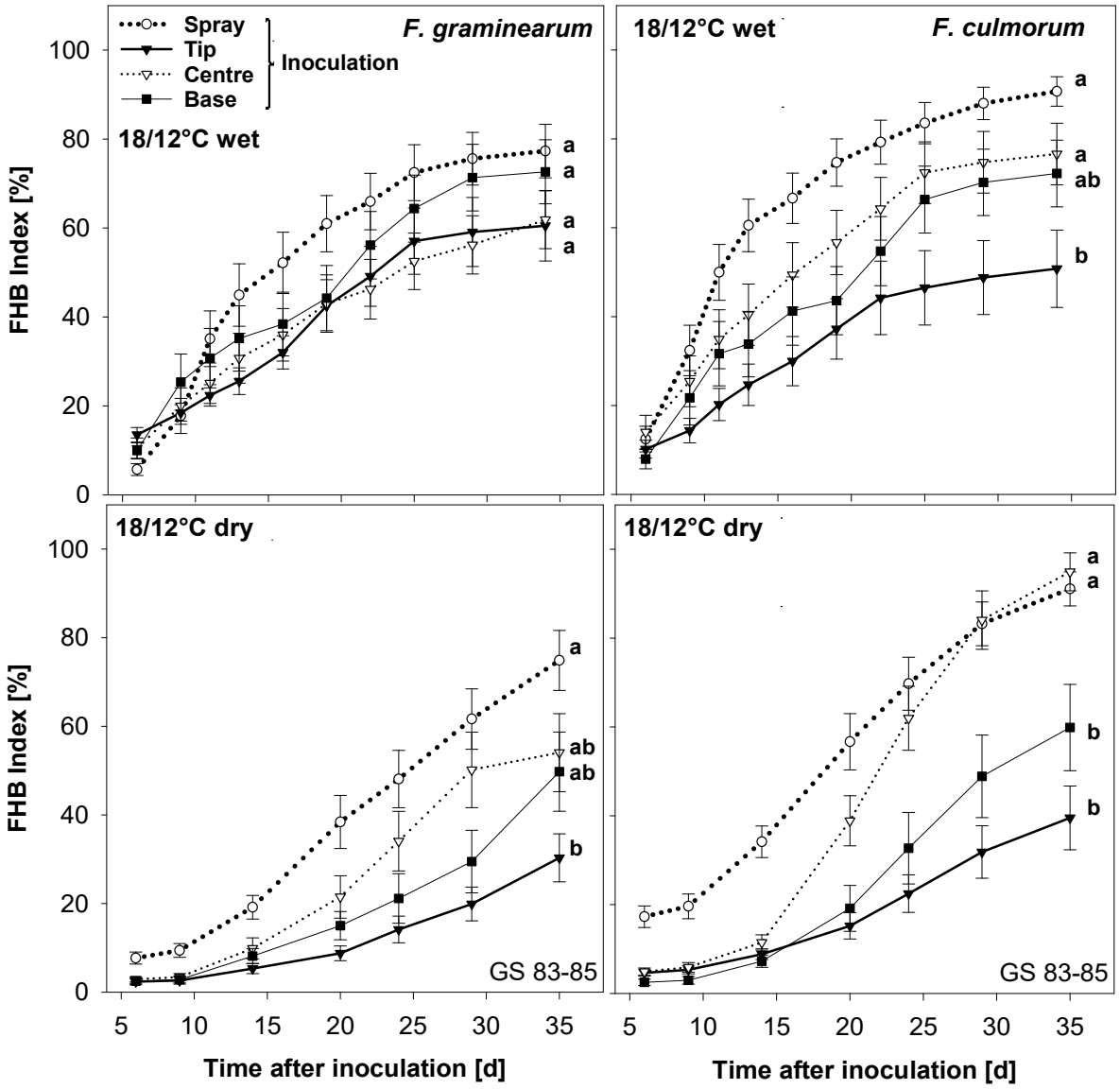

Figure 3.19 Progress curves of *Fusarium* head blight (FHB) at 18/12°C, under wet and dry conditions (with or without short-term spells of moisture, respectively) due to *F. graminearum* and *F. culmorum* establishment in wheat after spray, tip, centre and base inoculation of ears, measured as average proportion of symptomatic spikelets per ear (FHB index). Ears were inoculated at GS 61-65. (mean ± SE: n > 20). Same letters denote no significant difference at the same time point (Tukey HSD test, $P \leq 0.05$).

3.3.2.3 FHB index at 24/18°C

The effect of higher temperature scenarios (24/18°C) in FHB index progress curves is shown in Fig. 3.20.

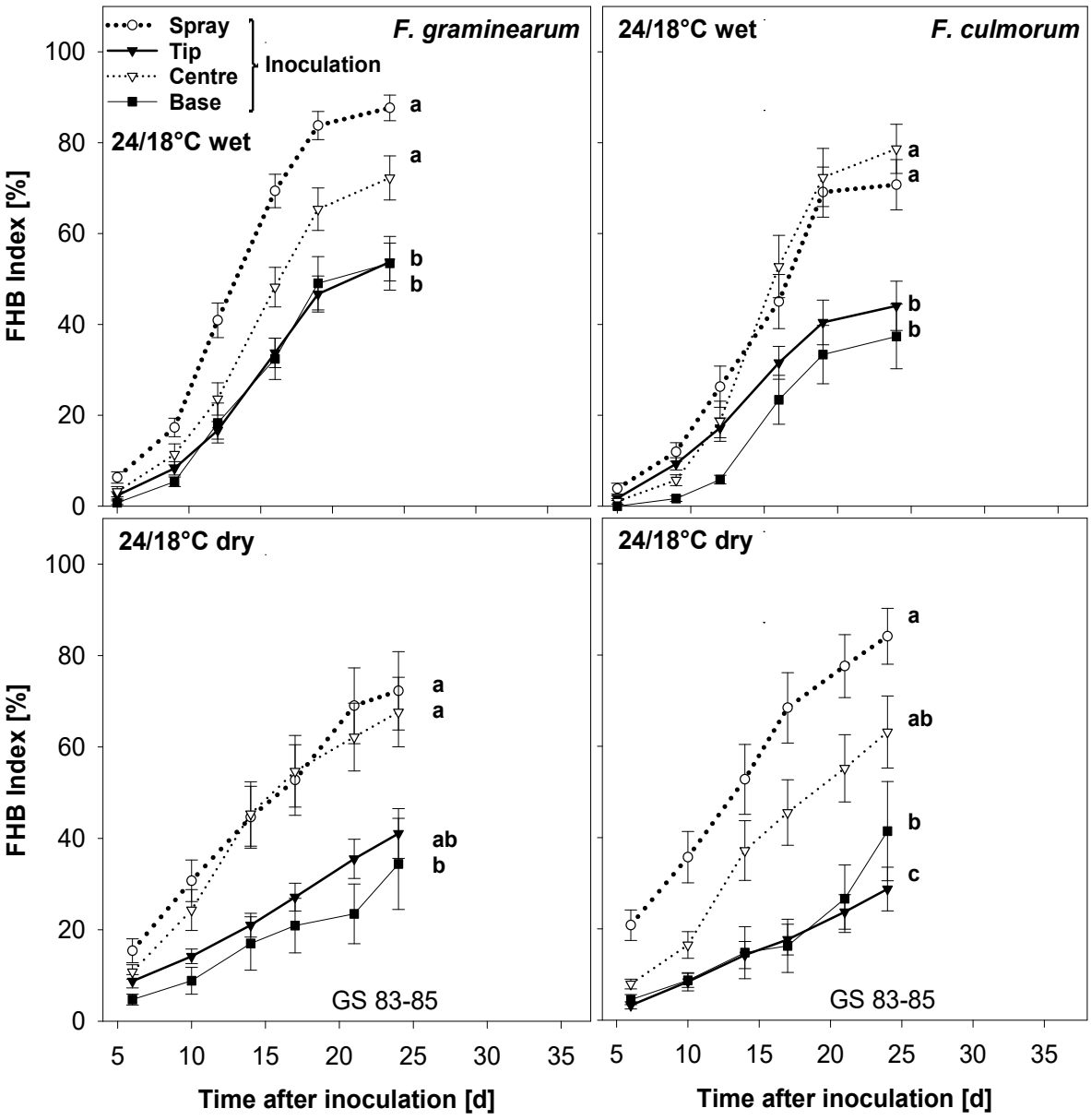

Figure 3.20 Progress curves of *Fusarium* head blight (FHB) at 18/12°C, under wet and dry conditions (with or without short-term spells of moisture, respectively) due to *F. graminearum* and *F. culmorum* establishment in wheat ears after spray, tip, centre and base inoculation of ears measured as average proportion of symptomatic spikelets per ear (FHB index). Ears were inoculated at GS 61-65. (mean ± SE: n > 20). Same letter denotes no significant difference at the same time point (Tukey HSD test, $P \leq 0.05$).

In total, the temperature (18/12°C versus 24/18°C) at identical light conditions had the effect of extending the growth stages of wheat ears and allowed, therefore, a longer visual assessment of the disease severity (FHB index).

Table 3.15 Effect of environmental conditions and spray, tip, centre and base inoculations of individual wheat ears with *Fusarium graminearum* and *F. culmorum* on the area under disease progress curves (AUDPC) (in % days). FHB was observed in two temperature regimes (18/12 and 24/18°C day/night) with or without short-term spells of moisture (wet or dry, respectively). Ears were inoculated at GS 61-65. (AUDPC: 18/12°C wet 28 days; 18/12°C dry 30 days; 24/18°C wet 19 days; 24/18°C dry 19 days, n > 20).

Environmental conditions	***Fusarium* species**	**Inoculation scenario**			
		Spray[a]	**Tip[c]**	**Centre[b]**	**Base[c]**
[a]18/12°C wet	*F. graminearum*	1559.52*	1162.90	1159.57*	1371.96
	F. culmorum	1927.53	996.79	1547.62	1361.54
[b]18/12°C dry	*F. graminearum*	1165.91*	364.91	771.17*	541.44*
	F. culmorum	1620.32	547.72	1314.26	746.78
[b]24/18°C wet	*F. graminearum*	1013.41*	531.34	739.60	527.64*
	F. culmorum	752.31	478.76	758.13	334.95
[c]24/18°C dry	*F. graminearum*	844.51	517.45*	729.50	289.12
	F. culmorum	933.21	257.25	608.42	286.37

* Significant difference between *Fusarium* species within infection scenario (*t*-test; $P \leq 0.05$).
abc Environmental conditions and inoculation scenarios with the same letter are not significantly different (Tukey's HSD; $P \leq 0.05$).

At this time point and under all environmental conditions, base and tip inoculations with both pathogens caused FHB indices not significantly different between each other with one exception; FHB indices of *F. culmorum* at 24/18°C dry (Fig. 3.20).

The 3-way ANOVA of the AUDPCs of the FHB indices (Tab. 3.15 and 3.7) showed a significant effect of the environmental conditions, and primary site of ear infection, while no significant effect by the *Fusarium* spp. was found. The conditions of 18/12°C wet, proved to be optimal for the epidemic development of FHB followed by 18/12°C dry and 24/18°C wet. In contrast, 24/18°C dry proved less suitability for the disease development, considering the AUDPC. Spray inoculation had the strongest effect on the AUDPC, whereas tip and base inoculation had the lowest and centre

inoculation had an intermediate effect. At 18/12°C, *F. culmorum* caused significant higher AUDPCs compared to *F. graminearum,* when the individual inoculation scenario was considered (spray and centre under wet conditions and spray, centre and base under dry conditions). In contrast, at 24/18°C wet *F. graminearum* showed higher AUDPC values which were significantly different after the spray and base inoculations, and after tip inoculation at 24/18°C dry (Tab. 3.15).

3.3.3 *Fusarium* infection on kernels

3.3.3.1 Overall rate of infected kernels

The overall FIK under different environmental conditions and at different primary site of ears infection with *F. graminearum* and *F. culmorum* is shown in (Fig. 3.21). *F. graminearum* caused the overall highest FIK at 24/18°C wet, while the lowest rate was obtained at 24/18°C dry and

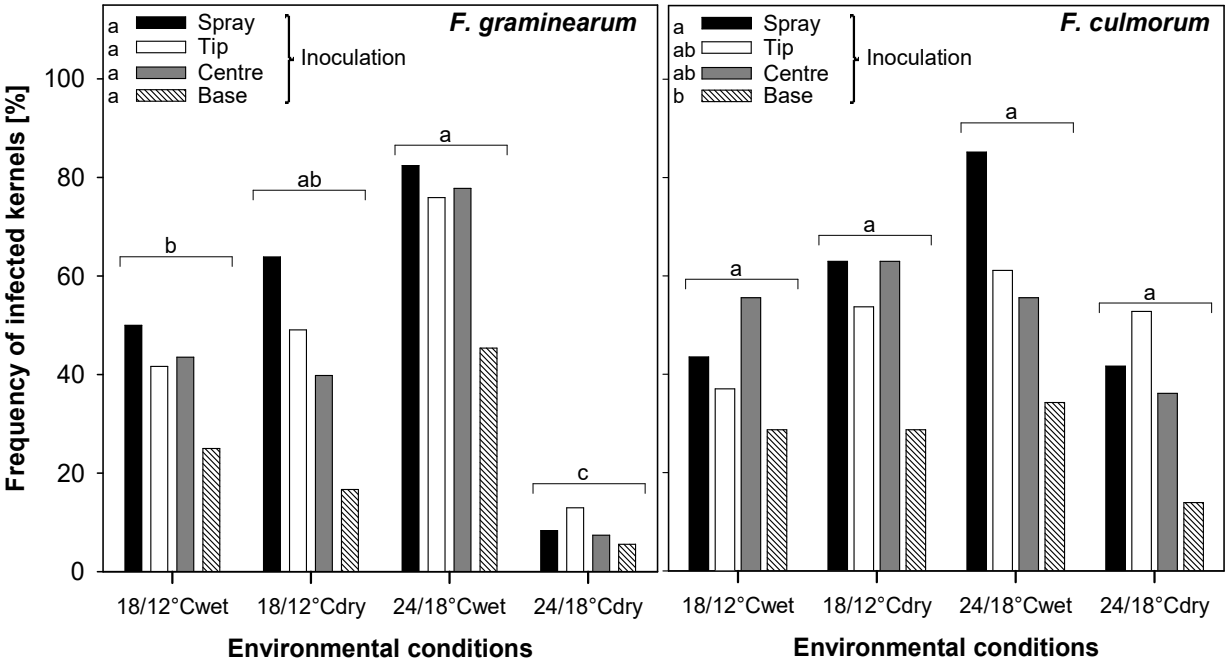

Figure 3.21 Infected kernels rate (FIK) with *F. graminearum* and *F. culmorum* under two temperature regimes [18/12°C and. 24/18°C, day/night] with or without short-term spells of moisture (wet or dry, respectively) after spray, tip, centre and base inoculation of ears at GS 61-65, (n=108). Columns with the same letter are not significantly different (Tukey HSD test, $P \leq 0.05$).

no significant effect was shown for the primary site of ears infection. In contrast, the FIK with *F. culmorum* was not significantly different comparing different environmental conditions. However significant differences were pronounced between infection scenarios. FIK after spray inoculation was the highest, while the lowest was observed after base inoculation.

When the observations from both *Fusarium* species were considered, the 3-way ANOVA of the FIK (Tab. 3.17) showed a significant effect of environmental conditions, the primary site of ear infection and *Fusarium* spp. Nevertheless, no interaction was found between any of these factors. In conclusion, *F. culmorum* was able to infect significantly more kernels than *F. graminearum* (Fig. 3.23). The conditions at 24/18°C wet were optimal for infecting kernels, showing significant differences compared to other conditions and at the same temperature regime. Dry condition proved to be less suitable in any case. 18/12°C wet and dry conditions occupied the intermediate FIK ranks, with no significant differences between each other. Infection after tip inoculation was associated with the highest FIK similar to infection after centre and spray inoculations, whereas infection after base inoculated caused the lowest rate.

3.3.3.2 Spatial distribution of infected kernels within ears

The gradient of FIK across single ears (Fig. 3.23), after considering the four environmental conditions, was a function of the inoculation site (primary site of infection within ear), whereas the levels at which the inoculation took place showed the highest FIK. The FIK from ears decreased slowly from tip-inoculated downward to the basal level with 37.50% and 25% for the infection with *F. culmorum* and *F. graminearum*, respectively.

The gradients of FIK of both *Fusarium* species resulting from base infection showed decreasing rates in the upwards direction compared to that after tip infection. Both *Fusarium* spp. showed the tendency to spread within ears preferably downwards not upwards. This effect became evident and was also verified after the centre inoculation. The frequency of infected kernels from spikelets 4 to 1 was only slightly lower than at the point of inoculation (spikelet 5), but re-isolation success decreased considerably from spikelet levels 5 to 9, especially for *F. graminearum.* No gradient was recognisable for the FIK after spray inoculations, but it can be seen how the basal and top levels are less infected in comparison to the central levels, especially for *F. culmorum* (Fig. 3.23).

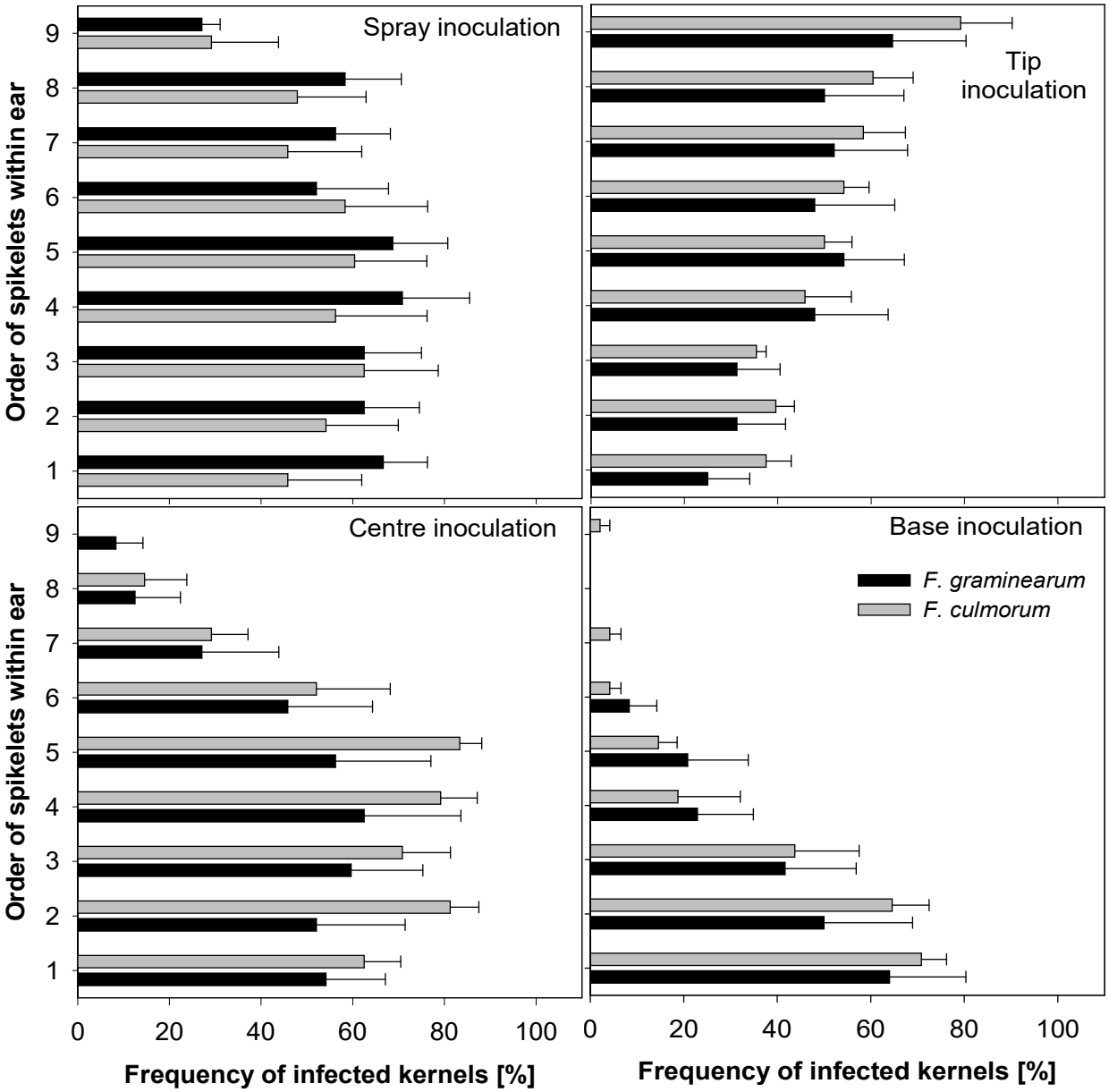

Figure 3.22 Effect of primary site of *Fusarium* infection of wheat ears and environmental conditions (18/12°C and 24/18°C, day/night), with or without short-term spells of moisture (wet or. dry, respectively), on the spatial distribution of infected kernels within ears at harvest. Ears had been inoculated by spraying, tip only, centre only, and base only with *F. graminearum* and *F. culmorum* at GS 61-65 (mean ±Se, n = 48).

3.3.3.3 Modelling of infection gradients

Estimated parameter values from fitting the exponential models (equations 8, 9 and 10) to the gradients of FIK under different environmental conditions and following different primary site of ear inoculation with *F. graminearum* and *F. culmorum* are shown in Table 6. Under different

environmental conditions, the base inoculation resulted in steep upward gradients which could be reasonably described by equation 8 for both *Fusarium* species ($R^2 \geq 0.82$) with values for the slope (*b*) between 0.27 and 0.76 (Tab. 3.16).

After the tip inoculation, the gradients were shallower, as revealed by equation 9. Except for the gradient at 24/18°C dry, this equation showed high goodness of fit to the frequency of infected kernels for *F. graminearum* ($R^2 \geq 0.61$ compared to ≥ 44 for *F. culmorum*). The values of slope parameter *c* (in downward direction) were between 0.06 and 0.16 and always significantly different from 0 except the one under 24/18°C dry conditions. These downward values were apparently lower than the upward direction values.

After centre inoculation, the pathogens spread upwards and downwards from the point of inoculation, but with a bias towards downwards for both *Fusarium* species. The gradients upwards (*b* values) were considerably steeper (0.98, 0.53, 0.27 and 0.07 for *F. graminearum* under the conditions 18/12°C wet, 18/12°C dry, 24/18°C wet and 24/18°C dry, respectively) than downwards (c values: 0.06, -0.02, 0.09 and -0.18 for *F. graminearum* under conditions 18/12°C wet, 18/12°C dry, 24/18°C wet and 24/18°C dry, respectively). This simulation was similar to that of the FIK of *F. culmorum* (Tab. 3.16). The c-values were not significantly different from 0 indicating that the frequency of infected kernels of the lower levels was constant under all environmental conditions. The b-values were not significantly different from 0, but for the gradient under 24/18°C dry conditions.

The application of equation 10 to the FIK after spray inoculation and different environmental conditions resulted in a reasonable goodness of fit ($R^2 \geq 0.43$ for both *Fusarium* spp.), except for *F. graminearum* at 18/12°C dry, $R^2 = 0.24$ and *F. culmorum* at 24/18°C dry conditions, $R^2 = 0.11$. However, the estimated parameters revealed in every viewed scenarios gradient and most cases the frequency of infected kernels could be considered as constant.

Table 3.16 Estimated parameter values of the exponential models (equations 8, 9 and 10) simulating the gradients of the frequency of infected kernels within single ears following spray, tip, centre and base inoculation with *F. graminearum* and *F. culmorum*. Parameter a simulates the frequency of infected kernels at the point of inoculation. Parameters b and c describe the slopes of the gradients in up- and downward direction from the inoculation point (n = 12).

Environmental conditions	Parameters	Inoculation scenario							
		F. graminearum				*F. culmorum*			
		Spray	**Tip**	**Centre**	**Base**	**Spray**	**Tip**	**Centre**	**Base**
18/12 °C wet	*a*	67.2 ± 9.7**	71.9 ± 5.0	78.6 ± 7.4	78.7 ± 8.8	43.1 ± 2.8	47.1 ± 5.1	82.9 ± 10.6	95.9 ± 15.3
	b	0.28 ± 0.11	-	0.98 ± 0.25	0.39 ± 0.07	0.06 ± 0.03*	-	0.45 ± 0.13	0.41 ± 0.11
	c	0.04 ± 0.06*	0.16 ± 0.02	0.06 ± 0.04*	-	-0.06 ± 0.03*	0.06 ± 0.03	0.05 ± 0.06*	-
	R^2	0.70	0.89	0.94	0.89	0.79	0.44	0.82	0.82
18/12 °C dry	*a*	68.9 ± 5.7	62.68 ± 4.15	55.11 ± 5.17	74.30 ± 3.24	76.34 ± 9.71	74.68 ± 5.05	97.76 ± 8.72	69.68 ± 9.85
	b	0.05 ± 0.04*	-	0.53 ± 0.12	0.64 ± 0.05	0.23 ± 0.08	-	0.58 ± 0.12	0.38 ± 0.09
	c	0.02 ± 0.04*	0.06 ± 0.02	-0.02 ± 0.04*	-	-0.01 ± 0.05*	0.09 ± 0.02	0.02 ± 0.03*	-
	R^2	0.24	0.71	0.94	0.98	0.74	0.78	0.94	0.84
24/1 °C wet	*a*	102.06 ± 3.04	101.10 ± 9.62	110.82 ± 8.31	110.51± 14.60	105.51± 11.34	93.77 ± 6.95	93.61 ± 13.05	86.11 ± 10.32
	b	0.12 ± 0.02	-	0.27 ± 0.05	0.27± 0.062	0.13 ± 0.05*	-	0.47 ± 0.14	0.29 ± 0.06
	c	0.08 ± 0.01	0.08 ± 0.02	0.09 ± 0.04*	-	0.06 ± 0.05*	0.12 ± 0.02	0.11± 0.07*	-
	R^2	0.92	0.61	0.88	0.83	0.54	0.77	0.81	0.86
24/18 °C dry	*a*	19.9 ± 6.52	18.56 ± 9.57*	6.15 ± 4.99*	15.86 ± 2.34	49.94 ± 11.98	76.25 ± 10.23	67.14 ± 9.19	69.05 ± 5.44
	b	0.51 ± 0.34*	-	0.07 ± 0.42*	0.34 ± 0.09	0.11 ± 0.12*	-	1.31 ± 0.56*	0.76 ± 0.12
	c	0.48 ± 0.32*	0.1 ± 0.14*	-0.18 ± 0.28*	-	0.06 ± 0.11*	0.10 ± 0.04	0.06 ± 0.06*	-
	R^2	0.43	0.08	0.13	0.82	0.11	0.50	0.89	0.95

* Value not significantly different from 0

** Estimated parameter value ± standard error

3.3.4 Kernel weight

It can be seen that *F. graminearum* caused less reduction in TKW at 18/12°C compared to that of *F. culmorum*, this was the opposite at the higher temperature regime of 24/18°C (Fig. 3.23).

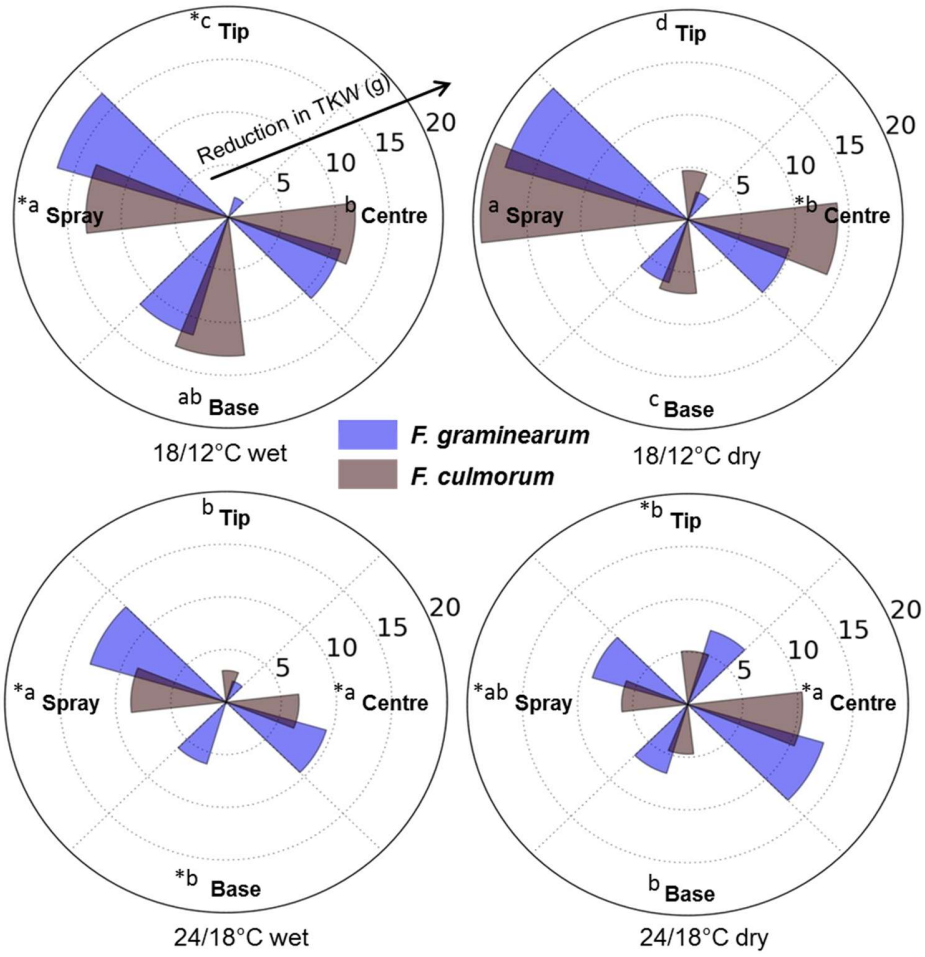

Figure 3.23 Effect of primary site of *Fusarium* infection of wheat ears at different environmental conditions (18/12°C and. 24/18°C, day/night, with or without short-term spells of moisture, wet or. dry, respectively) on reducing thousand kernels weight (RTKW) (in g compared to non-inoculated control). The same letter denotes no significant difference in RTKW between treatments of inoculations within the same environmental conditions (Tukey HSD test, $P \leq 0.05$). Asterisk denotes significant difference between *Fusarium* spp. within the same environmental conditions (t-test, $P \leq 0.05$). Ears had been inoculated with *F. graminearum* and *F. culmorum* by spraying, tip only, centre only, and base only at GS 61-65.

Lower temperatures (18/12°C) were associated with a stronger reduction in TKW in comparison to higher temperatures (24/18°C), no matter, if short terms spell of moisture, were applied or not.

Spray inoculation caused the highest reduction in TKW under all environmental conditions and was highest at 18/12°C wet (43.66% = 16.63 g reduction compared to the non-inoculated control). Meanwhile, the centre and base inoculation occupied the intermediate ranks regarding reducing the TKW, and the tip inoculation did not cause any reduction in some scenarios, or only minor reductions, of FHB (Fig. 3.23).

The 3-way ANOVA of the FIK (Tab. 3.17) showed a significant reducing effect of environmental conditions, the primary site of ear infection and *Fusarium* spp. on the TKW. A significant effect was observed in the interaction of Environmental conditions (EC)× Primary site of ears infection (PSI), EC× *Fusarium* spp. (FS) moreover, EC×PSI×FS (Tab. 3.17).

Table 3.17 Three-way ANOVA of the area under disease progress curves (AUDPC), reduction in thousand kernels weight (RTKW) and overall rates of infected kernels (FIK). For AUDPC and FIK, data were ln-transformed. DF: degree of freedom; F values including the level of significance, (* $P \leq 0.5$, ** $P \leq 0.05$), are presented in the remaining columns.

	Factors						
Variables	**Environmental conditions (EC)**	**Primary site of ears infection (PSI)**	**Pathogens: *Fusarium* spp. (FS)**	**EC× PSI**	**EC× FS**	**PSI× FS**	**EC× PSI× FS**
DF	3	3	1	9	3	3	9
AUDPC	63.46**	68.98**	0.21	4.28*	9.10**	3.66**	1.40
IKR	34.64**	10.95**	6.62*	1.17	14.33	1.45	0.71
TKW	48.12**	246.75**	16.31**	37.61**	17.82**	3.03*	3.96**

3.3.5 Correlations among *Fusarium* infection parameters

A significant correlation was found between AUDPC and TKW for the observations from spray and base inoculations (P = 0.66 and 0.8, respectively). When environmental conditions were considered (Fig. 3.24), a significant correlation was proved between AUDPC and TKW (r = 0.83, 0.82, 0.95 and 0.94 for 18/12°C wet, 18/12°C dry, 24/18°C wet and 24/18°C dry, respectively). Observations from all inoculation scenarios and environmental conditions (n = 32), showed a significant correlation as well (r = 0.67) (Tab. 3.18)

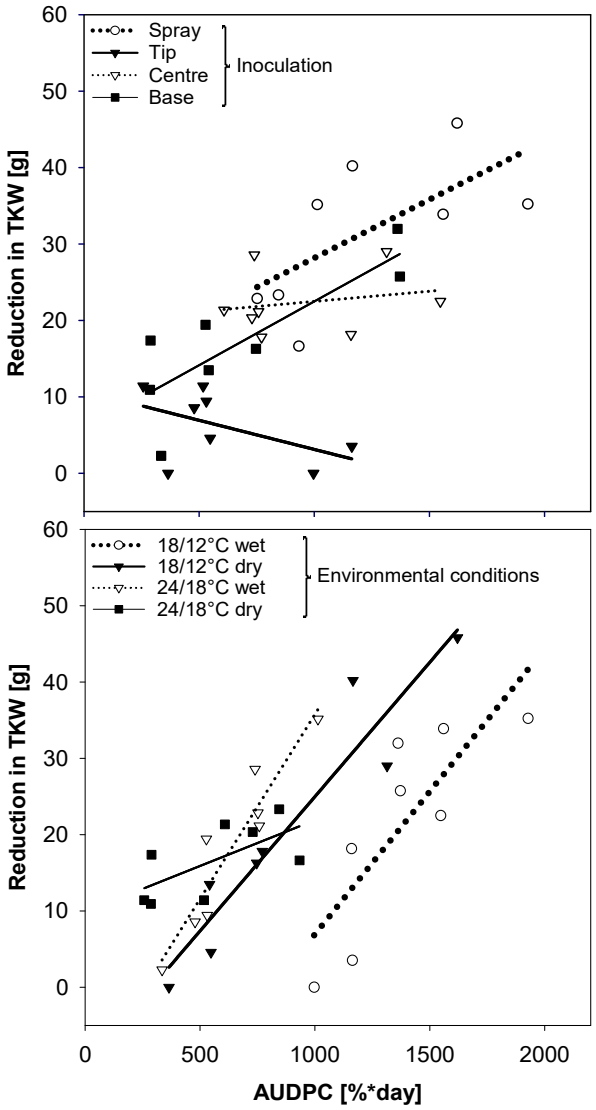

Figure 3.24 Correlation between areas under disease progress curves (AUDPC, includes observations of FHB after spray, tip, centre and base inoculation with *F. graminearum* and *F. culmorum*) and the reduction in thousand kernels weight (TKW). Symbols stand for the observations and lines are the linear regression lines, (n =8).

Except for the cases of tip and centre inoculations, AUDPC proved to be a good predictor of the reduction of TKW according to the linear regression. In contrast, neither AUDPC nor TKW can predict the FIK at any scenario of FHB development investigated in this study (Tab. 3.18).

Table 3.18 Coefficient of determinations (R^2) and Pearson coefficients (r) of linear regression and correlation tests, respectively, among the area under disease progress curves (AUDPC), reduction in thousand kennels weight (TKW) and Frequency of infected kernels (FIK) considering the primary site of ear infection by *F. graminearum* and *F. culmorum* and different environmental conditions (18/12°C and. 24/18°C, day/night; with or without short-term spells of moisture, wet or. dry, respectively).

		Inoculation scenarios (n = 8)				**Environmental conditions (n = 8)**				***Fusarium* spp. (n = 16)**		**Combination of all scenarios (n = 32)**
						18/12°C		**24/18°C**				
		Spray	**Tip**	**Centre**	**Base**	**wet**	**dry**	**wet**	**dry**	***F. graminearum***	***F. culmorum***	
AUDPC×TKW	r	0.66*	-0.50	0.21	0.83*	0.82*	0.95**	0.94**	0.65*	0.55*	0.76*	0.67*
	R^2	0.44	0.25	0.04	0.69	0.66	0.90	0.88	0.42	0.31	0.58	0.45
AUDPC×FIK	r	-0.07	-0.16	0.31	0.24	0.32	0.63*	0.72*	-0.02	0.23	0.19	0.21
	R^2	0.006	0.02	0.10	0.06	0.10	0.40	0.51	0.0003	0.053	0.035	0.04
TKW×FIK	r	0.32	-0.03	0.67*	0.07	0.029	0.52	0.63*	-0.25	0.29	0.27	0.26
	R^2	0.006	0.0008	0.46	0.005	0.0009	0.27	0.39	0.06	0.085	0.08	0.07

* Correlation is significant at the 0.05 level (1-tailed)

** Correlation is significant at the 0.01 level (1-tailed)

3.4 Infrared Thermography to visualise the spatio-temporal dynamics of *Fusarium* head blight within ears

3.4.1 Early detection using Infrared Thermography

IRT was able to detect the infection with *F. graminearum* before symptoms become visible at 2 dai (Fig. 3.25). At 2, 7, and 17 dai, the infection caused higher temperature on infected spikelets in comparison to the non-inoculated ones. At 17 dai, the upper non-inoculated part of the ear showed higher temperature compared to the base of the same ear. During the early stage of infection development, 2 dai, the temperature difference between infected and non-infected spikelets was about 0.5°C. At the advanced level of symptoms development, these differences were more pronounced (Fig. 3.25).

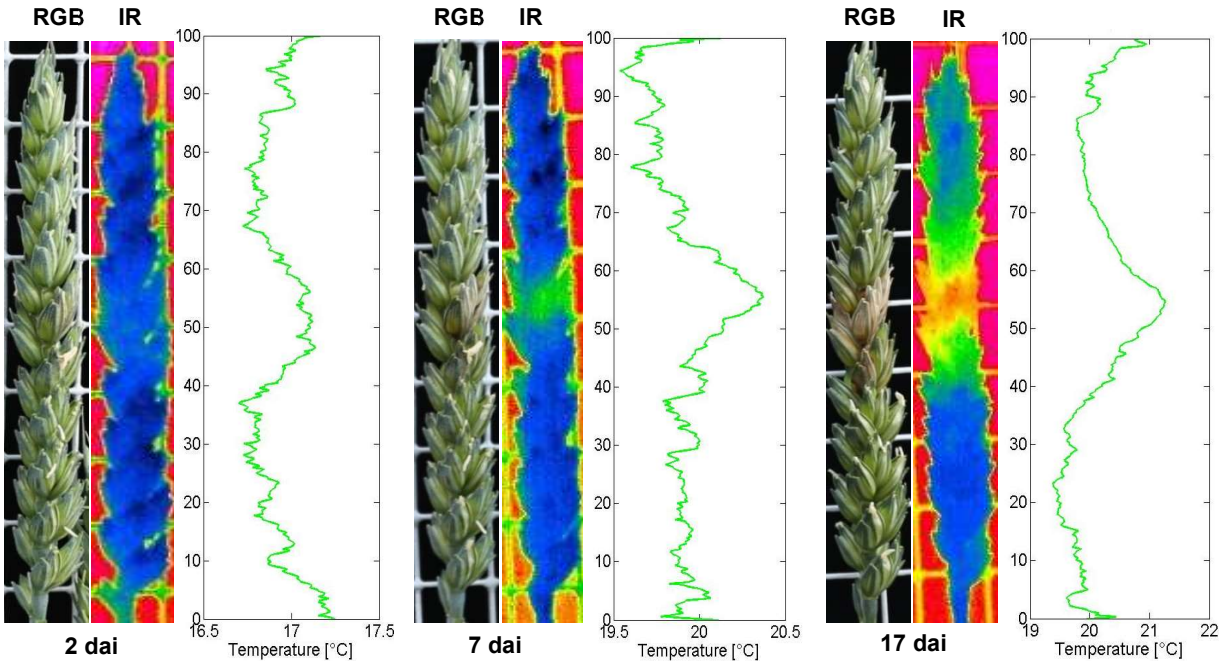

Figure 3.25 Spatial-temporal dynamics of *Fusarium* head blight development after *F. graminearum* inoculation by injecting the inoculum at three central spikelets of wheat ears visualised by digital images (RGB), false colour images of ear temperature (IR), temperature profile (green lines). Ears were divided into 100 regions horizontally and temperature mean of each region is presented along ears (y-axes). Ears were inoculated at GS 60-65.

3.4.2 Disease severity

The progress curves of diseases severity (FHB index) of both *Fusarium* species after ear infection at different primary sites are shown in Fig. 3.26. The infection after spray inoculation with both species caused the highest disease severity in comparison to that after injecting the inoculum in single spikelets. *F. culmorum* was more aggressive than *F. graminearum* after spray inoculation ($P \leq 0.05$) at 6 dai. The difference in aggressiveness between *Fusarium* species was also observed 25 dai with significant higher FHB index caused by *F. culmorum.*

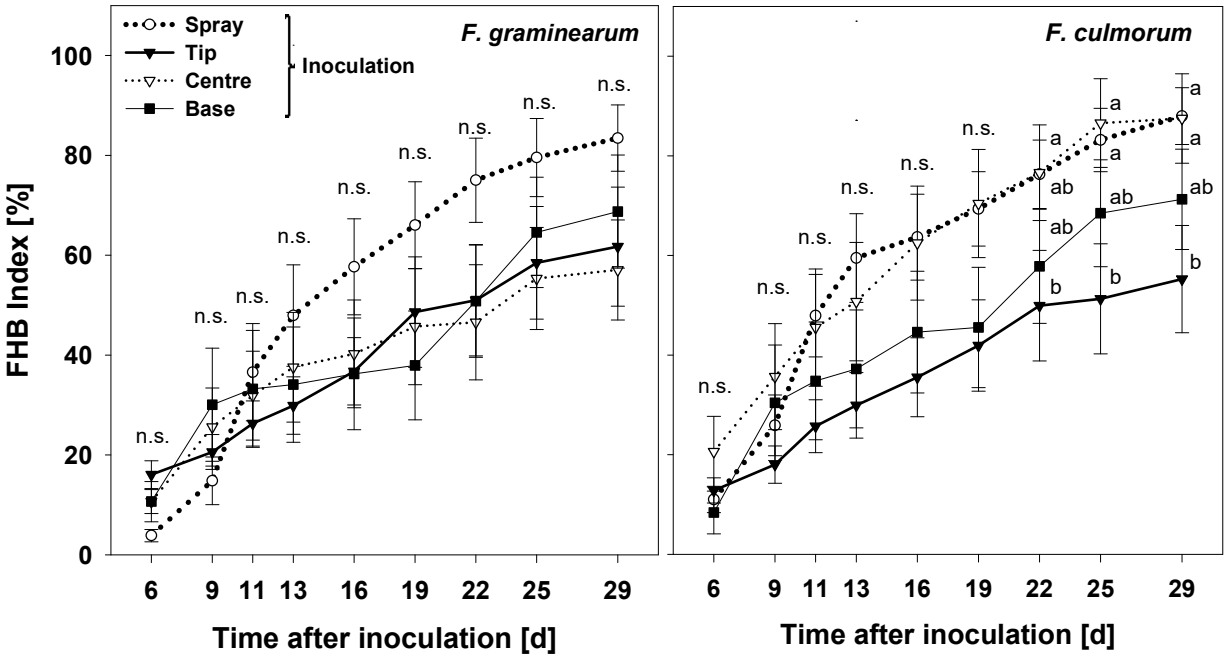

Figure 3.26 Progress curves of *Fusarium* head blight due to *F. graminearum* (left) and *F. culmorum* (right) in wheat ears after spray, tip, centre and base inoculation of ears measured as average proportion of symptomatic spikelets per ear (FHB index). Ears were inoculated at GS 61-65. Means with different letters at the same date differ significantly according to Tukey's HSD, $P \leq 0.05$, n.s. stands for no significant differences at the same date, (mean ± SE: n = 11-13).

A sudden increase of FHB symptoms was observed 19 dai on ears after base inoculation with both *Fusarium* species which was not observed in the case of other inoculation scenarios. For the four inoculation scenarios, the FHB indices developed similarly until 13 dai, when FHB index was significantly lower after tip inoculation (Fig. 3.26).

Spray inoculation resulted in the highest disease severity, significantly higher than that after tip inoculation when AUDPC was considered (Tab. 3.19). Base and centre inoculation caused AUDPCs not significantly different from that after tip and spray inoculation. AUDPC values demonstrated that the aggressiveness of *F. culmorum* was higher than that of *F. graminearum* after centre inoculation (Tab. 3.19).

Table 3.19 Effect of spray, tip, centre and base inoculation of individual wheat ears with *Fusarium graminearum* and *F. culmorum* on the area under disease progress curve of *Fusarium* head blight (AUDPC in % days, n = 11-13). Ears were inoculated at GS 61-65.

***Fusarium* spp.**	**Inoculation scenario**			
	Spray	**Tip**	**Centre**	**Base**
F. graminearum	1277.3	940.0	1037.9	872.5
F. culmorum	1420.9	903.3	1575.9*	1223.5
Overall mean	1352.0a	920.1b	1284.ab	155.6ab

* Significant difference between *Fusarium* species within infection scenario (*t*-test; $P \leq 0.05$).
ab Means with the same letter are not significantly different (Tukey's HSD; $P \leq 0.05$).

3.4.3 Effect of FHB on temperature of wheat ears

3.4.3.1 Spatial patterns of ear temperature

The effect of *Fusarium* infections at an early and late stage after inoculation (9 dai and 29 dai, respectively) on spatial patterns of ear temperature is shown in Fig. 3.27. Ears of non-inoculated control showed homogenous patterns of ear temperature with a low rate of heterogeneity between the topical and the downwards florets within single spikelet. The ears of this treatment tended to show higher heterogeneity in temperature at late growth stages near ripeness, 29 dai (Fig. 3.27).

Fusarium infection after tip inoculation was accompanied with a higher temperature at the location of symptoms development and did not affect the temperature of the rest of the same ear. Infected spikelets of centre and base inoculation showed a lower increase in spikelets temperature at 9 dai and were accompanied by increased temperature of the upper parts of ears. At 29 dai, ears of non-inoculated control showed lower temperature compared to that of infected ones. Tip infected ears showed lower temperature compared to ears of other infection scenarios at the same point of assessment (Fig. 3.27).

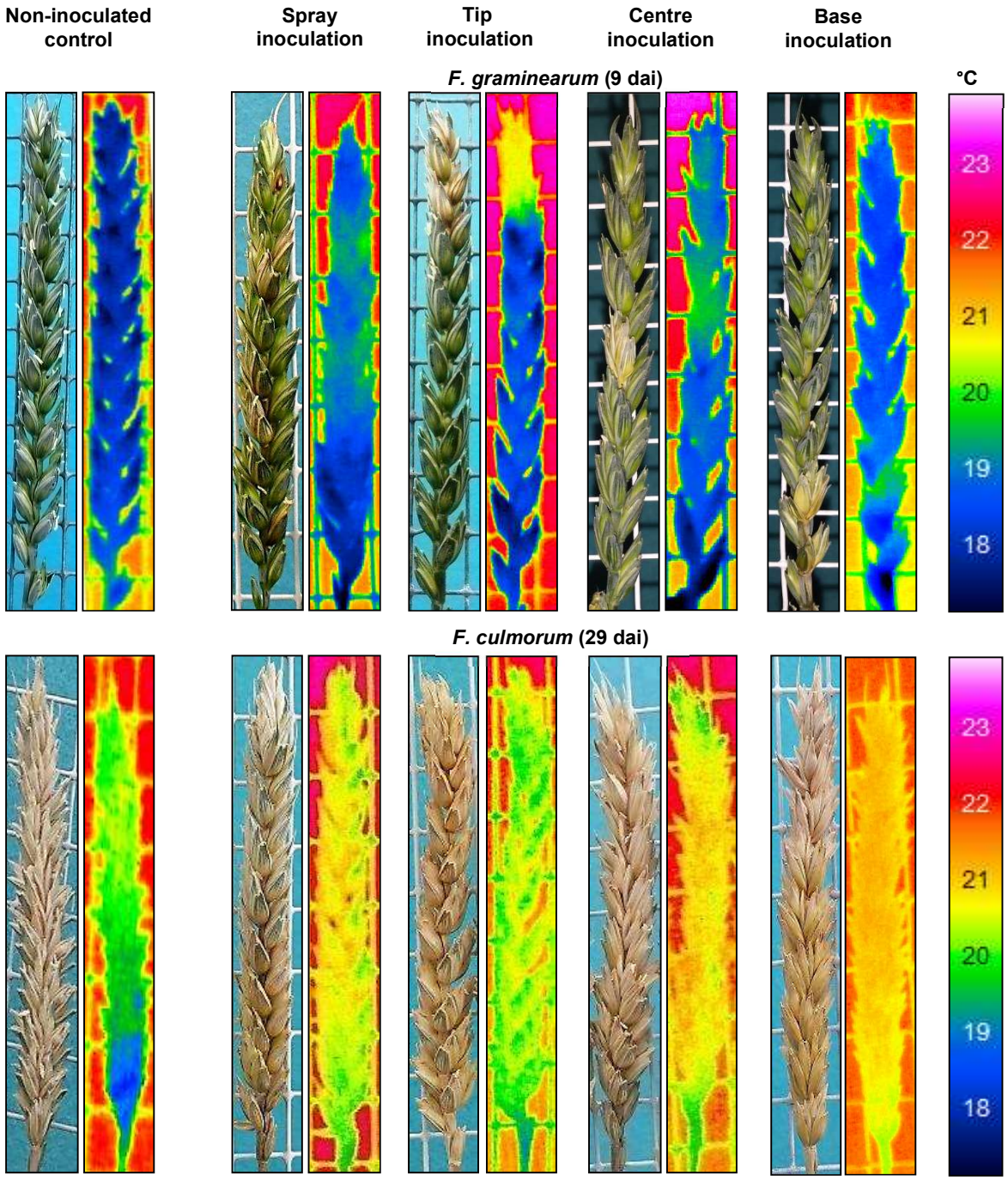

Figure 3.27 Effect of the primary site of *Fusarium* inoculation of wheat ears on spatial patterns of ear temperature, RGB images (left) and IR images (right), at 9 dai by *F. graminearum* (top) and 29 dai by *F. culmorum* (bottom), respectively. Ears were inoculated at GS 61-65.

3.4.3.2 Temperature heterogeneity within individual ears

The temperature span (TS) within infected ears was significantly higher than that within non-inoculated control ears. The degree of heterogeneity decreased over time after anthesis and was not significantly different from non-inoculated control ears at late assessment dates of measuring (GS 77-83, Fig. 3.28). After tip and centre inoculation, FHB caused the highest TS which was significantly different from the other treatments. The differences were observed in most of the monitoring days with the highest TS values 11 dai for tip inoculated ears with *F. graminearum*. Starting at 22 dai, TS decreased and was not significantly different from other treatments including the non-inoculated control for inoculated ears with *F. graminearum*.

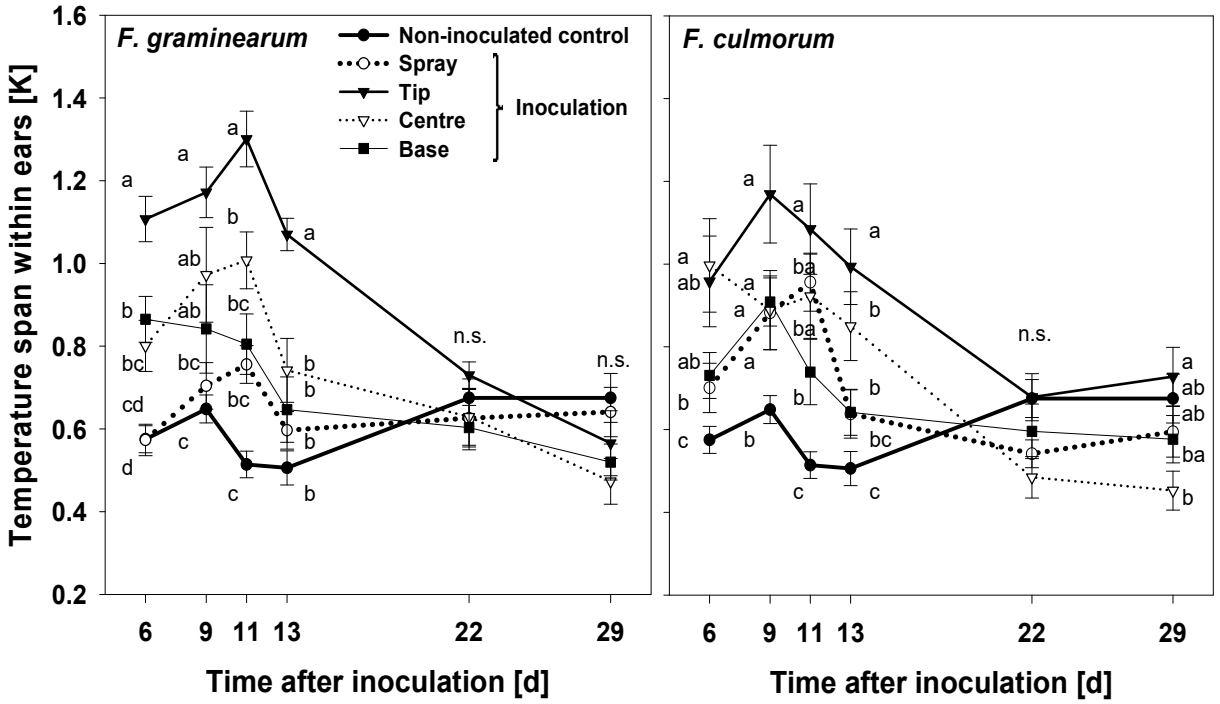

Figure 3.28 Effect of the primary site of *Fusarium* inoculation of wheat ears and *Fusarium* species on the progress of temperature span within ears. Ears were inoculated with *F. graminearum* (left) and *F. culmorum* (right) at GS 61-65. Means with different letters at the same date differ significantly according to Tukey's HSD, $P \leq 0.05$, n.s. stands for no significant differences at the same date, (mean ± SE: n = 11-13).

The non-inoculated control tended to show higher heterogeneity in ear temperature over time and was significantly higher than that after centre inoculation with *F. culmorum* at 29 dai. The effect of FHB on within-ear temperature heterogeneity was not affected by the inoculated *Fusarium* species when TS curves were considered (Fig. 3.28). Similar trends of differences were observed

when the area under temperature span curves was investigated. FHB after spray and base inoculations was associated with the lowest heterogeneity of ears temperature as AUTSCs showed. In contrast, *Fusarium* infections after centre and tip inoculations were associated with the highest AUTSC values (Tab. 3.20).

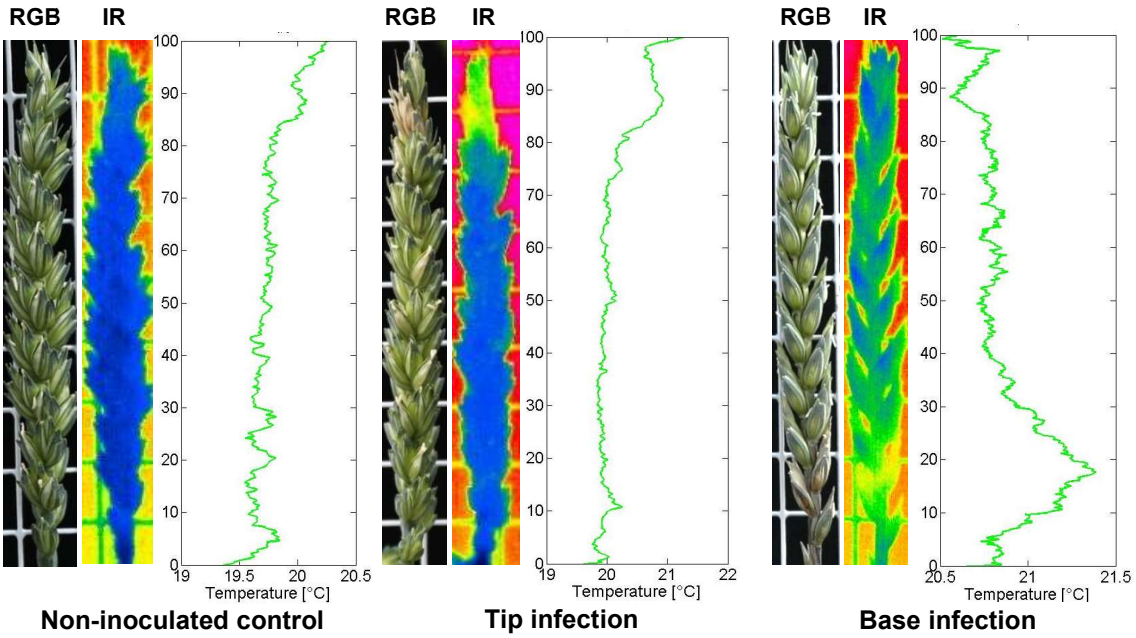

Figure 3.29 Spatial patterns of ear temperature after *F. graminearum* inoculation by injecting the inoculum at topical spikelets (tip infection) or at basal spikelets (base infection) of wheat ears compared to non-inoculated control. Patterns are visualised by digital images (RGB), false colour images of ear temperature (IR), temperature profile (green lines). Ears were divided into 100 regions (correspond y-axes) and temperature mean of each region is presented along ears. Ears were inoculated at GS 60-65.

Table 3.20 Effect of spray, tip, centre and base inoculation of wheat ears with *F. graminearum* and *F. culmorum* on the area under temperature span curve (measured in K days) and compared to non-inoculated control. (n = 11-13). Ears were inoculated at GS 61-65.

***Fusarium* spp.**	**Non-inoculated control**	**Inoculation scenario**			
		Spray	**Tip**	**Centre**	**Base**
F. graminearum	-	14.7	18.3	16.4	15.2
F. culmorum	-	14.6	16.3	15.6	14.8
Overall mean	13.6 c	14.6 bc	17.3 a	16.0 ab	14.9 abc

* Significant difference between *Fusarium* species within infection scenario (*t*-test; $P \leq 0.05$).
abc Means with the same letter are not significantly different (Tukey's HSD; $P \leq 0.05$).

The effect of the primary site of ear infection with *Fusarium* species on temperature heterogeneity can be seen in Fig. 3.29. Base infection increased the average of ear temperature not only at the position of the infection but also at the upper part of the ears in comparison to the ears of non-inoculated control. In contrast, *Fusarium* infection after tip inoculation does not affect the down part of the same ear, and higher increase in temperature has been shown at the symptomatic spikelets (Fig. 3.29).

3.4.3.3 Temperature difference between ear and ambient air

The temperature difference (TD) between ambient air and ear temperature decreased over time for all treatments including the non-inoculated control which had the highest values throughout the experiments (Fig. 3.30). FHB increased the average temperature of ears compared with that of non-inoculated ears and thereby reduced the TD values significantly. During the period of temperature increase (6-13 dai), *F. culmorum* proved to be more aggressive than *F. graminearum* as indicated by TD values (Fig. 3.30).

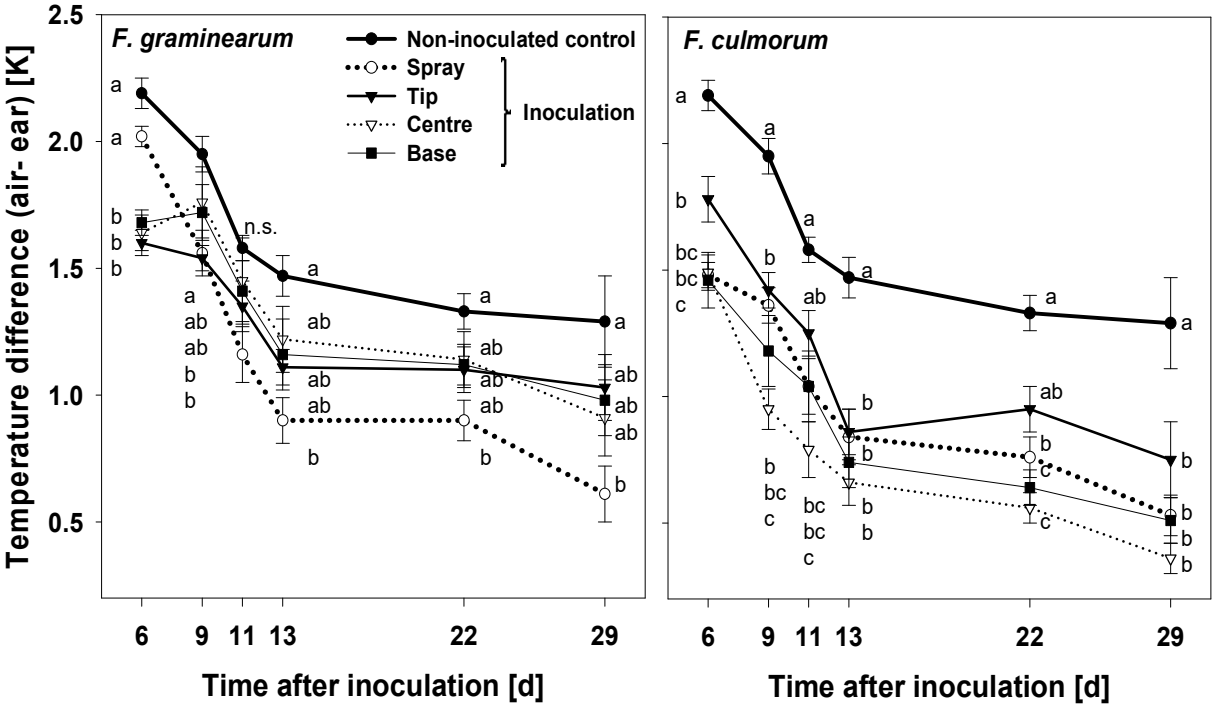

Figure 3.30 Effect of the primary site of *Fusarium* inoculation of wheat ears and *Fusarium* species on the progress of temperature difference (air - ear). Ears were inoculated with *F. graminearum* (left) and *F. culmorum* (right) at GS 61-65. Means with different letters at the same date differ significantly according to Tukey's HSD, $P \leq 0.05$ (mean ± SE: n = 11-13).

At 29 dai, when the visual assessment was not accurate anymore, TD values still showed significant differences between inoculated and non-inoculated ears, respectively (Fig. 3.30). The area under temperature difference curves (AUTDCs) showed significant differences among all treatments compared to the non-inoculated control. Differences between *Fusarium* species in AUTDCs were most pronounced after centre and base inoculation, again demonstrating a higher aggressiveness of *F. culmorum* over *F. graminearum* (Tab. 3.21).

Table 3.21 Effect of spray, tip, centre and base inoculation of wheat ears with *F. graminearum* and *F. culmorum* on the area under temperature difference curve (measured in K days) compared to non-inoculated control. (n = 11-13). Ears were inoculated at GS 61-65.

***Fusarium* spp.**	**Non-inoculated control**	**Inoculation scenario**			
		Spray	**Tip**	**Centre**	**Spray**
F. graminearum	-	23.5	23.2	29.1*	27.4*
F. culmorum	-	19.7	20.2	14.8	18.8
Overall mean	34.9 a	21.6 b	21.7 b	22.0 b	23.1 b

* Significant difference between *Fusarium* species within infection scenario (*t*-test; $P \leq 0.05$).
abc Means with the same letter are not significantly different (Tukey's HSD; $P \leq 0.05$).

3.4.4 Relationship between disease severity and thermal response

Visual estimations of disease severity and the temperature differences between air-ears (TD) were negatively correlated. These relationships were found when infection scenarios were combined for each *Fusarium* species and the all individual scenarios (Fig. 3.31). Overall, and irrespective of inoculation scenario, there was a significant linear regression between FHB index and TD (R^2 = 0.68 and 0.64 for *F. graminearum* and *F. culmorum*, respectively) 13dai (Tab. 3.22). When the different inoculation scenarios of both pathogens were considered (Fig. 3.31), linear regression varied from strong, e.g. for tip inoculation of *F. culmorum* (R^2 = 0.84), to not significant, e.g. for base inoculation of *F. culmorum* (R^2 = 0.24) (Tab. 3.22).

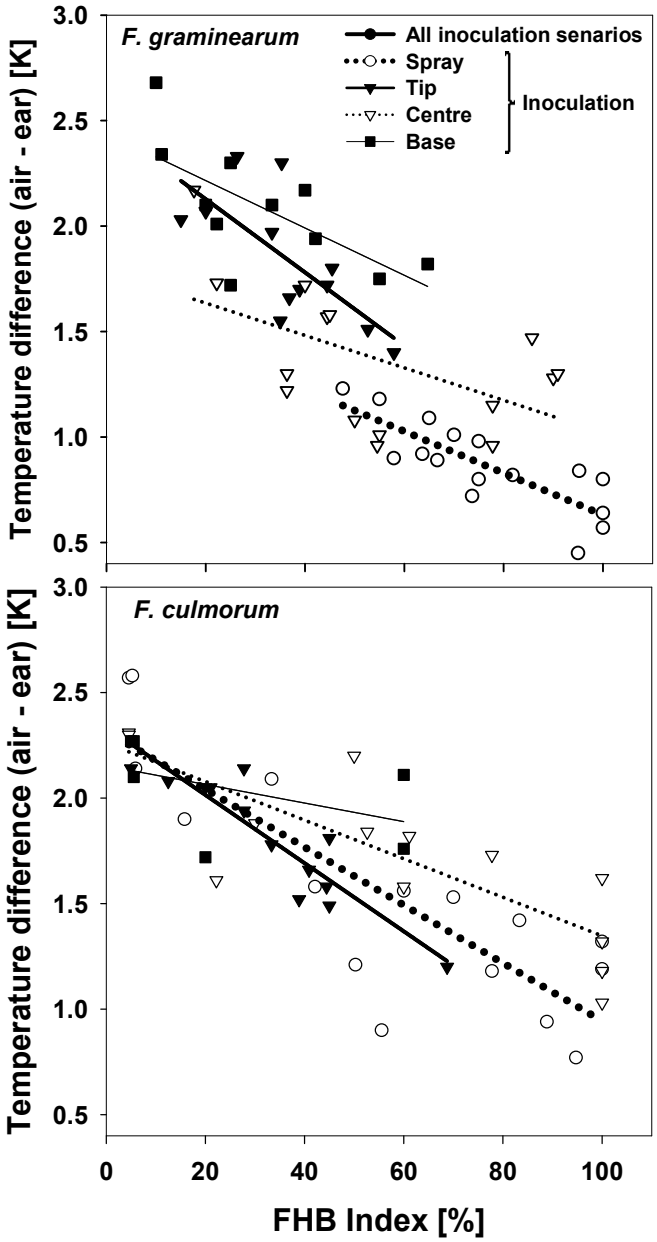

Figure 3.31 Relationship between visual estimation of *Fusarium* head blight (FHB index) and the temperature difference between air and ears 13 days post-*Fusarium* inoculation of wheat. Ears had been inoculated with *F. graminearum* and *F. culmorum*, respectively, by spraying, tip only, centre only, and base only at GS 61-65 ($n \geq 6$). Symbols stand for observations, lines represent linear estimation.

Table 3.22 Estimated parameter values of the linear regression between FHB index and the temperature difference between air and ears. Parameter *b* is the slope, *a* is the intercept. Ears had been inoculated with *F. graminearum* and *F. culmorum*, respectively, by spraying, tip only, centre only, and base only at GS 61-65. (n ≥6).

	Parameters	**Inoculation scenario**				**Combination of all scenarios**
		Spray	**Tip**	**Centre**	**Base**	
F. graminearum	*a*	1.62±0.15**	2.47±0.21	1.79±0.20	2.44±0.14	2.41±0.10
	b	-0.01±0.002	-0.02±0.005	-0.008±0.003	-0.01±0.004	-0.02±0.002
	R^2	0.66	0.51	0.29	0.46	0.69
F. culmorum	*a*	2.32±0.15	2.34± 0.08	2.26±0.13	2.15± 0.14	2.44±0.07
	b	-0.014±0.002	-0.02±0.002	-0.009±0.002	-0.004±0.004*	-0.011±0.002
	R^2	0.72	0.84	0.66	0.24	0.64

* Value not significantly different from 0

** Estimated parameter value ± standard error

3.5 Fusion of sensor data for monitoring *Fusarium* head blight at spikelets level

3.5.1 Disease development

The first symptoms of FHB were visible 3 dai with small necrotic lesions (1%) on glumes of ears inoculated with *F. graminearum*. Starting 5 dai, *F. culmorum* infection was associated with visible symptoms not significantly different from those by *F. graminearum*. FHB symptoms of both *Fusarium* species increased sharply 7 dai with no significant difference between the pathogen species (Fig. 3.32). The asymptotic stage of symptoms development was reached between 21 and 30 dai. Senescence started 21 dai and could be monitored easily through non-inoculated spikelets. At the last time point of assessment, the non-inoculated ears showed average percentage of 56.66 senescence (visually estimated), 30 dai (GS 83) (Fig. 3.32).

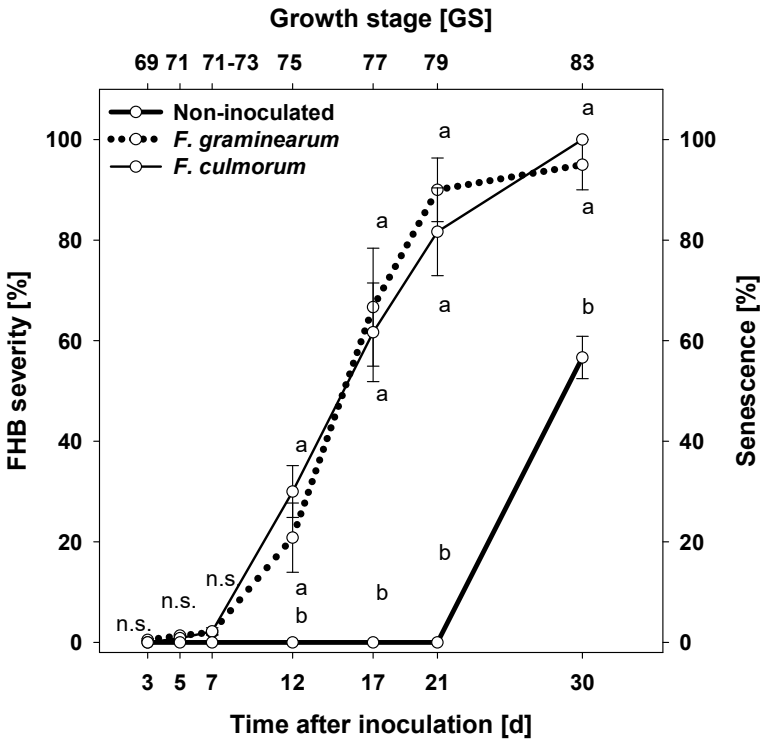

Figure 3.32 Progress curves of *Fusarium* head blight (% diseased spikelet area) due to *F. graminearum* (dotted line) and *F. culmorum* (solid line) in wheat spikelets after spray inoculation compared to non-inoculated control (bold solid line stands for senescence). Ears were inoculated at GS 61-65. Different letters at the same date differ significantly according to Tukey's HSD, $P \leq 0.05$ (mean ± SE: n = 6). n.s., not significantly different.

3.5.2 Effect of *Fusarium* infection on spikelet temperature

Infection of spikelets by *Fusarium* species affected the transpiration and altered temperature average and heterogeneity of those spikelets compared to non-inoculated control ones. The infection reduced TDs of inoculated spikelets as compared with the non-inoculated control 5 dai and was significant until 21 dai. TDs of non-inoculated control were higher than those of infected spikelets with both pathogens until senescence.

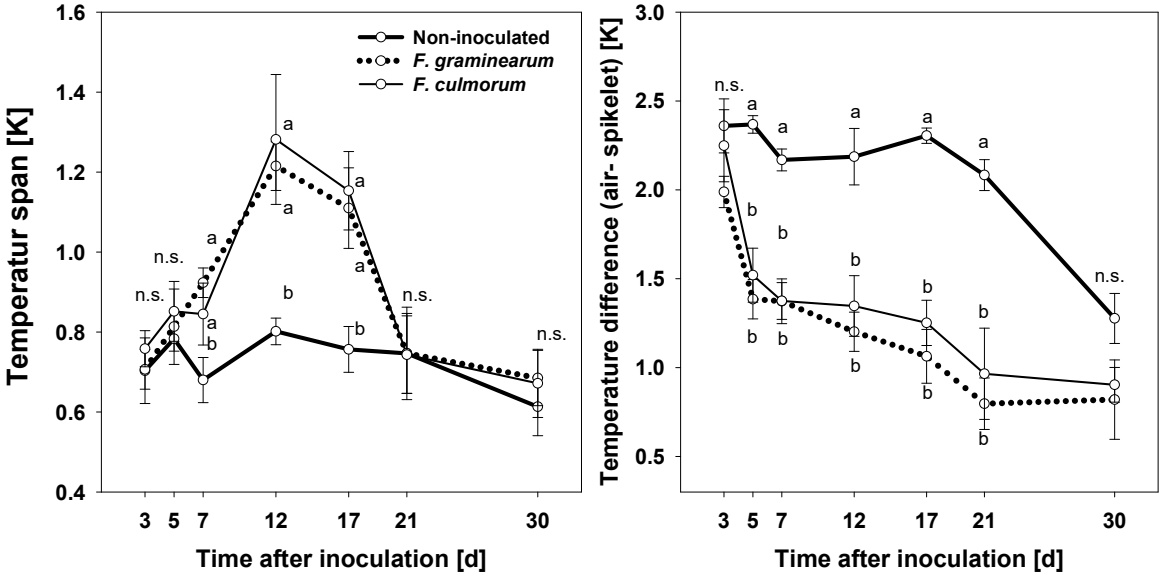

Figure 3.33 Effect of FHB caused by *F. graminearum* (dotted lines) and *F. culmorum* (solid lines) on the development of temperature span curves (a) and average temperature difference curves [air – spikelet] (a) compared to non-inoculated control (bold solid lines). Ears were spray-inoculated at GS 61-65. Different letters at the same date differ significantly according to Tukey's HSD, $P \leq 0.05$ (mean ± SE: n = 6). n.s., not significantly different.

Temperature span (TS) (Fig. 3.33), which indicates temperature heterogeneity within individual spikelets, increased 7 dai. Significant increases in TSs were observed starting at 7 dai for infected spikelets compared to non-inoculated control. The maximum TSs was observed at 12 dai, then the infected spikelets showed lower temperature heterogeneity. At 21 dai, GS 79, TSs of both infected and non-inoculated control spikelets were not significantly different (Fig. 3.33).

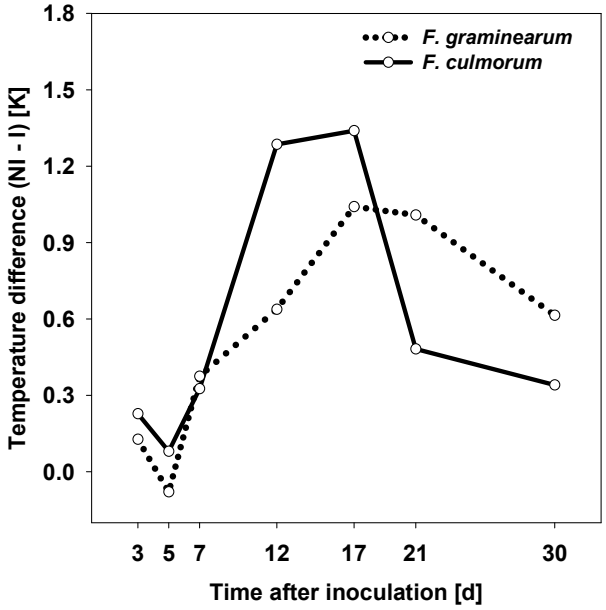

Figure 3.34 Effect of *Fusarium* head blight caused by *F. graminearum* (dotted line) and *F. culmorum* (solid line) on average temperature difference curves compared to non-inoculated control [non-inoculated control (NI) – inoculated (I)]. Ears were spray inoculated at GS 61-65.

The infection with *Fusarium* species reduced the average temperature of inoculated ears in comparison to the non-inoculated control ears after 3-5 dai, before symptoms become visible (Fig. 3.34). The temperature of infected ears increased over time; at 17 dai the temperature difference reached 1.04°C and 1.34°C for infected ears with *F. graminearum* and *F. culmorum*, respectively. After this time point, the temperature difference between infected and non-inoculated ears started to reduce and reached 0.61°C and 0.34°C for infected ears (*F. graminearum* and *F. culmorum*, respectively) in comparison to non-inoculated control (Fig. 3.34).

3.5.3 Effect of *Fusarium* infection on spikelet chlorophyll fluorescence

Fusarium head blight caused by both *Fusarium* species affected the photosynthetic activities of spikelet tissue at early infection stages and stopped it at bleached symptoms stage. The maximal fluorescence of dark-adapted spikelet was significantly reduced in spikelets infected by *F. graminearum* compared with those of *F. culmorum* and non-inoculated control 7 dai (Fig. 3.35). Infection of *F. graminearum* significantly reduced Fm 7 dai compared to non-inoculated control.

Starting 12 dai, *Fusarium* infection by both species significantly reduced Fm, and the differences were also pronounced 30 dai.

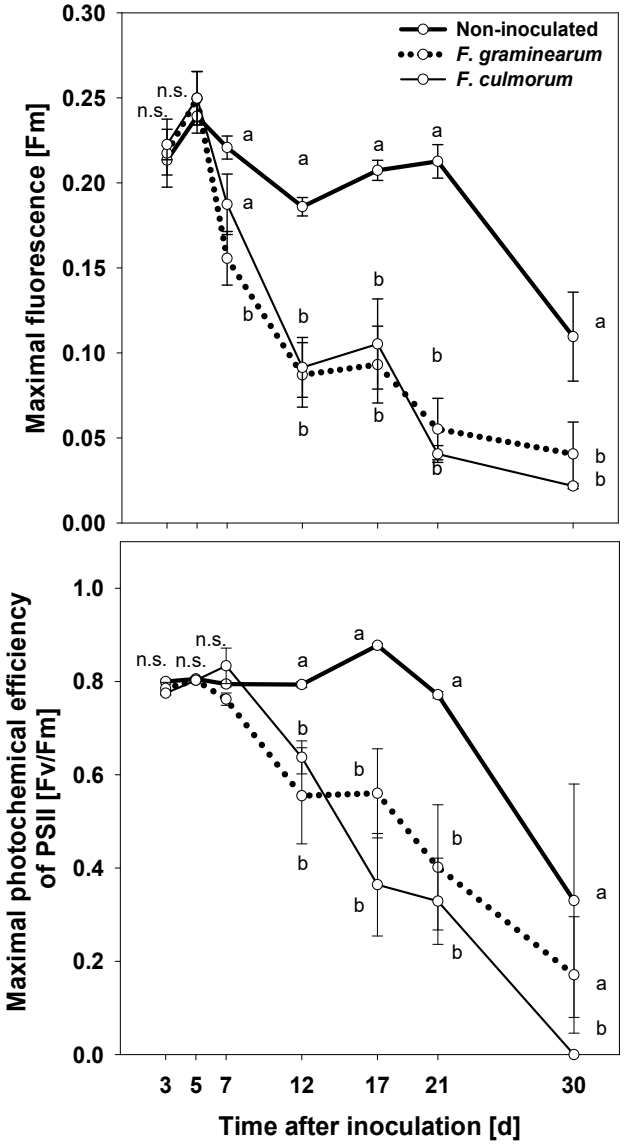

Figure 3.35 Effect of *Fusarium* head blight caused by *F. graminearum* (dotted lines) and *F. culmorum* (solid lines) on maximal fluorescence yields of dark-adapted spikelets [Fm] (a) and maximal photochemical efficacy of photosynthesis II [Fv/Fm in comparison to non-inoculated control (bold solid lines). Ears were spray inoculated at GS 61-65. Different letters at the same date differ significantly according to Tukey's HSD, $P \leq 0.05$ (mean ± SE: n = 6). n.s., not significantly different.

The maximal photochemical efficacy of photosynthesis II [Fv/Fm] was not affected by *Fusarium* infection during the first week after inoculation. Starting from 12 dai, Fv/Fm was significantly reduced until 30 dai for the infection with *F. culmorum* (Fig. 3.35).

Photochemical quantum yield Y[II] was able to differentiate between infected spikelets and non-inoculated ones during the first week after inoculation (Fig. 3.36). 12 dai, *Fusarium* infection reduced Fv/Fm and Y[II] significantly as compared to non-inoculated control. At the last time point of assessing, GS 83, Y[II] showed no significant difference between infected and non-inoculated control (Fig. 3.36).

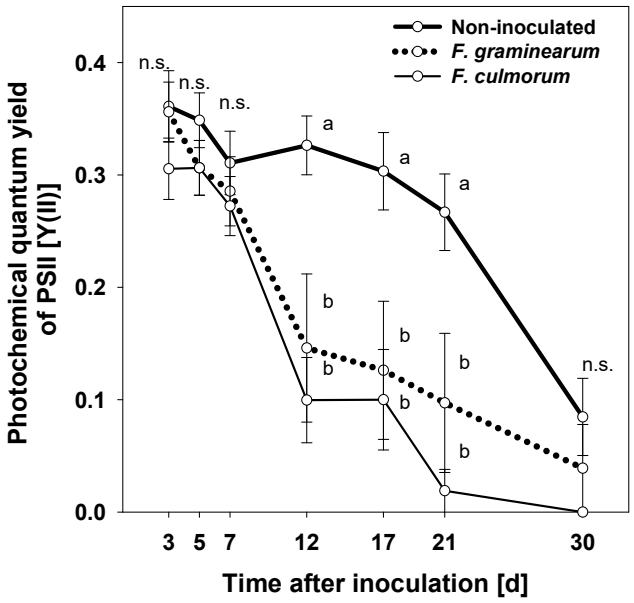

Figure 3.36 Effect of *Fusarium* head blight caused by *F. graminearum* (dotted lines) and *F. culmorum* (solid lines photochemical quantum yield Y[II] in comparison to non-inoculated control (bold solid lines). Ears were spray inoculated at GS 61-65. Different letters at the same date differ significantly according to Tukey's HSD, $P \leq 0.05$ (mean ± SE: n = 6). n.s., not significantly different.

3.5.4 Correlations among parameters of sensors and visual assessments

Sensor data were correlated to each other according to Pearson's method (Fig. 3.37). Indices of the sensors were significantly correlated to each other and to disease severity of visual assessment with different degrees of strength. However, TS was an exception. It showed no significant correlation with the other traits. The observed correlations were high and varied from 0.64 to 0.84. Pearson's

correlation method confirmed positive correlation among all selected indices, apart from VA which showed a negative correlation to sensor data (the strongest, -0.88 to Fv/Fm) (Fig. 3.37).

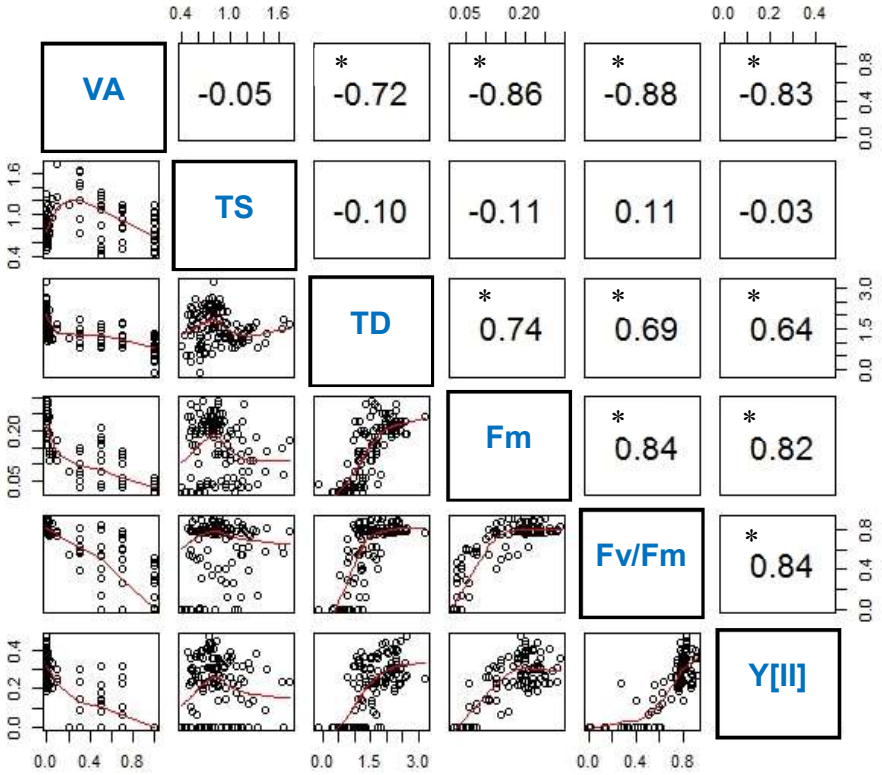

Figure 3.37 Correlation matrix among visual assessment of FHB and senescence (VA) and sensor data: temperature difference between air and spikelet (TD), temperature span within spikelet (TS), maximal fluorescence of dark-adapted spikelets (Fm), maximal photochemical efficacy (Fv/Fm) and photochemical quantum yield of photosynthesis II (Y[II]), (n = 126 pairs, Pearsons equivalent coefficient), Asterisk indicates significant correlation ($P \leq 0.01$).

Early and late symptoms of FHB compared to non-symptomatic spikelets in infected and non-inoculated control ears are shown in Fig. 3.38. The development of FHB symptoms could be assessed with the help of the non-invasive sensors 3 dai. Infected spikelets were warmer than spikelets from non-inoculated control and, exhibited an elevated temperature close to that of air 5 dai for the infection with both *Fusarium* species. At late infection stage, infected spikelets were wholly bleached and had almost the same temperature as the ambient air temperature. The chlorophyll fluorescence index Fm could detect the tissues where the infection had started 3 dai

especially for spikelets infected with *F. graminearum*. Over time, Fm was reduced to equalise the 0 values at 21 dai (Fig. 3.38).

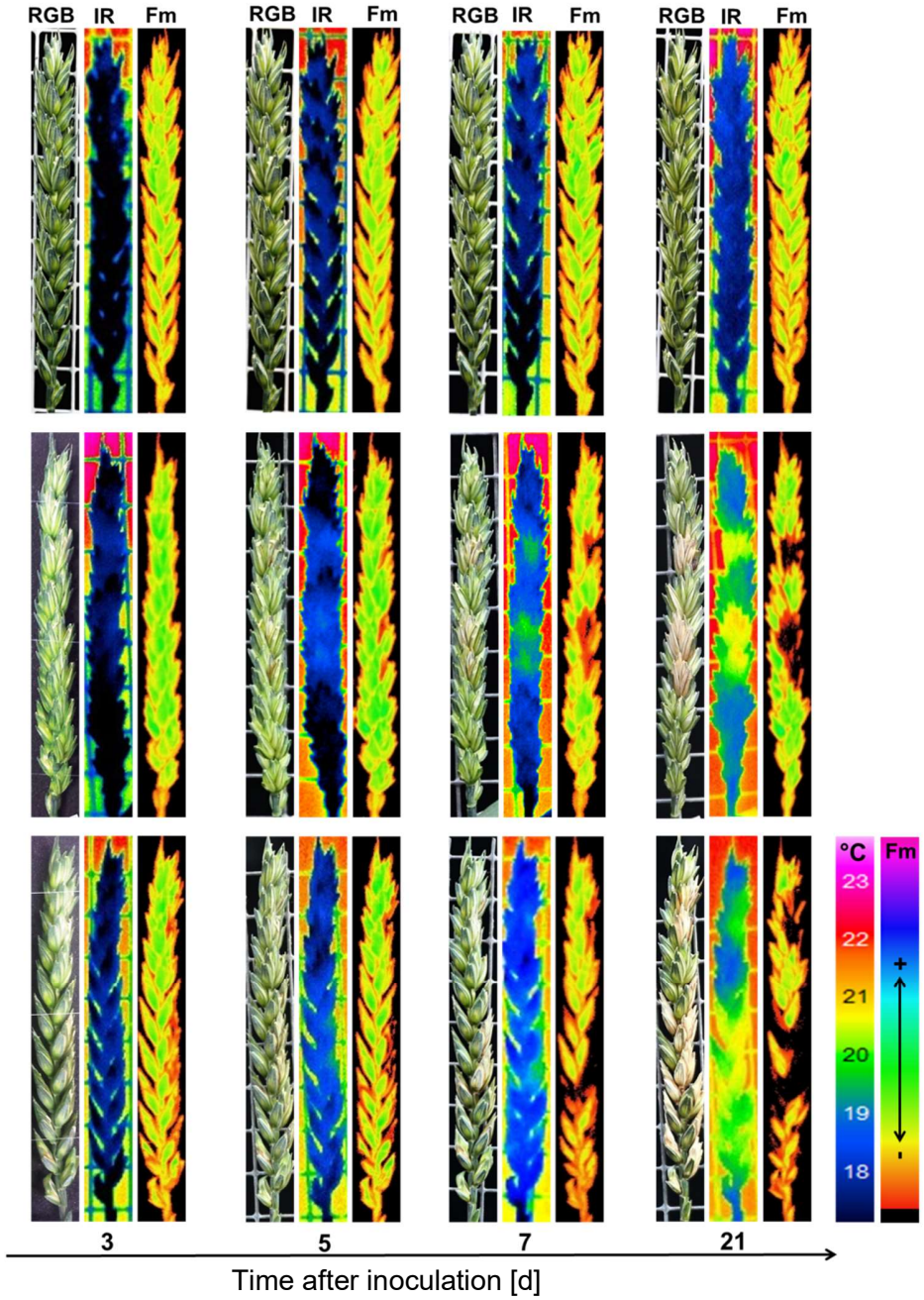

Figure 3.38 Spatio-temporal dynamics of *Fusarium* head blight caused by *F. graminearum* and *F. culmorum* compared to non-inoculated control visualised by digital images (RGB), false colour images of ear temperature (IR) and maximum chlorophyll fluorescence (Fm).

3.5.5 Classification of healthy and diseased spikelets by fusion of sensor data

Visual estimation of FHB and multisensory data, including TS and TD of IRT and Fm, Fv/Fm and Y[II] of CFI, were subjected to stepwise discriminant analysis for each time point of FHB estimation (Fig. 3.39). The features of different sensors used in the stepwise discriminant analysis were not always the same for each time points of assessment.

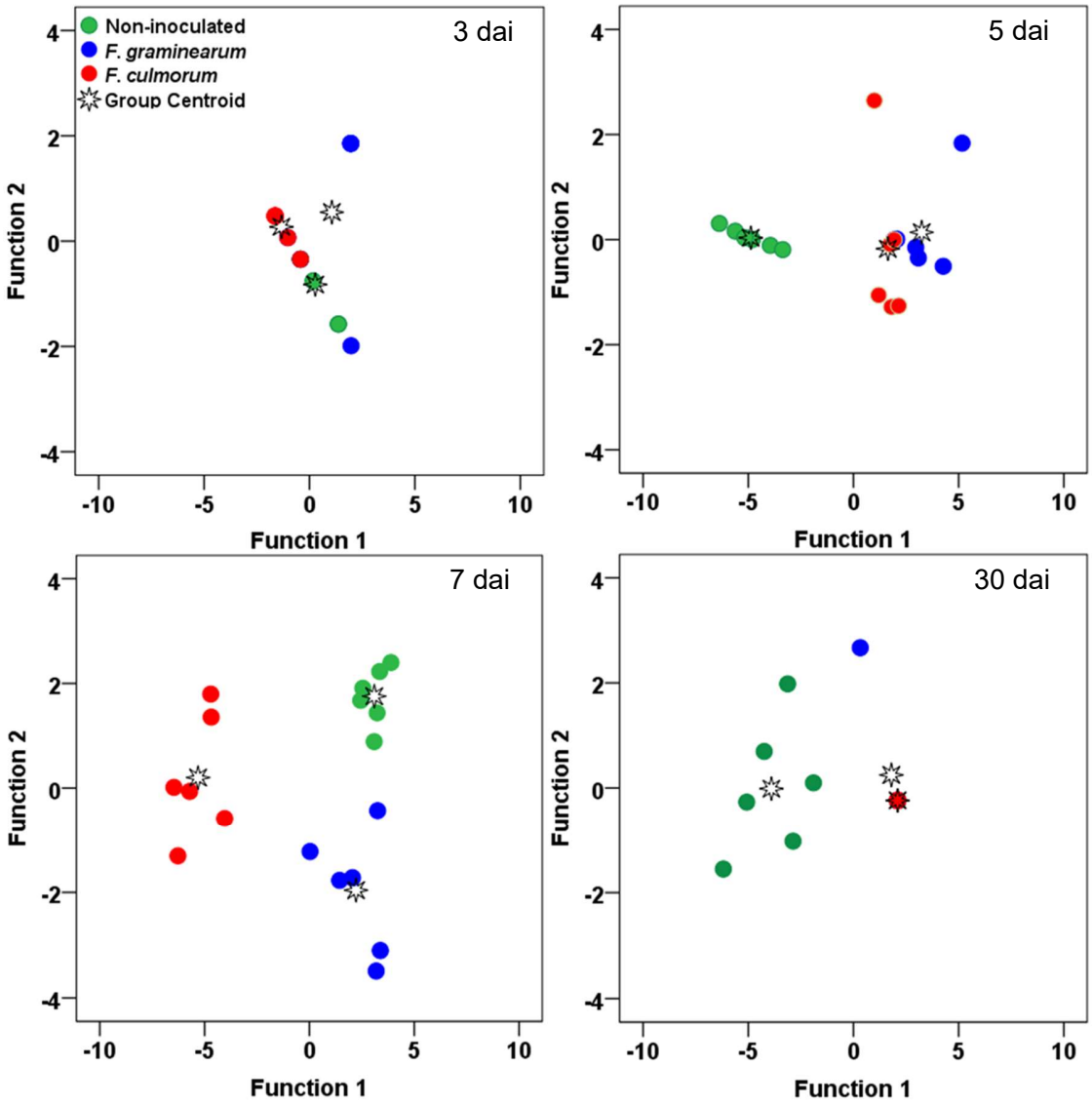

Figure 3.39 Scatter plots for discrimination of *Fusarium* head blight caused by *F. graminearum* and *F. culmorum* compared with non-inoculated control by fusion of sensor data from thermography, chlorophyll fluorescence, hyperspectral imaging and visual assessment using stepwise discriminant analysis for each assessment (3, 5, 7, and 30 dai) date. n = 6

At 3 dai, the group's centroids of all treatments were near to each other. However, the accuracy of the prediction was 77.8% (Tab. 3.23). The group's centroids were more separated over the time. The accuracy of the prediction in parallel improved to reach 100% starting at 7 dai. From 21 dai on, the group's centroids of *F. graminearum* and *F. culmorum* were again close to each other, and the discrimination was reduced to 72.2% (Tab. 3.23).

Table 3.23 Confusion matrix for the classification result of the stepwise discriminant analysis for each assessment date shows the predicted and the original estimation for each treatment.

Date	**Original group membership**	**Predicted group membership**		
		Non-inoculated control	***F. graminearum***	***F. culmorum***
3 dai	Non-inoculated control	6	0	0
	F. graminearum	2	3	1
	F. culmorum	1	0	5
	Accurate prediction 77.8%			
5 dai	Non-inoculated control	6	0	0
	F. graminearum	0	4	2
	F. culmorum	0	0	6
	Accurate prediction 88.9%			
7 dai	Non-inoculated control	6	0	0
	F. graminearum	0	6	0
	F. culmorum	0	0	6
	Accuracy 100%			
12 dai	Non-inoculated control	6	0	0
	F. graminearum	0	6	0
	F. culmorum	0	0	6
	Accuracy 100%			
17 dai	Non-inoculated control	6	0	0
	F. graminearum	0	6	0
	F. culmorum	0	0	6
	Accuracy 100%			
21 dai	Non-inoculated control	6	0	0
	F. graminearum	0	4	2
	F. culmorum	0	3	3
	Accuracy 72.2%			
30 dai	Non-inoculated control	6	0	0
	F. graminearum	0	1	5
	F. culmorum	0	0	6
	Accuracy 72.2%			

4. DISCUSSION

The genus *Fusarium* includes some of the most damaging plant pathogens leading to significant annual losses worldwide (Elmer 2015). A wide range of economically important plants suffers from *Fusarium* infection like *Allium cepa* bulbs in Germany which can be infected by up to 24 toxigenic *Fusarium* spp. (Boehnke et al. 2015). In wheat, *Fusarium* head blight (FHB) is the most devastating disease caused by many species (Parry et al. 1995). *Fusarium* species differ in the geographical distribution according to environmental conditions (Infantino et al. 2012; Popovski and Celar 2013). Even at a local area with similar environmental conditions a high diversity in *Fusarium* species profile was found (Schlang 2010). *Fusarium* species also varied in their ability to produce mycotoxins, which is affected by the environmental conditions as well (Meyer 2006). Disease management is a big challenge because of the lack of resistant sources. Moreover, resistance to this disease is a complicated trait that might be controlled by a complicated gene network (Bedawy 2013). Fungicides against FHB provide limited control (Lienemann 2002). The Azole fungicide group, which include the highest effective fungicides against this disease, does not provide 100% control efficacy (Meier 2003). The current problematic situation of FHB triggers applying innovative research methods to promote our understanding of this complex disease. Site-specific application of fungicides following precision agriculture techniques might efficiently contribute against FHB. Precision agriculture integrates sensors, methods of data analysis and pest management systems to optimise agricultural practices according to the spatial and temporal variability in the field (Mahlein 2016). Integrating such sensors for studying FHB under controlled conditions was recently reported by Al Masri et al. (2017). Further steps in studying this disease by applying sensors under field and controlled conditions were achieved, interpreted and brought into context in the followings.

4.1 Impact of foliar wheat diseases and their control by fungicides on *Fusarium* head blight

The wheat crop can be infected by many pathogens singly or simultaneously. The simultaneous attacks of different organs of the same host plant by different pathogens are well described in the literature (Jesus Junior et al. 2014). The infections can alter the plant's physiology, for instance by increasing the susceptibility of the plant to the infection by other pathogens (Paula et al. 2010). Moreover, in the case of foliar wheat diseases, it increases the chance of leaf infection by *Fusarium* spp. and may contribute an extra source of inoculum for the occurrence of FHB (Ali and Francl 2001). An investigation of the relationship between foliar wheat diseases including their fungicidal control with wheat head blight was carried out in two field trials of 2014 and 2015 planting seasons. In the 2015 experiment, the nitrogen level (N100 and N50) was introduced as a new factor, and the hyperspectral reflectance of the wheat canopy was measured at GS 73. Additionally, two treatments of fungicides were introduced in the 2015 experiment, one against foliar wheat disease and another one against FHB.

Foliar diseases varied in their presences and reactions to the investigated factors between Tobak and Pamier within the same environmental conditions which are in line with the previous findings by Zhang et al. (2006). For example, higher nitrogen levels increased the severity of brown rust on Pamier which was earlier confirmed by Ma et al. (2004). Only in the 2014 experiment, Tobak showed a higher susceptibility to brown rust as already reported (Anonymous 2013). The management of foliar pathogens with fungicides may help in reducing FHB intensity by decreasing the amount of inoculum (Ali and Francl 2001). Even with no visible symptoms on leaves, *Fusarium* infection can develope on maize leaves (Xuan 2014). A positive correlation was found between the presences of foliar diseases and leaf infection with *Fusarium* species which is an indication of higher FHB occurrence as has been observed in both years. Among the 17 *Fusarium* spp. associated with FHB (Parry et al. 1995), 10 species were isolated from wheat kernels in 2014 and 2015 experiments. Although *Fusarium poae* is considered to be a relatively low virulent pathogen of cereals, recent studies by Stenglein (2009) identified this pathogen as a frequently occurring pathogen with FHB in wheat which is in accordance with the finding of the current research. Visible

symptoms of FHB manifested earlier in 2014 field trial compared to 2015, an indication that the environmental condition has a substantial effect on the development of wheat and establishment of FHB infection.

Wheat canopy grown with N50 was associated with lower FHB incidence on both varieties. However, this relationship was not significant which is in line with the findings of Teich and Hamilton (1985), Fauzi and Paulitz (1994) and Aufhammer et al. (2000) who reported no relationship between N levels and FHB occurrence. In contrast, a positive correlation was reported by Lemmens et al. (2004), Ma et al. (2004) and Muhammed et al. (2010). The later explained this enhancement by more suitability of *Fusarium* conidia to germinate at higher nitrogen levels. Yang et al. (2010) and Hofer et al. (2016) claimed a negative correlation. Hofer et al. (2016) explained this relationship by the influencing of canopy characteristics and possibly its physiology through N fertilisation which restricted *Fusarium* grain infection.

Tobak showed higher susceptibility to FHB than Pamier in both trials which is in line with (Anonymous 2013). FHB incidence was not significanty correlated to kernels infection (expressed as FIK) and TKW, which might be attributed to the primary site of ear infection (Al Masri et al. 2017). The overall low correlations among FHB severity, infected kernels and TKW are explained by the pathogen spread within ears downwards more than upwards and the effect on yield formation which is lower for infections of the upper parts of ears. Additionally, higher temperature after anthesis accelerated the development of ears and helped kernels to escape the expansion of *Fusarium* infection within ears through the senescence. Among investigated parameters, only FDF was negatively correlated with TKW, which showed that the foliar diseases on the flag leaf are associated with a significant effect on TKW. This relationship is not straightforward when it comes to investigation (Zhang et al. 2006). The non-significant relationship between TKW and FHB, as proved in this research, is in accordance with Alvarez et al. (2010), but contradicts the findings of Lemmens et al. (2004) and Brennan et al. (2005) who proved a significant correlation.

In total, the linear regression analysis between FHB incidence and foliar wheat diseases proved that FHB is a function of foliar diseases which was evident by observations of 2014 and 2015 experiments. Moreover, observations by the marginal variety of Sokrates in the 2015 experiment revealed similar results. The extension of the vegetation phase of wheat canopy due to the application of fungicides like benzimidazoles, triazoles and strobilurins (Fletcher and Nath 1984;

Beck 2002; Berdugo 2013) were also observed in the present study during the 2015 experiment in some Sokrates plots (3×3 m). Strobilurins and triazoles fungicidal groups might influence the phytohormones and reduce the oxidative stress associated with plant senescence which in total extend the green period of the wheat canopy (Cromey et al. 2004; Jaleel et al. 2006). Based on this effect, areas of (~1×3 m) of the marginal variety, which received fungicides against foliar diseases, showed extended vegetation period and allowed the possibility of additional observations of FHB incidence.

The assessment of proteins content of kernels (RPR, PR) from the 2015 experiment revealed a significant effect of N levels on both varieties which is in accordance with Zhao et al. (2005). The application of foliar urea at the start of grain filling and fungicides to control foliar diseases of wheat might eliminate the reduction in grain proteins (Dimmock and Gooding 2002). In the current research, the fungicide application against foliar diseases showed no effect on protein content. However, fungicide application against FHB had a significant effect on Tobak regarding protein content. Protein deposition and starch synthesis during the development of kernels are functions of different mechanisms (Jenner et al. 1991). *F. graminearum* infection does not profoundly alter the grain protein profile and does not significantly disturb the early process of grain ontogeny. However, it impacts molecular changes during the grain filling stage which impact the starch synthesis and storage proteins (Chetouhi et al. 2014). In both varieties and among all factors, the percentage of protein and starch was not changed due to FHB, suggesting that the pathways for protein/starch biosynthesis and disease response are different. This is in line with the findings of Wang et al. (2005) and Martin et al. (2017). Similar investigations on the effect of *Fusarium* infection on protein content have shown rough increases (Boyacioğlu and Hettiarachchy 1995) and decreases in starch content (Boyacioğlu and Hettiarachchy 1995) which was not recognised in the current research when all investigated factors were considered.

Hyperspectral reflection, measured by hand-held ASD FieldSpec spectroradiometer was characteristic for vital wheat canopy under field conditions in comparison with other reports (Asner 1998; Pradhan et al. 2014; Yue et al. 2017). It has provided a high sensitivity in measuring the canopy status at GS 73, considering the applications of fungicide and the nitrogen levels before any visible symptoms of FHB. Fungicide application affects not only the foliar and head diseases of wheat but also influences the physiology of wheat which is in turn delays senescence of flag

leaves (Berdugo et al. 2013). The application of bixafen and fluoxastrobin had a significant effect on leaf reflectance (Berdugo et al. 2013). These differences in reflectance were most pronounced in the VIS range at 550-650 nm especially at advanced growth stages of wheat because of the delay of senescence. However, at GS 71 very marginal effect of fungicide application were found in comparison to non-treated control. This finding supports the hypothesis of the current study that foliar diseases and the potential FHB occurrence are the key factors affecting the reflectance spectra at GS 73 when to compare similar N-supply treatments.

Nitrogen concentration in plants significantly affects pigment concentration which in turn affects leaf colour (Pradhan et al. 2014). The spectral reflectance in NIR (760-1120 nm) of N100 treatments showed comparatively higher than that of N50 which is in line with the findings of (Pradhan et al. 2014). They reported additionally lower reflection in the visible range for treatments with nitrogen deficiency which was not observed in the current research. The higher reflection at NIR is attributed to the higher leaf area index in N100 which is positively correlated to nitrogen fertilisation (Chang et al. 2005).

Hyperspectral reflectance was widely applied to characterise different foliar crops diseases. Kuska et al. (2015) investigated the resistance reaction of different barley genotypes to *Blumeria graminis* f.sp. *hordei* and proved the potential of hyperspectral imaging (HIS) to characterise this pathosystem based on the level of resistance and susceptibility of the infected barley genotype. Yellow rust in winter wheat has increased the reflectance in the VIS and reduced it at NIR (Jing et al. 2007). The reflectance of wheat canopy decreased with the increased powdery mildew index at NIR range (Cao et al. 2013). The potential of HSI in detecting and characterising FHB after symptoms become visible has been reported by Bauriegel et al. (2011), Bauriegel and Herppich (2014). Reflectance spectra measured in the current work are not oriented to measure the effect of a specific wheat disease because it is under field condition and after anthesis. In other words, a combination of head blight and foliar diseases has the potential to occur even without visible symptoms which affect the reflectance spectra. Therefore, parameters that are related to specific physiological aspects need to be derived from the measured reflectance spectra for further investigations.

Spectral vegetative indices (SVIs) indicate specific parameters of plant functions and reduce the data dimensionality of reflectance spectra (Delalieux et al. 2009; Mahlein 2010). The 11 SVIs

investigated in the current study were categorised into three classes including pigments-based indices (NDVI, PRI, BGI2, PSSRa, b and c), plant senescence reflection index (PSRI) and water indices (WI1, 2, 3 and 4). Pigments are controlled by the chemical and the biological activity of host plant (Sims and Gamon 2002). N level has a significant impact on most of the pigment-based indices except PRI, and the most pronounced impact was on NDVI. This finding can be attributed to the importance of N in pigment formation of the wheat canopy. Also, the application of fungicide to control foliar diseases revealed a significant impact on chlorophyll content expressed as PSSRa and PSSRc on Tobak canopy and thus may have affected the photosynthetic apparatus with negative implication on grain yield. The presence of pigment including chlorophyll-a and chlorophyll-b plays a critical role affecting spectral reflection (Moroni et al. 2013).

Because of the vitality of wheat canopy of both variety in GS 73, Photochemical senescence refection index (PSRI) was very close to zero and not affected by different treatments. The reflection in the SWIR region was higher at low N levels which might be attributed to lower canopy water content (Pradhan et al. 2014). Low N levels might lead to a reduction in transpiration which increases the canopy temperature and in turn, lowers plant water status (Aggarwal et al. 2006). In the current investigation, only the combination of N50 and foliar diseases presence was associated with lower water content as indicated with W1.

Using indices to extract and interpret data of HSI might be promising to develop sensors that can measure specific bands and report the casual stress factor specifically (Mahlein et al. 2010). Moreover, they can be a good indicator when they are correlated to each other and to those from measuring the quality and quantity of harvested kernels. The SVIs were mostly correlated to each other which is in line with the finding of Mahlein (2010), and some of them showed a significant correlation to quality and quantity parameters of kernels which is of great importance in the application of sensors. FHB incidence was significantly correlated to PRI and BGI2 which might provide a valuable non-invasive predictor of FHB before symptoms become visible. The spectral changes during FHB development are related to modifications in carotenoid (500 to 533 nm) and, in particular, of chlorophyll contents (560 to 675 nm and 682 to 733 nm) (Bauriegel and Herppich 2014) which is in accordance with the findings of the current results. However, they also referred to changes in between 927 and 931 nm which were not observed in the current research.

SVIs were used to study foliar wheat diseases, but individually. Nicolas (2004) investigated the correlation between the severity of *Zymoseptoria tritici* infection and the yield of wheat and proved a negative correlation between GY and NDVI. Huang et al. (2007) correlated the visual assessment of YR to PRI and proved the potential of PRI for quantifying yellow rust in winter wheat; similar results were found by Jing et al. (2007) using PSSRa. However, none of the foliar diseases parameters (AUDPC or FDF) showed any relationship to any of the investigated SVIs. This missing relationship might be attributed to the low presence of foliar diseases at measuring time (GS 73). Additionally, the presence of the ears at this growth stage can be the reason.

Spectral reflectance is potentially useful as a predictor of grain protein content and quality in wheat (Zhao et al. 2005; Li-Hong et al. 2007). NDVI, PSSR a, b and c were highly correlated to proteins content of kernels in the 2015 experiment. Grain yield showed a significant correlation to all investigated SVIs whereas TKW was significantly correlated only with water indices. Similar results have been reported by Prasad et al. (2007), Li-Hong et al. (2007) and Pradhan et al. (2014) regarding the correlation of GY to NDVI and WI.

The epidemiological implications of foliar diseases co-occurring on the same crop are essential because the establishment of disease management strategies depends on the knowledge of disease interactions (Jesus Junior et al. 2014). In studying the interaction between foliar wheat diseases and FHB, it was not possible to control foliar diseases without the application of fungicide which had a side-effect on *Fusarium* pathogens on leaves. Therefore, the new outlook from the current study is to investigate this kind of interaction under controlled conditions in which foliar pathogens are manageable without fungicide application. In the current research, the correlation among different parameters of 2015 experiment was made in an attempt to imitate the conditions in the field where different factors of stress interact in wheat canopies. The current research proved the relationship between foliar diseases including their control by fungicides and FHB which provides new insight into FHB control. Moreover, out of 11 SVIs investigated, BGI2 and PRI proved their potential in predicting *Fusarium* infection on ears under field conditions and before symptoms become visible.

4.2 Impact of primary infection site of *Fusarium* species on head blight development

Wheat is most susceptible to the infection by *Fusarium* species at anthesis (Xu et al. 2007). Anthesis starts at the central spikelet of ears and extends up- and downwards (Brown et al. 2010). For a wheat canopy in the field, the period of anthesis, i.e. the period of highest susceptibility, expands when main stem and tillers of plants differ in the developmental stage and thus increases the probability of FHB. The heterogeneity in growth stages on the scales canopy, plant, ear, and even spikelet results in differences in susceptibility to *Fusarium* infection and the well-known phenomenon of the coexistence of diseased and healthy ears, spikelets, and kernels in the field. FHB incidence of cv. Passat reached 90-93% at the asymptotic stage after spray inoculation by *F. graminearum* and *F. culmorum*, respectively. The interaction between wheat varieties and *Fusarium* species, the duration of the favourable conditions of FHB and the timing of the inoculation, within anthesis phase, are some non-genetic factors of host plants which make the understanding of the disease even more complicated (Bai and Shaner 2004). Only in rare cases, the level of *Fusarium* infection results in homogenous regions of FHB incidences close to 100%.

After lesion extension, the characteristic symptoms of FHB, bleached spikelets, start to become visible. The penetration of host tissues occurred from the inner surface of lemma, glume and palea and on the upper side of the ovary (Kang and Buchenauer 2000). The pathogen spread downwards to rachilla and rachis node following both inter and intracellular growth. Afterward, the infection develops up- and downwards from the rachis node. Series of alterations occurred in ears tissues, including degeneration of host cytoplasm and organelles, the collapse of parenchyma cells, the disintegration of digestion of host cell walls (Kang and Buchenauer 2000) which lead to the typical bleached symptoms of FHB. FHB index did not significantly differ among inoculation scenarios 6 dai. Miedaner et al. (2003) reported that spray and centre inoculation resulted in similar levels of disease severities. The infection spread from one spikelet to others was not consistent within the same infection scenario. Some ears were entirely infected from locally infected spikelet, in others; the infection was restricted to inoculated spikelets without any pathogen spread although spikelets were bleached. This spread is not well understood yet (Brown et al. 2010). At 10 dai, the sections of lemma proved the mycelium growth on the surface to the inner part of the floret which might be enhanced with the short-term application of moisture. Kang and Buchenauer (2000) reported that

networks of hyphae are formed starting from 2 dai on the inner surfaces of lemma and glume and palea, but not on their outer surface.

The spread of *Fusarium* spp. from rachilla can plug the rachis and can affect the movement of water and nutrients to the top of ears (Lemmens et al. 2004). Centre and base infection caused very often complete plug of the rachis and typical bleached spikelets above the inoculated spikelets. This mechanism of symptom development is absent after tip inoculation which may explain why FHB index after tip inoculation was low compared to the other inoculation scenarios. FHB is considered as a monocyclic or one cycle disease for the infection with *F. graminearum* and *F. culmorum*. In other words, after the infection has taken place, very few secondary infections develop from the primary infection by conidia formed in infected tissues (Wegulo 2012). The progress of monocyclic diseases is mostly described by monomolecular functions that show a high goodness of fit (Campbell and Madden 1990). The development of FHB after combing all infection scenarios and for individual infection scenarios showed the shape of monomolecular functions.

The pathogenic aggressiveness varies among *Fusarium* species (Goswami and Kistler 2005) and isolates. The same *Fusarium* species may behave differently under different temperature and humidity conditions (Meier 2003; Brennan et al. 2005). In the current study, a regime of 18/12°C day/night was applied considered to represent cool, wet summer conditions in central Europe. The higher aggressiveness of *F. culmorum* in producing FHB symptoms is in accordance with the reports on the predominance of *F. graminearum* and *F.culmorum* in warmer and cooler regions, respectively (Parry et al. 1995; Osborne and Stein 2007). Meier (2003) made the same observations when FHB developed after centre inoculation of *F. graminearum* and *F.culmorum* under similar environmental conditions. *F. graminearum* has been reported to increase over *F. culmorum* in several countries of Europe, such as in the UK and northern Germany (Jennings et al. 2004, Desjardin 2006). These increments could be justified by the increase of maize cultivation during the recent decades in these countries, like in Germany as reported by Desjardin (2006).

Investigating the effect of FHB on yield loss as estimated from EW showed that *F. culmorum* does not affect yield loss in most of the infection scenarios, except after base infection. In contrast, the reduction in TKW was significantly different from the non-inoculated control for all infection scenarios except the one after tip inoculation. The infection with *F. graminearum* resulted in significant reduction of both EW and TKW with exception to the infection after tip inoculation.

This finding revealed the non-reflection of visual assessment of FHB of *F. graminearum* and *F. culmorum* in the reduction in grain yield.

Resistance to kernel infection plays a crucial role in FHB epidemics (Mesterhazy 2002). However, non-genetic factors like the position of the primary site of infection may influence *Fusarium* infection of kernels and grain filling in different ways. Bleached spikelets (at the tip) are associated with reduced TKW, but kernels may be not infected by *Fusarium* spp. (Lemmens et al. 2004). With primary infection of the ear's base, FHB significantly reduced TKW, but the upper kernels where not infected and only 31.3% of total kernels were infected. After tip inoculation, in contrast, the pathogen was able to infect the kernels even at the ear's base and resulted in 45.9% infected kernels. The up and downward spread of the pathogen after centre inoculation confirmed that the downward colonisation of ears is stronger than upwards. Argyris et al. (2005) noticed that tissue desiccation could play a barrier role against pathogen growth and prevent it from expansion to the upper bleached spikelets. The observed patterns of *Fusarium* spread within ears also confirmed more recent studies by Brown et al. (2010) and Malbrán et al. (2012) for centre infection with *F. graminearum*.

The condition 18/12°C day/night allowed the pathogens to develop downwards and colonise the upper part of stems and flag leaves. This development was significantly affected by the primary site of ear infections. The spray and base inoculations, which caused infections in the basal part of ears, allowed a better movement of the infection to the upper part of stems and then the flag leaf. In contrast, this development of pathogen did not reach the stems after tip inoculations and with a lower degree after centre inoculation because of the ripening at later stages of ear developments. After spray inoculation, FHB caused the highest disease severity (AUDPC) and the highest reduction in grain weight. A strong negative correlation between disease severity and grain yield was described by Lemmens et al. (2004) and Brennan et al. (2005). Tip inoculation resulted in the lowest AUDPC values and no kernels weight reduction (the number of kernels per ear was not assessed). Although FHB index and AUDPC after centre and base inoculations were not significantly different from that after tip inoculation, centre and base inoculations resulted in significant TKW reductions. These results demonstrate an only weak relationship between disease severity and reducing kernels weight. Moreover, the higher aggressiveness of *F. culmorum* compared to *F. graminearum* as measured in AUDPC was not retrieved in a stronger reduction of

TKW. This suggests that the *Fusarium* species responsible for FHB determines the shape of the relationship between disease severity and yield effects and verifies the assumption of Brennan et al. (2005). Effects of the primary site of infected spikelet within ears and the specific *Fusarium* spp. involved in FHB may explain why Alvarez et al. (2010) did not observe a correlation between disease severity and grain loss.

Bai and Shaner (2004) studied types of resistance to the initial infection referred to as Type I resistance, and to the further development of the pathogen within an ear, described as Type II. They estimated resistance to Type I and Type II by spray and single floret inoculation, respectively. The exponential functions developed in this study are useful tools to simulate resistance Type II when the frequency of *Fusarium*-infected kernels was assessed for the different spikelet levels. Parameter *a* estimates the infection success at the site of inoculation, while *b* and *c* characterise the slopes as indicators for up and downwards spread of the pathogen. Kiyosawa and Shiyomi (1972) were the first who used the exponential function to describe gradients of plant diseases in fields. On-ear level, the site of primarily infected spikelet proved to play a crucial role in the infection gradients.

DON accumulation in harvested grain is not fully understood in relation to FHB intensity according to many reports. Paul et al. (2005) have conducted a meta-analysis of 163 reports studying FHB and proved that FHB index is significantly correlated with DON. In contrast, Alvarez et al. (2010) reported that TKW is a good indicator of DON accumulation in the harvested kernel. In the current study, different infection scenarios provided detailed results about FHB regarding both FHB index and TKW. Mycotoxin analysis based on different primary sites of ear infection might provide valuable insight into understanding the relationship between DON accumulation and FHB intensity.

4.3 Characterising the impact of environmental conditions on *Fusarium* head blight development within ears

Temperature, air humidity and the availability of water are the most critical environmental factors that influence the epidemic outbreak of FHB (Brennan et al. 2005; Popovski and Celar 2013). A particularly interesting topic for future research is studying the effects of climatic conditions on *Fusarium* diseases which may prove useful strategies for developing novel methods of disease management (Popovski and Celar 2013). Investigating the tip, centre and base *Fusarium* infection scenarios which were above discussed, was made under 18/12°C day/night and wet conditions (Al Masri et al. 2017). The same scenarios of infection were developed by inoculating *F. graminearum* and *F. culmorum*, but different environmental conditions were applied after infection (48 h of incubation) until ripening.

Differences in FHB incidences were not only observed between *Fusarium* species or among inoculation scenarios (injecting the inoculum or spray inoculation) but also depending on the environmental conditions after infection. This finding verifies the claims of many reports about the complex nature of this disease. FHB incidences developed at 18/12°C wet were higher than that under dry conditions. The results suggested that the infection after incubation (48 h) was possible only under wet conditions, meaning short-term spells of moisture. Xu et al. (2007) reported that the incidence of infection in wheat ears is increased when the period of wetness and temperature is longer. The data presented here suggest that the differences in disease incidences between *Fusarium* spp. were most pronounced at 18/12°C accompanied by dry conditions. In this environment *F. culmorum* caused disease incidences significantly higher than *F. graminearum*. Rossi et al. (2001) reported that the relative humidity increased the frequency of glume infections by *F. culmorum,* whereas these conditions were unfavourable for *F. graminearum*. The interaction between wheat ears and *Fusarium* species was different at 24/18°C where both *Fusarium* species caused similar FHB incidences. These results confirm former findings that fungal pathogens that are associated with FHB behave differently in different environments (Xu and Nicholson 2009). However, the interaction between wheat varieties and *Fusarium* species, the duration of the favourable conditions for FHB and the timing of the inoculation, within the anthesis phase, are some non-genetic factors of host plants which make the understanding of this disease even more complex (Bai and Shaner 2004).

Al Masri et al. (2017) have proved that this development is variable when the position of the primary site of ear infection is considered (tip, centre or base). The current study proved further that this development is affected by the environmental conditions under which the disease is developing. For example, tip and base infections caused low disease severity under all environmental conditions in comparison to that after spray and centre inoculations with exception to that at 18/12°C wet for the infection with *F. graminearum*. The kinetics of *Fusarium* infections after single spikelet inoculations within ears are indicators for the resistance Type II to FHB (Dweba et al. 2017). If a *Fusarium* infection was associated with symptoms, Champeil et al. (2004) called this resistance Type III (which meets the FHB index in this study). The current findings urged the importance of considering these factors when studying Type II or Type III of FHB resistance.

The prolongation of the growth stages of wheat at 18/12°C, in comparison to 24/18°C, gave *F. graminearum* the time to develop and colonise areas from ears similar to that of other infection scenarios. On the other hand, higher temperature shortened the growth stages of ear development and in consequence lower areas of ears were infected. However, at 24/18°C wet FHB index reached the asymptotic stage of the disease progress curves in a shorter time, which means acceleration in disease development can be revealed from slopes estimated by a logistic function. Brennan et al. (2005) reported similar results and explained this behaviour with a higher susceptibility of the host or a higher aggressiveness of pathogens, or a combination of both at higher temperatures. Lovell et al. (2004) explained this acceleration as a result of the fact that the fungus is growing according to thermal time and consequently the symptoms at the lower temperature (16°C) take longer time. Doohan et al. (2003) showed that trichothecene production by *F. culmorum* and *F. graminearum* is favoured by warm and humid conditions, which might be another reason causing this acceleration.

At 18/12°C, the aggressiveness of *F. culmorum* was more than of *F. graminearum* compared to that at 24/18°C, as revealed by FHB index and AUDPC. Rossi et al. (2001) reported that *F. graminearum* is more aggressive at 28-29°C compared to *F. culmorum* which showed high pathogenicity at 18 and at 26.5°C. The reported optimal growth temperatures are 24-28°C for *F. graminearum* and 20-25°C for *F. culmorum* (Popovski and Celar 2013). The spread of *F. graminearum* in wheat spikes can be described as a function of DON which means that the strains

that produce DON spread within ears much better than DON nonproducing strains (Bai 2001). In conclusion, the higher aggressiveness of *F. culmorum*, resulting in symptoms, is in accordance with the reports on the predominance of *F. graminearum* and *F.culmorum* in warmer and cooler regions, respectively (Parry et al. 1995; Osborne and Stein 2007).

In total, the comparison of disease progress curves of FHB index and incidence showed clearly that the monomolecular function describes the disease incidence well, whereas the FHB index was better described by the logistic function. However, this parameter under 18/12°C wet conditions seemed to be better described by the monomolecular function. The development of *Fusarium* infection at ears is defined as a monocyclic disease after the infection has taken place; very few secondary infections develop from the primary infection by conidia formed in infected tissues (Wegulo 2012). The progress of monocyclic diseases is mostly described by monomolecular functions, which show a high goodness of fit (Campbell and Madden 1990). The relationship between the incidence and severity of FHB in winter wheat was frequently investigated (Groth et al. 1999; Xu et al. 2004; Paul et al. 2005). For example, Paul et al. (2005) reported that the severity was more precisely predicted when incidences occurred at low numbers, compared to incidences occurring with high numbers. Such kind of investigations might be executed in the future when a new factor like the primary site of ear infection is considered.

Kernel infection by *Fusarium* species can be attributed to genetic or non-genetic factors like the position of the primary site of ear infection (Mesterhazy 2002; Al Masri et al. 2017). Furthermore, the influence of the environmental conditions was apparent as 24/18°C wet conditions increased the average rate of infected kernels significantly with *F. graminearum* compared to dry conditions. Meier (2003) made similar observations when FHB developed after spray inoculation of *F. graminearum, F.culmorum, F. poae* and *F. avenaceum* under wet environmental conditions.

Tip infection caused the lowest disease severity, FHB index, but its FIK was not different from that after spray or centre inoculations, which were associated with the highest symptoms. Former reports verified the infection development of *F. graminearum* in the rachis in both symptomatic and symptomless ears after ears had been inoculated (Malbrán et al. 2014). However, bleached spikelets (at the upper part of primary infected spikelets) are associated with shrunken kernels, but may not be infected by *Fusarium* spp. (Lemmens et al. 2004). While a primary infection of the ears' bases was reported, the upper kernels where not infected under all applied environmental

conditions. The up and downward development of the pathogens after centre inoculation confirmed that the downward colonisation of ears is stronger than upwards under both temperature regimes. Brown et al. (2010) confirmed the observed patterns of *Fusarium* spread within ears for centre infection with *F. graminearum*. The exponential functions used to describe the gradients of infected kernels within ears at 18/12°C wet (Al Masri et al. 2017), also proved high goodness of fit to these gradients at 18/12°C dry and most of the gradients at 24/18°C wet and dry. Only at 24/18°C dry, tip and centre inoculations with *F. graminearum* developed infections on kernels without gradients, at the same time displaying a low rate of infected kernels in comparison to *F. culmorum,* at the same conditions. Similar observations were made by Meier (2003) for FHB developed after centre inoculations of *F. graminearum* and *F.culmorum* under wet and dry environmental conditions.

Significant effects of all investigated factors (*Fusarium* species, the primary site of ear infection and environmental conditions) on TKW were found in the current study. Earlier observations revealed that the reduction in TKW was higher at temperatures higher than 20°C, compared to that at 16°C (Brennan et al. 2005). Also, Mentewab et al. (2000) showed a reduction in TKW and the visible symptoms of FHB at 25°C, compared to 15°C. The here presented results revealed that the lower temperatures were associated with higher AUDPCs and a lower RTKW, especially for infections after spray inoculations. In general, spray inoculation has the highest effect on TKW while tip inoculation did not affect.

Former work showed an intermediate effect of centre and base inoculations on RTKW at 18/12°C wet (Al Masri et al. 2017). These observations were also found for the infection at 18/12°C dry and 24/18°C wet and dry. However, differences in the aggressiveness between *Fusarium* species regarding TKW cannot be concluded from the 3-ways ANOVA because of the interactions that were found between them. The resulting reduced TKW revealed that the effects of FHB by both pathogens are significantly dependent on the relations between the three factors: pathogen, environment, and primary site of ears infection. However, from most of the t-tests, comparing *Fusarium* spp. on levels of individual infection scenarios, it can be concluded that *F. graminearum* was more aggressive than *F. culmorum*. Nevertheless, previously there has been no significant difference in pathogenicity between *F. graminearum* and *F. culmorum* regarding AUDPC and TKW accounting for the timing of *Fusarium* infection (Siou et al. 2014).

A given FHB value, regarding symptoms, can be associated with rather different levels of *Fusarium* damaged kernels and yield losses depending on the environmental conditions, even if the correlations between the parameters were generally close (Mesterházy et al. 2005). The current study has proved a positive correlation between AUDPC and RTKW at the four applied environmental conditions. However, when the primary site of ear infection was considered, FHB systems expressed as AUDPC after centre and tip infections showed no significant correlation with the RTKW. One conclusion that can be retrieved is: the more the ears are infected at the tip and in the centre, the lower is the correlation between AUDPC and RTKW. The effects of the primary site of infected spikelet within ears may explain why Alvarez et al. (2010) did not observe a correlation between disease severity and grain loss.

In summary, this research shows that the growth stages of wheat are affected by environmental conditions, which as a consequence affects the interaction between *Fusarium* spp. and wheat. It proved that under lower temperatures the disease has a broader time frame to develop, possibly enabling it to reach the flag leaves. This research demonstrates the importance of considering the primary site of ear infection as a critical factor to understand the later development of FHB, confirming it under different environmental conditions. In conclusion, differences in the aggressiveness of *Fusarium* species were not apparent in this work. However, the improved understanding of the epidemiological development of FHB, at ears level, could help researchers to understand the poor correlation between visible symptoms and losses in TKW and FIK. Nevertheless, further research is necessary to determine if these results are consistent across wheat varieties. Moreover, it would be interesting to assess the effect of environmental conditions on the mycotoxin accumulation in grain independency of the primary site of ear infection.

4.4 Infrared Thermography to visualise the spatio-temporal dynamics of *Fusarium* head blight within ears

The heterogeneity in growth stages on scales of plants, tillers and main stems, ears, spikelets position within ears, and even of spikelets and florets along the rachilla are associated with differences in the phenological development of ears (Brown et al. 2010; Lukac et al. 2012). This heterogeneity in development stages affects transpiration and water status of ears. These differences might explain the temperature span (TS) of non-inoculated control ears that was in the range 0.51-0.57 °C. Blum (1985) has reported that the transpiration ratio (Carbon exchange rate/transpiration) was not homogenous within ears. Over time, the heterogeneity of ear temperature increased because of the ripeness which was observed under greenhouse conditions to begin at topical spikelets downwards.

The development of FHB from small necrotic lesions on glumes to thoroughly bleached spikelets was associated with a low relative water content of spikelets. In the current study, the potential of IRT was proved to detect FHB before symptoms become visible. IRT is suitable for detecting plant diseases as they cause disorder in plant transpiration and water content (Jones et al. 2009; Mahlein et al. 2012; Oerke et al. 2014; Mahlein et al. 2016). However, the above early pre-symptomatic detection was not proved in all experiments. The signal of emitted IR-radiation from ears estimated by the thermocamera is affected by factors like the reflection of IR- radiation from other objects nearby ears, depending on the environmental conditions outside the greenhouse compartment where the measurements took place, namely sunshine. Other factors are related to the ears and the 3 dimensions of the ears after being fixed to grids at measurement. There are difficulties specific to the application of thermography, some related to thermocamera like obtaining fast, uniform and highly energetic thermograms over a large surface of objects and other factors like the effect of thermal added and losses values and the emissivity issue as well (Maldague 2002).

FHB basically causes an increased temperature of infected spikelets compared to non-inoculated control because of reduced transpiration due to the reduced water supply. The increase in tobacco leaf temperature after tobacco mosaic virus infection was associated with an accumulation of salicylic acid, known to cause closure of stomatal cells (Chaerle et al. 1999). *Fusarium oxysporum* f. sp. *cucumerinum* (FOC) on cucumber caused stomata closure in leaves and resulted in lower

transpiration rate and subsequently increased leaf temperature (Wang et al. 2012). The symptoms resulting from the infection with the nematode *Heterodera schachtii* on sugar beet were associated with higher temperature because of lower water supply (Schmitz et al. 2004). In contrast, the subcuticular growth of *Venturia inaequalis* on apple leaves caused a localised decrease in leaf temperature before symptoms became visible because of higher transpiration rate at infection sites (Oerke et al. 2010). The characteristic thermal reaction of lower temperature in grapevines was detectable before the symptoms become visible on leaves after inoculation with *Plasmopara viticola* (Stoll et al. 2008). An initial increase of transpiration – similar to the transient increase caused by downy mildews in cucumber (Oerke et al. 2006) – was never observed for Fusarium-infected wheat spikelets.

The variation of temperature within non-inoculated ears was low as reflected in low TS values. FHB caused higher TS values, mainly when the ear's tip was the primary site of infection. The growth of the pathogens from rachilla to rachis may shut off the water supply to the non-inoculated spikelets (Lemmens et al. 2004) and, in turn, causes an increase in ear temperature according to the degree of the shut-off. After tip inoculation, FHB developed downwards without an effect on water movement to lower, non-inoculated spikelets. A sharp increase in temperature was observed between symptomatic and non-symptomatic spikelets and the range between minimum and maximum temperature within ears was wide. In the other infection scenarios, FHB was associated with an increase in total ear temperature because of a lower water status of almost the whole ear which led to lower TS values.

The overall ear temperature, expressed as TD, was linearly correlated to FHB index. The linear regression proved that the temperature difference between ears and air is a function of FHB index. FHB reduced the water content of ears which had temperatures close to that of the surrounding air. Therefore, *Fusarium* infection reduced TD values compared to non-inoculated ears. The variation in linear regression from strong, e.g. for tip inoculation of *F. culmorum* (R^2 = 0.84), to non-significant, e.g. for base inoculation of *F. culmorum* (R^2 = 0.24), is because of the impact of the primary site of ears infection. The infected tip ears have no blocking of assimilates that might take place in base and centre infection. Consequently, this scenario of infection was not associated with reducing the supply of water to the lower part of the ear. Therefore, the visual estimation matches the thermal assessment of the infection better than that of base and centre infection. At these

infection scenarios, the upper parts are scored to be healthy, but the thermal assessments showed higher temperature. FHB, however, is not the sole factor determining TD. The relative humidity of the ambient air determining the leaf-to-air water vapour pressure deficiency as well as the senescence of plant tissue associated with reduced relative water content is the main factors influencing transpiration and TD of plant tissue (Oerke et al. 2006). The observations in this study demonstrate that even when wheat started to become senescent, the transpiration of non-infected ears resulted in lower ear temperature and allowed to discriminate between infected and non-infected ears. TS values proved to be especially valuable for the interpretation of IR images of wheat ears in early growth stages after anthesis. The use of temperature extremes is sensitive to small, localised changes in ear temperature and independent from a reference temperature as used by Jones et al. (2002). The temperature of the ambient air was used in this study as a reference for calculating TD. At advanced growth stages, when the within-ear temperature heterogeneity of infected ears decreased, TD was more efficient in detecting FHB infection because of differences in the stage of overall ear senescence.

Bai and Shaner (2004) studied types of resistance Type I and Type II by spray and single floret inoculation of central spikelets, respectively. In the current study, the single floret inoculation was done in different locations within the ear, not only at the centre, and a significant effect of the inoculation site was proved. Moreover, thermography allowed estimating the effect of single spikelet infection on the entire ear and to predict the part that will be bleached, which is not possible with naked eyes or traditional methods of disease assessments. In contrast to visual assessments of FHB severity, thermography was suitable to differentiate between FHB scenarios involving different sites of primary infection of ears. The temperature heterogeneity within ears measured as temperature span was especially useful in early infection stages. This technique may be used with high spatial resolution to track non-invasively the spread of *Fusarium* species from one spikelet level to the other to quantify type II resistance. Although the thermographic detection of *Fusarium* infections in the field cannot be used in practical disease control – when ear colonisation becomes detectable several days after the primary infection and fungicide applications for FHB control are not available anymore or are of low efficacy – the technology may be applied in breeding for FHB resistance. Studying the responses of various resistance sources to fungal attack is also optimal to investigate using this sensor.

4.5 Fusion of sensor data for monitoring *Fusarium* head blight at spikelets level

Precision agriculture is a set of technologies and data processing methods, including sensors, to optimise production systems in agriculture with the aim to maintain the quality of the environment (Gebbers and Adamchuk 2010). In this regard, an increasing interest in remote sensing methods has been attracted during the recent years, and it is expected to play a major role in detecting and monitoring plant diseases in the next 30-40 years (Lucas 2010). Implementation of precision agriculture concepts to manage FHB might contribute very significantly to secure cereal production systems. An early detection and subjective monitoring of FHB using proximal sensor methods, IRT and CFI separately or together will promote our knowledge about FHB and in accordance improve disease management keeping in mind maintaining the environment.

Progress curves of FHB on the scale of spikelets developed in the current study showed faster disease development compared to that after considering the whole ears as reported by Al Masri et al. (2017) after following the same procedure of inoculation. The rating scales and the available spatial area for disease development can explain this difference. The early symptoms of FHB from a small necrotic lesion on glumes (until 5%) to thoroughly bleached spikelets were associated with a relatively low water content of spikelets. FHB basically causes an increased temperature of infected spikelets compared to non-inoculated because of reduced transpiration due to reduced water supply (Al Masri et al. 2017). This disorder in spikelets was associated not only with spikelet temperature but also with photosynthesis activities measured by CFI.

The application of IRT was successful in detecting and monitoring FHB under field and controlled conditions (Oerke et al. 2014; Al Masri et al. 2017). An early detection of this disease at pre-symptomatic stage using IRT was possible in the current study when single spikelets were considered. This early detection was attributed to increasing spikelet temperature not more than 0.3°C which means extraordinary conditions of measuring. Oerke et al. (2010) reported the possibility to detect the infection with *Venturia inaequalis* on apple leaves (apple scab) before symptoms become visible. Moreover, Gomez (2014) proved the ability of IRT to predict the infection with *Peronospora parsa* (downy mildew) on rose under controlled conditions. The structure of spikelets and ears compared to that of leaves regarding transpiration apparatus led to a

higher temperature of ears compared to that of leaves (Ayeneh et al. 2002). That might explain the higher sensitivity of IRT to detect apple scab and downy mildew on leaves pre-symptomatically compared to the case of FHB.

When symptoms appeared, infected spikelets showed higher temperature compared to non-inoculated ones which is in accordance with Oerke et al. (2014) and Al Masri et al. (2017). Preventing or reducing the movement of the assimilate upwards from the preliminary infection site into the ears (Lemmens et al. 2004) leads to a higher temperature. When single spikelets are considered, the higher temperature is an outcome of the destruction of the transpiration apparatus of spikelets where necrosis is formed. Additionally, the plug of rachilla when the *Fusarium* infections move from floret to rachilla can have a similar effect as reported by Lemmens et al. (2004) and Al Masri et al. (2017).

Reduction in the average temperature of infected spikelets was proved, 3-5 dai, as compared to the non-inoculated control. The reduction in ear temperature before bleached symptoms of FHB appeared might be explained by the reaction of ear's tissues to *Fusarium* infection with higher and uncontrolled transpiration rate. The infection with *Venturia inaequalis* on apple leaves led to dropped temperature and was visible on thermograms before symptoms become visible (Oerke et al. 2010). The same behaviour was reported for downy mildew of cucumber by Oerke et al. (2006) and of grapevine leaves by Stoll et al. (2008). However, the reduction in ear temperature during 2-5 dai still needs further investigations under 100% controlled conditions.

The higher temperature of infected ears, after being normalised (TD), allowed an early detection of FHB as early as 5 dai and proved better capability in this regard as compared to temperature span (TS) which confirmed the finding of Al Masri et al. (2017). TS of single infected spikelets showed curves similar to that of the entire infected ears. The effect of the senescence, lower water content, might explain the reason why TS did not vary 21 dai between the infected and the non-inoculated spikelets. IRT revealed its high potential not only in FHB-early detection but also in a more accurate assessment of this disease compared to visual estimation (Al Masri et al. 2017) which was confirmed in the current study as well. Chaerle et al. (2007) reported that IRT provides higher potential of non-invasive measurement when combined with CFI to characterise plant diseases which were investigated in the current study.

Biotic and abiotic stresses in plants have been widely studied using CFI during the last decade (Chaerle et al. 2007; Cséfalvay et al. 2009; Scholes and Rolfe 2009; Kuckenberg et al. 2009; Bürling et al. 2011; Bauriegel et al. 2011; Oerke et al. 2014). It provides a direct non-invasive measurement of cell function and information about the impacts of fungal pathogens on host metabolism (Scholes and Rolfe 2009). The most sensitive reporters of grapevine infection with *Plasmopara viticola* were the maximum quantum yield (Fv/Fm) and the effective quantum yield Y[II] of PSII (Cséfalvay et al. 2009) which is in line with the current findings. The potential of CFI to characterise FHB in wheat was first investigated by Bauriegel et al. (2010). They demonstrated the possibility of using Fv/Fm to discriminate between healthy and infected ears first at GS 75 and the limitation of the method at the beginning of ripening. FHB was detectable using CFI as early as 5 dai in the current work, which is in accordance with the studies of Bauriegel et al. (2010 and 2011). However, the early infection could be distinguished by a few pixels with lower Fm values. Cséfalvay et al. (2009) reported the suitability of CFI for the early detection of *Plasmopara viticola* of grapevine 3 days before symptoms became visible and recommended using CFI at high resolution for disease detection under field conditions. Kuckenberg et al. (2009) proved the possibility to early and precisely detect powdery mildew and leaf rust in wheat before symptoms became visible or significant changes in the normalised differenced vegetative index (NDVI) became pronounced. In accordance with the present study, they used the parameter of fast chlorophyll fluorescence kinetics Fm. However, they reported that Fv/F0 had the most pronounced response to both diseases.

The increased number of parameters resulting from the combination of IRT and CFI has improved the early detection of FHB which has been proved by discriminant analysis which is in accordance with the recommendation of Chaerle et al. (2007). Moreover, this multisensory method has proved the possibility to differentiate among *Fusarium* spp. infections, which was not possible by the visual assessment. Fusion of HSI and CFI data was used by Moshou et al. (2005) on yellow rust (*Puccinia striiformis*) and they proved the accuracy of discrimination of the disease by 94.5% and at the same time reduced the error of measurements by 11.3% and 16.5% for CFI and HSI, respectively using QDA. They used self-organising map (SOM) which decreased the overall classification error even to 1%. Berdugo et al. (2014) applied a sensor fusion approach using discriminant analysis and proved the early detection possibility of *cucumber mosaic virus* (CMV), *cucumber green mottle mosaic virus* (CGMMV), and the powdery mildew of the fungus

Sphaerotheca fuliginea in cucumber. Differentiation between FHB depending on the pathogen was possible by a principal component analysis which proved the ability to significantly differentiate among all treatments at assessment points, especially when systems become visible and before senescence started. Plugging the rachis as already discussed has an effect on water movements upwards which can be detected by IRT but not by CFI. In contrast, CFI is sensitive to detect the local *Fusarium* infection at early stages (≤ 5%) when symptoms appear on glumes which is difficult to capture by IRT.

IRT and CFI are unspecific-stress detectors (Lindenthal et al. 2005; Mahlein et al. 2012; Oerke et al. 2014). To the extent of our knowledge, the current study is the first one that involved IRT and CFI in simultaneous measurement to detect and monitor FHB. Also, it is the first one that correlates the indices of these sensors and applies the fusion of sensor data approach. The finding of the current study provides new knowledge of great importance not only for the application in precision agriculture but also for modern resistance phenotyping of FHB. The finding of the current study contributes very significantly to manage FHB using non-destructive proximal sensing that provides a highly accurate assessment. However, further studies are still required like hyperspectral imaging to discover the potential of these sensor data in combination under controlled and field conditions.

5. SUMMARY

The main objectives of the presented research were to investigate the epidemiology of *Fusarium* head blight (FHB) under field and controlled conditions using innovative methods. Proximal sensing methods were integrated into this work based on its successful application in characterising various plant diseases. *Fusarium* and foliar pathogens infections influence the optical properties of wheat at canopy and ear levels. Prior to FHB occurrence, *Fusarium* inoculum is transferred from the residue of previous crops to ears through the canopy. Wheat leaves might be infected by obligate or non-obligate pathogens which could result in antagonism or synergism. At this level, the critical question of research was to address the effect of foliar wheat diseases and their control with fungicides on Fusarium infection at ears. To assess the vital situation of the canopy, a non-imaging hyperspectral system was applied, and spectral parameters from reflectance spectra were calculated. After inoculum reached the ears, the infection takes place at spikelets that are at anthesis. As anthesis is heterogeneous within single ears, the infection occurs mostly in a few spikelets of individual ears. This was established in the current work through developing the different primary site of infection within ears by base, centre and tip inoculations. Inoculation was done by *F. graminearum,* and *F. culmorum* and different environmental conditions were subjected to monitor their effect on FHB extension within ears. At ears level, proximal sensing of ears temperature was addressed using Infrared Thermography under controlled conditions. Detailed investigations at spikelet levels were then fulfilled using fusion of sensor data of Infrared Thermography and chlorophyll fluorescence Imaging.

In total, the results obtained in this research can be summarised as follows:

- Under field conditions, the severities of the foliar wheat diseases septoria leaf blotch (*Zymoseptoria tritici*), brown rust (*Puccinia trticina*) and yellow rust (*Puccinia striiformis*) influenced the development of ear Fusarioses and was significantly reduced by the application of fungicides. FHB occurrence was significantly reduced especially in Tobak which showed higher susceptibility in comparison to Pamier. Nitrogen levels showed no relationship to *Fusarium* infection in ears but affected the reflectance spectra of wheat

canopy mostly between 760 and 1120 nm and spectral reflectance indices (SVIs). The presence of foliar wheat diseases showed significant correlation with *Fusarium* infection at F-2, especially by *F. equiseti* in 2014 and *F. graminearum* and *F. culmorum* in 2015 experiments. This relationship was not verified for kernels infection with *Fusarium* spp. which were mostly infected with *F. poae*. However, observation from both years revealed a significant correlation between foliar wheat diseases and FHB incidence (r = 0.63 and 0.53 in the 2014 and 2015 experiments, respectively). Among 11 SVIs investigated in the 2015 trial, blue-green index 2 (BGI2) and photochemical reflectance index (PRI) showed significant correlation with FHB (r = 0.4 for both). *Fusarium* infection in ears was not responsible for yield reduction. However, foliar diseases which were assessed only on the flag leaf at GS 83 proved significant correlation to thousand kernels weight (TKW).

- *Fusarium* infection after inoculation under controlled conditions showed no significant differences between *F. graminearum* and *F. culmorum* regarding disease incidence. The asymptotic phase of FHB incidence was reached at 13 dai. Infection development at 18/12°C wet conditions by *F. culmorum* caused significantly higher disease severity neither reflected in the frequency of infected kernels nor in thousand kernels weight (TKW). Centre and base infection reduced EW similar to that obtained after spray inoculation. These scenarios of infections reduced EW significantly compared to tip infection and non-inoculated control. Spray inoculations had the highest infection and later reduction on TKW whereas tip infection did not affect. Centre and base infection had intermediate effects on TKW, although FHB levels did not differ with the same trend among inoculation scenarios. The overall low correlations among FHB severity, infected kernels, and TKW are explained by the pathogen spread within ears – downwards better than upwards – and the effect on yield formation which is lower for infections of the upper parts of ears. An exponential model showed high goodness of fit for gradients of infected kernels within ears ($R^2 \geq 70$) except for tip infection with *F. culmorum*.

- *F. graminearum* and *F. culmorum* infections, expressed as FHB incidence, were under wet conditions higher than under dry environment. A monomolecular function showed high goodness of fit to incidence curves at both wet and dry conditions ($R^2 \geq 97$ and 70, respectively). Lower temperatures after anthesis delayed ripening of wheat ears which

allowed more disease development within ears and affected the shape of the disease progress curves. The logistic function showed high goodness of fit to these curves (FHB index) except that at 18/12°C wet. The higher temperature of 24/18°C and wet environment triggered *F. graminearum* to infect kernels much more than that obtained at dry conditions. *Fusarium* species developed downward better than upward within ears, as infected kernels revealed, except for the infection by *F. graminearum* at 24/18°C and dry conditions which showed no gradients. Grain yield loss expressed as TKW was at highest at low temperatures and wet conditions (18/12°C wet). This reduction can be estimated using the area under disease progress curves (AUDPC), r = 0.67 for combined observations. In contrast, neither AUDPC nor TKW were correlated to kernel infection at harvest.

- FHB was detectable before symptoms became visible using Infrared Thermography (IRT). After symptoms appear, *Fusarium* infection significantly increased the temperature span (TS) within ears starting at 6 dai. Infections starting at the ear tip caused higher TS compared to that of ear centre and base. Higher aggressiveness, reflected in FHB index, of *F. culmorum* compared to that of *F. graminearum* resulted in a higher temperature of infected ears when the area under temperature difference curves (AUTDC) was considered. The temperature difference between air and ear (TD) was negatively correlated with FHB index with R^2 = 0.68 and 0.64 for *F. graminearum* and *F. culmorum*, respectively. The destructed transpiration system of inoculated ears enabled disease detection at late growth stages of ears when senescence started, 29 dai, in comparison to non-inoculated control.

- Time-series measurements with IRT and Chlorophyll Fluorescence Imaging (CFI) allowed the visualisation of temperature and photosynthesis heterogeneity within the infected spikelets. Altered transpiration caused significantly increased temperature starting at 5 dai. The early detection was also confirmed by CFI via maximal fluorescence yields of dark-adapted spikelets (Fm) starting at 5 dai. The selected features derived from sensor data were significantly correlated with each other except of the temperature span (TS). Fusion of sensor data through linear discriminant analysis allowed differentiating between treatments starting at 3 dai with 77.8% accuracy of prediction. Moreover, it allowed discriminating between spikelets infected with *F. graminearum* from those infected with *F. culmorum* with 100% accuracy of prediction.

Valuable insights in understanding FHB development were revealed through the current research using sensors. The findings contribute highly to more efficient control of FHB and enrich the concepts of precision agriculture of wheat. The relationship between this disease and foliar wheat diseases and their control with fungicides can be engaged to improve the efficacy of Integrated Plant Protection measures against *Fusarium* infection. Moreover, Infrared thermography and Chlorophyll Fluorescence Imaging have the potential of monitoring FHB more precisely and subjectively. Such new findings can contribute also significantly in selection processes of breeding for FHB resistance.

6. REFERENCES

Abildgren, M. P., Lund, F., Thrane, U., & Elmholt, S. (1987). Czapek-Dox agar containing iprodione and dicloran as a selective medium for the isolation of *Fusarium* species. *Letters in Applied Microbiology*, *5*(4), 83–86.

Aggarwal, P. K., Kalra, N., Chander, S., & Pathak, H. (2006). InfoCrop: A dynamic simulation model for the assessment of crop yields, losses due to pests, and environmental impact of agro-ecosystems in tropical environmentals. I. Model description. *Agriculture systems, 89*(1), 1–25.

Al Masri, A., Hau, B., Dehne, H. W., Mahlein, A. K., & Oerke, E. C. (2017). Impact of primary infection site of *Fusarium* species on head blight development in wheat ears evaluated by IR-thermography. *European Journal of Plant Pathology*, *147*(4), 855–868.

Ali, S., & Francl, L. (2001). Progression of *Fusarium* species in wheat leaves from seedling to adult stages in North Dakota. In: Proceedings of the 2001 National *Fusarium* Head Blight Forum, pp. 99.

Alvarez, C. L., Somma, S., Moretti, A., & Fernández Pinto, V. (2010). Aggressiveness of *Fusarium graminearumsensu stricto* isolates in wheat kernels in Argentina. *Journal of Phytopathology, 158*(3), 173–181.

Amarasinghe, C. C., Tamburic-Ilincic, L., Gilbert, J., Brûlé-Babel, A, L., & Dilantha Fernando, W. G. (2013). Evaluation of different fungicides for control of *Fusarium* head blight in wheat inoculated with 3ADON and 15ADON chemotypes of *Fusarium graminearum* in Canada. *Canadian Journal of Plant Pathology, 35*(2), 200–208.

Anonymous, (2013). Beschreibende Sortenliste Getreide. Mais Öl-und Faserpflanzen Leguminosen Rüben Zwischenfrüchte, Bundessortenamt. Hannover, Germany. http://www.bundessortenamt.de /internet30/ filea-dmin/Files/PDF/bsl_getreide_2013.pdf. Accessed on 28 January 2016.

Argyris, J., TeKrony, D., Hershman, D., Van Sanford, D., Hall, M., Kennedy, B., Rucker, M., & Edge, C. (2005). *Fusarium* head blight infection following point inoculation in the greenhouse compared with movement of *Fusarium graminearum* in seed and floral components. *Crop Science, 45*(2), 626–634.

Asner, G. P. (1998). Biophysical and biochemical sources of variability in canopy reflectance. *Remote Sensing of Environment*, *64*(3), 234–253.

Aufhammer, W., Kübler, E., Kaul, H. P., Hermann,W., Höhn, D., & Yi, C. (2000). Infection with head blight (*F. graminearum*, *F. culmorum*) and deoxynivalenol concentration in winter wheat as influenced by N fertilization. *Pflanzenbauwissenschaften*, *4*(2), 72–78.

Ayeneh, A., Van Ginkel, M., Reynolds, M. P., & Ammar, K. (2002). Comparison of leaf, spike, peduncle and canopy temperature depression in wheat under heat stress. *Field Crops Research, 79*(2–3), 173–184.

Bai, G. H. (2001). Deoxynivalenol-nonreducing *Fusarium graminearum* causes initial infection, but does not cause disease spread in wheat spikes. *Mycopathologia, 153*(2), 91-98.

Bai, G., & Shaner, G. (2004). Management and resistance in wheat and barley to *Fusarium* head blight. *Annual Review of Phytopathology, 42*,135–161.

Baker, N. R. (2008). Chlorophyll Fluorescence: A Probe of Photosynthesis In Vivo. *Annual Review of Plant Biology*, *59*(1), 89–113.

Bauriegel, E., Giebel, A., & Herppich, W. B. (2010). Rapid *Fusarium* head blight detection on winter wheat ears using chlorophyll fluorescence imaging. *Journal of Applied Botany and Food Quality*, *83*, 196–203.

Bauriegel, E., Giebel, A., & Herppich, W. B. (2011). Hyperspectral and chlorophyll fluorescence imaging to analyse the impact of *Fusarium culmorum* on the photosynthetic integrity of infected wheat ears. *Sensors*, *11*(4), 3765–79.

Bauriegel, E., & Herppich, W. B. (2014). Hyperspectral and Chlorophyll Fluorescence Imaging for Early Detection of Plant Diseases, with Special Reference to *Fusarium* spec. Infections in wheat. *Agriculture*, *4*(1), 32–57.

Beck, C., Oerke, E-C., & Dehne, H-W. (2002). Impact of strobilurins on physiology and yield formation of wheat. *Mededelingen (Rijksuniversiteit te Gent. Fakulteit van de Landbouwkundige en Toegepaste Biologische Wetenschappen)*, *67*(2), 181–187.

Bedawy, I. M. A. (2013). Association Mapping of QTLs for *Fusarium* Head Blight Tolerance in a Structured Barley Population. Ph.D. Dissertation, University of Bonn, Bonn, Germany. http://hss.ulb.uni-bonn.de/2013/3186/3186.pdf. Accessed on 18 October 2017

Berdugo, C. A., Mahlein, A. K., Steiner, U., Dehne, H. W., & Oerke, E. C. (2013). Sensors and imaging techniques for the assessment of the delay of wheat senescence induced by fungicides. *Functional Plant Biology*, *40*(7), 677–689.

Berdugo, C. A., Zito, R., Paulus, S., & Mahlein, A. K. (2014). Fusion of sensor data for the detection and differentiation of plant diseases in cucumber. *Plant Pathology*, *63*(6), 1344–1356.

Berthiller, F., Brera, C., Iha, M. H., Krska, R., Lattanzio, V. M. T., MacDonald, S., Malone, R. J., C. Maragos, Solfrizzo, M., Stranska-Zachariasova, M., Stroka, J., & Tittlemier S. A. (2017). Developments in mycotoxin analysis: an update for 2015-2016. *World Mycotoxin Journal*, *10*(1), 5–29.

Blackburn, G. A. (1998). Quantifying Chlorophylls and Caroteniods at Leaf and Canopy Scales. *Remote Sensing of Environment*, *66*(3), 273–285.

Blandino, M., Pilatim A., Reyneri, A., & Scudellari, D. (2010). Effect of maize crop residue density on Fusarium head blight and on deoxynivalenol contamination of common wheat grains. *Cereal Research Communications*, *38*(4), 550–559.

Blažek, J., Jirsa, O., & Hrušková, M. (2005). Prediction of Wheat Milling Characteristics by Near-Infrared Reflectance Spectroscopy. *Czech journal of food sciences, 23*(4), 145–151.

Bock, C. H., Poole, G. H., Parker, P. E., & Gottwald, T. R. (2010). Plant Disease Severity Estimated Visually, by Digital Photography and Image Analysis, and by Hyperspectral Imaging. *Critical Reviews in Plant Sciences*, *29*(2), 59–107.

Boehnke, B., Karlovsky, P., Pfohl, K., Gamliel, A., Isack Y., & Dehne, H. W. (2015). Identification of different *Fusarium* spp. in *allium* spp. in Germany. *Communications in Agricultural and Applied Biological Sciences*, *80*(3), 453–463.

Bottalico, A., & Perrone, G. (2002). Toxigenic *Fusarium* species and mycotoxins associated with head blight in small-grain cereals in Europe. *European Journal of Plant Pathology, 108*(7)*,* 611–624.

Boyacioğlu, D., & Hettiarachchy, N. S. (1995). Changes in some biochemical components of wheat grain that was infected with *Fusarium graminearum*. *Journal of Cereal Science, 21*(1), 57–62.

Brennan, J. M., Egan, D., Cooke, B. M., & Doohan, F. M. (2005). Effect of temperature on head blight of wheat caused by *Fusarium culmorum* and *F. graminearum*. *Plant Pathology*, *54*(2), 156–160.

Brown, N. A., Urban, M., van de Meene, A. M. L., & Hammond-Kosack, K. E. (2010). The infection biology of *Fusarium graminearum*: Defining the pathways of spikelet to spikelet colonisation in wheat ears. *Fungal Biology, 114*(7), 555–571.

Bürling, K., Hunsche, M., & Noga, G. (2011). Use of blue-green and chlorophyll fluorescence measurements for differentiation between nitrogen deficiency and pathogen infection in wheat. *Journal of Plant Physiology*, *168*(14), 1641–1648.

Caloni, F., & Cortinovis, C. (2010). Effects of fusariotoxins in the equine species. *Veterinary Journal, 186*(2), 157–161.

Campbell, C. L., & Madden L. V. (1990). Introduction to Plant Disease Epidemiology. New York: John Wiley and Sons.

Cao, X., Luo, Y., Zhou, Y., Duan, X., & Cheng, D. (2013). Detection of powdery mildew in two winter wheat Varieties using canopy hyperspectral reflectance. *Crop Protection*, *45*, 124–131.

Carter, G. A., & Knapp, A. K. (2001). Leaf optical properties in higher plants: linking spectral characteristics to stress and chlorophyll concentration. *American Journal of Botany*, *88*(4), 677–684.

Chaerle, L., Van Caeneghem, W., Messens, E., Lambers, H., Van Montagu, M., & Van Der Straeten, D. (1999). Presymptomatic visualization of plant-virus interactions by thermography. *Nature Biotechnology, 17*(8), 813–816.

Chaerle, L., Valcke, R., & Van der Straeten, D. (2003). Imaging techniques in plant physiology and agronomy: from simple to multispectral approaches. In: Hemantaranjan, A. (Ed.), Advances in plant physiology. Rajasthan: Jodhpur.

Chaerle, L., Leinonen, I., Jones, H. G., & Van Der Straeten, D. (2007). Monitoring and screening plant populations with combined thermal and chlorophyll fluorescence imaging. *Journal of Experimental Botany*, *58*(4), 773–784.

Chakraborty, S. & Newton, A. C. (2011). Climate change, plant diseases and food security: An overview. *Plant Pathology*, *60*(1), 2–14.

Champeil, A., Doré, T., & Fourbet, J. F. (2004). *Fusarium* head blight: Epidemiological origin of the effects of cultural practices on head blight attacks and the production of mycotoxins by *Fusarium* in wheat grains. *Plant Science*, *166*(6), 1389–1415.

Chang, K. W., Shen, Y., & Lo, J. C. (2005). Predicting rice yield using canopy reflectance measured at booting stage. *Agronomy Journal*, *97*(3), 872–878.

Chetouhi, C., Bonhomme, L., Lecomte, P., Cambon, F., Merlino, M., Biron, D. G., & Langin, T. (2014). A proteomics survey in wheat susceptibility to *Fusarium* head blight during grain development. *European Journal of Plant Pathology*, *141*(2), 407–418.

Cortinovis, C., Pizzo, F., Spicer, L. J., & Caloni, F. (2013). *Fusarium* mycotoxins: Effects on reproductive function in domestic animals-A review. *Theriogenology*, *80*(6), 557–564.

Couture, L. (1980). Assessment of severity of foliage diseases of cereals in cooperative evaluation tests. *lnventaire des maladies des plantesau Canada*, *60*(1), 8–10.

Cromey, M. G., Butler, R. C., Mace, M. A., & Cole, A. L. J. (2004). Effects of the fungicides azoxystrobin and tebuconazole on *Didymella exitialis*, leaf senescence and grain yield in wheat. *Crop Protection*, *23*(11), 1019–1030.

Cséfalvay, L., Gaspero, G. Di, Matouš, K., Bellin, D., Ruperti, B., & Olejníčková, J. (2009). Pre-symptomatic detection of *Plasmopara viticola* infection in grapevine leaves using chlorophyll fluorescence imaging. *European Journal of Plant Pathology, 125*(2), 291–302.

Curran, P. J. (1989). Remote sensing of foliar chemistry. *Remote Sensing of Environment*, *30*(3), 271–278.

Danner, M., Locherer, M., Hank, T., & Richter, K. (2015). Spectral Sampling with the ASD FieldSpec 4 – Theory, Measurement, Problems, Interpretation. EnMAP Field Guides Technical Report, GFZ Data Services. http://doi.org/10.2312/enmap.2015.008. Accessed on 12 October 2017.

Delalieux, S., Somers, B., Verstraeten, W. W., van Aardt, J. A. N., Keulemans, W., & Coppin, P. (2009). Hyperspectral indices to diagnose leaf biotic stress of apple plants, considering leaf phenology. *International Journal of Remote Sensing*, *30*(8), 1887–1912.

Desjardin, A. E. (2006). *Fusarium* Mycotoxins: Chemistry, Genetics, and Biology. Saint Paul: American Phytopathological Society Press.

Dimmock, J. P. R. E., & Gooding, M. J. (2002). Influence of foliar diseases, and their control by fungicides, on the protein concentration in wheat grain: a review. *Journal of Agricultural Science*, *138*(4), 349–366.

Doohan, F. M., Brennan, J., & Cooke, B. M. (2003). Influence of climatic factors on *Fusarium* species pathogenic to cereals. *European Journal of Plant Pathology*, *109*(7), 755–768.

Dweba, C. C., Figlan, S., Shimelis, H. A., Motaung, T. E., Sydenham, S., Mwadzingeni, L., & Tsilo, T. J. (2017). *Fusarium* head blight of wheat: Pathogenesis and control strategies. *Crop Protection*, *91*(1), 114–122.

Elmer, W. (2015). Introduction to the special issue of "Management of *Fusarium* Diseases" for the Journal of Crop Protection. *Crop Protection*, *73*(3), 1.

FAO. (2017). FAO Statistics Division: http://www.fao.org/worldfoodsituation/csdb/en/. Accessed on 04 October 2017.

Fauzi, M. T., & Paulitz, T. C. (1994). The effect of plant growth regulators and nitrogen on *Fusarium* head blight of the spring wheat variety max. *Plant Disease*, *78*(3), 289–292.

Ferrigo, D., Raiola, A., & Causin, R. (2016). *Fusarium* toxins in cereals: Occurrence, legislation, factors promoting the appearance and their management. *Molecules*, *21*(5), 627–662.

Fletcher, R. A., & Nath, V. (1984). Triadimefon reduces transpiration and increases yield in water-stressed plants. *Physiologia Plantarum*, *62*(3), 422–426.

Gamon, J. A., Peñuelas, J., & Field, C. B. (1992). A Narrow-Waveband Spectral Index That Tracks Diurnal Changes in Photosynthetic Efficiency. *Remote Sensing Environment*, *44*, 35–44.

Gao, B., (1996). NDWI a normalized difference water index for remote sensing of vegetation liquid water from space. *Remote Sensing of Environment*, *58*, 257–266.

Garbetta, A., Debellis, L., de Girolamo, A., Schena, R., Visconti, A., & Minervini, F. (2015). Dose-dependent lipid peroxidation induction on ex vivo intestine tracts exposed to chyme samples from fumonisins contaminated corn samples. *Toxicology in Vitro*, *29*(5), 1140–1145.

Gäumann, E. (1947). Enniatin, ein neues, gegen Mykobakterien wirksames Antibiorikum, *Experientia*, *3*(5), 202–203.

Gebbers, R., & Adamchuk, V. I. (2010). Precision Agriculture and Food Security. *Science, 327*(5967), 828–831.

Genty, B., Briantais, J. M., & Baker, N. R. (1989). The relationship between the quantum yield of photosynthetic electron transport and quenching of chlorophyll fluorescence. *Biochimica et Biophysica Acta*, *990*(1), 87–92.

Gerlach, D. (1977). Botanische MFIKotechnik, eine Einführung. Stutgart: Georg Thieme Verlag.

Gilbert, J. & Tekauz, A. (2000). Review: Recent developments in research on *Fusarium* head blight of wheat in Canada. *Canadian Journal of Plant Pathology*, *22*(1), 1–8.

Goetz, A. F. H., Vane, G., Solomon, J. E., & Rock, B. N. (1985). Imaging Spectrometry for Earth Remote Sensing. *Science*, *228*(4704), 1147–1153.

Gomez, S. (2014). Infection and spread of *Peronospora sparsa* on Rosa sp. (Berk.) - amicroscopic and a thermographic approach. Ph.D. Dissertation, University of Bonn, Bonn, Germany. http://hss.ulb.uni-bonn.de/2014/3473/3473. Accessed on 25 June 2014

Goswami, R. S., & Kistler, H. C. (2005). Pathogenicity and in planta mycotoxin accumulation among members of the *Fusarium graminearum* species complex in wheat and rice. *Phytopathology, 95*(12), 1397–1404.

Govindjee (2004). Chlorophyll a fluorescence: a bit of basics and history. In Papageorgiou, G. C., & Govindjee (Ed.), Chlorophyll a Fluorescence: A signature of photosynthesis. Dordrecht: Springer.

Groth, J. V., Ozmon, E. A., & Busch, R. H. (1999). Repeatability and relationship of incidence and severity measures of scab of wheat caused by *Fusarium graminearum* in inoculated nurseries. *Plant Disease*, *83*, 1033–1038.

Guo, Z. (2015). Ecological interactions of Fusarium species and the meal beetle Tenebrio molitor. Ph.D. Dissertation, University of Bonn, Bonn, Germany. http://hss.ulb.uni-bonn.de/2015/4154/4154.pdf. Accessed on 12 October 2017.

Hardinsky, M.A. & Lemas, V. (1983). The influence of soil salinity, growth form, and leaf moisture on the spectral reflectance of *Spartina alternifolia* canopies. *Photogrammetric Engineering and Remote Sensing*, *49*, 77–83.

Herebian, D., Zühlke, S., Lamshöft, M., & Spiteller, M. (2009). Multi-mycotoxin analysis in complex biological matrices using liquid chromatography-electrospray ionization-mass spectrometry: an experimental study using triple stage quadrupole and linear ion trap-Orbitrap technology. *Journal of Separation Science*, *32*(7), 939-948.

Hillnhütter, C., Mahlein, A. K., Sikora, R. A., & Oerke, E. C. (2011). Remote sensing to detect plant stress induced by *Heterodera schachtii* and *Rhizoctonia solani* in sugar beet fields. *Field Crops Research, 122*, 70–77.

Hofer, K., Barmeier, G., Schmidhalter, U., Habler, K., Rychlik, M., Hückelhoven, R., & Hess, M. (2016). Effect of nitrogen fertilization on *Fusarium* head blight in spring barley. *Crop Protection*, *88*(5), 18–27.

Hooker, D. C., Schaafsma, A. W., & Tamburic-Ilincic, L. (2002). Using Weather Variables Pre- and Post-heading to Predict Deoxynivalenol Content in Winter Wheat. *Plant Disease*, *86*(6), 611–619.

Huang, W., Lamb, D. W., Niu, Z., Zhang, Y., Liu, L., & Wang, J. (2007). Identification of yellow rust in wheat using in-situ spectral reflectance measurements and airborne hyperspectral imaging. *Precision Agriculture*, *8*(4–5), 187–197.

Infantino, A., Santori, A., & Shah, D. A. (2012). Community structure of the *Fusarium* complex in wheat seed in Italy. *European Journal of Plant Pathology*, *132*(4), 499–510.

Ishii, H. (2005). Impact of fungicide resistance in plant pathogens on crop disease control and agricultural environment. *Japan Agriculture Research Quarterly*, *40*(3), 205-211.

Jacquemoud, S., & Ustin, S. L. (2001). Leaf optical properties: a state of the art. In: Proceedings of the 8th International Symposium Physical Measurements & Signatures in Remote Sensing, pp. 223–232.

Jaleel, C. A., Gopi, R., Alagu Lakshmanan, G. M., & Panneerselvam, R. (2006). Triadimefon induced changes in the antioxidant metabolism and ajmalicine production in *Catharanthus roseus* (L.) G. Don. *Plant Science*, *171*(2), 271–276.

Jenner, C. F., Ugalde, T. D., & Aspinall, D. (1991). The Physiology of Starch and Protein Deposition in the Endosperm of Wheat. *Australian Journal of Plant Physiology*, *18*(3), 211–226.

Jennings, P., Coates, M. E., Walsh, K., Turner, J. A., & Nicholson, P. (2004). Determination of deoxynivalenol- and nivalenol-producing chemotypes of *Fusarium graminearum* isolated from wheat crops in England and Wales. *Plant Pathology, 53*(5), 643–652.

Jensen, J. R. (2002). Remote sensing of the environment – An earth resource perspective. New Jersey: Prentice Hall.

Jestoi, M. (2008). Emerging *Fusarium*-mycotoxins fusaproliferin, beauvericin, enniatins, and moniliformin: a review. *Critical Reviews in Food Science and Nutrition*, *48*(1), 21–49.

Jestoi, M., Rokka, M., Yli-Mattila, T., Parikka, P., Rizzo, A., & Peltonen, K. (2004). Presence and concentrations of the *Fusarium*-related mycotoxins beauvericin, enniatins and moniliformin in Finnish grain samples. *Food Additives and Contaminants*, *21*(8), 794–802.

Jesus Junior, W. C., Paula Júnior, T. J., Lehner, M. S., & Hau, B. (2014). Interactions between foliar diseases: concepts and epidemiological approaches. *Tropical Plant Pathology*, *39*(1), 1–18.

Jing, L., Jinbao, J., Yunhao, C., Yuanyuan, W., Wei, S., & Wenjiang, H. (2007). Using hyperspectral indices to estimate foliar chlorophyll a concentrations of winter wheat under

yellow rust stress. *New Zealand Journal of Agricultural Research*, *50*(5), 1031–1036.

Jones, H. G., & Schofield, P. (2008). Thermal and other remote sensing of Plant Stress. *Generaland Applied Plant Physiology*, *34*(1-2),19–32.

Jones, H. G., Serraj, R., Loveys, B. R., Xiong, L., Wheaton, A., & Price, A. H. (2009). Thermal infrared imaging of crop canopies for the remote diagnosis and quantification of plant responses to water stress in the field. *Functional Plant Biology*, *36*(11), 978–989.

Jones, H. G., Stoll, M., Santos, T., De Sousa, C., Chaves, M. M., & Grant, O. M. (2002). Use of infrared thermography for monitoring stomatal closure in the field: Application to grapevine. *Journal of Experimental Botany*, *53*(387), 2249–2260.

Kang, Z., & Buchenauer, H. (2000). Cytology and ultrastructure of the infection of wheat spikes by *Fusarium culmorum*. *Mycological Research*, *104*(9), 1083–1093.

Karnovsky, M. J. (1965). A formaldehyde-glutaraldehydehyde fixative of high osmolarity for use in electron microscopy. *The Journal of Cell Biology*, *27*, 137–138.

Kitajima, M., & Butler, W. L. (1975). Fluorescence quenching in photosystem II of chloroplasts. *Biochimica et Biophysica Acta*, *376*(1), 116–125.

Kiyosawa, S., & Shiyomi, M. (1972). A theoretical evaluation of the effects of mixing resistant variety with susceptible variety for controlling plant diseases. *Annals of the Phytopathological Society of Japan*, *38*(1), 41–51.

Krause, G. H., & Weis, E. (1991). Chlorophyll fluorescence andphotosynthesis: the basics. *Annual Review of Plant Physiology and Plant Molecular Biology*, *42*, 313–249.

Kriss, A. B., Paul, P. A., & Madden, L. V. (2010). Relationship between yearly fluctuations in *Fusarium* head blight intensity and environmental variables: a window-pane analysis. *Phytopathology*, *100*(8), 784–797.

Kuckenberg, J., Tartachnyk, I., & Noga, G. (2009). Temporal and spatial changes of chlorophyll fluorescence as a basis for early and precise detection of leaf rust and powdery mildew infections in wheat leaves. *Precision Agriculture*, *10*(1), 34–44.

Kuska, M., Wahabzada, M., Leucker, M., Dehne, H. W., Kersting, K., & Oerke, E. C., Steiner, U., & Mahlein, A. K. (2015). Hyperspectral phenotyping on the microscopic scale: towards automated characterization of plant-pathogen interactions. *Plant methods*, 11: 28.

Lancashire, P. D., Bleiholder, H., Van den Boom, T., Langeluddecke, P., Stauss, R., Weber, E., & Witzenberger, A. (1991). A uniform decimal code for growth stages of crops and weeds. *Annals of Applied Biology*, *119*(3), 561–601.

Lemmens, M., Krska, R., Buerstmayr, H., Josephs, R., Schuhmacher, R., Grausgruber, H., & Ruckenbauer, P. (2003). *Fusarium* head blight reactions and accumulation of deoxynivalenol, moniliformin and zearalenone in wheat grains. *Cereal Research Communications*, *31*(3–4), 407–414.

Lemmens, M., Haim, K., Lew, H., & Ruckenbauer, P. (2004). The effect of nitrogen fertilization on *Fusarium* head blight development and deoxynivalenol contamination in wheat. *Journal of Phytopathology*, *152*(1), 1–8.

Lenthe, J. H., Oerke, E. C., & Dehne, H. W. (2007). Digital infrared thermography for monitoring canopy health of wheat. *Precision Agriculture*, *8*(1–2), 15–26.

Leucker, M., Mahlein, A. K., Steiner, U., & Oerke, E. C. (2016). Improvement of lesion phenotyping in Cercospora beticola – sugar beet interaction by hyperspectral imaging. *Phytopathology*, *106*(2), 177–184.

Lichtenthaler, H. K., Buschmann, C., & Knapp, M. (2005). How to correctly determine the different chlorophyll fluorescence parameters and the chlorophyll fluorescence decrease ratio RFd of leaves with the PAM fluorometer. *Photosynthetica*, *43*(3), 379–393.

Lienemann, K. (2002). Auftreten von Fusarium-Arten an Winterweizen im Rheinland und Möglichkeiten der Befallskontrolle unter besonderer Berücksichtigung der Weizensorte. Ph.D. Dissertation, University of Bonn, Bonn, Germany. http://hss.ulb.uni-bonn.de/2002/0157/0157.pdf. Accessed on 12 October 2017.

Li-Hong, X., Wei-Xing, C., & Lin-Zhang, Y. (2007). Predicting grain yield and protein content in winter wheat at different N-supply levels using canopy reflectance spectra. *Pedosphere*, *17*(5), 646–653.

Lindenthal, M., Steiner, U., Dehne, H. W., & Oerke, E. C. (2005). Effect of downy mildew development on transpiration of cucumber leaves visualized by digital infrared thermography. *Phytopathology*, *95*(3), 233–40.

Lovell, D. J., Powers, S. J., Welham, S. J., & Parker, S. R. (2004). A perspective on the measurement of time in plant disease epidemiology. *Plant Pathology*, *53*(6), 705–712.

Lucas, J. a. (2010). Advances in plant disease and pest management. *The Journal of Agricultural Science*, *149*, 91–114.

Lukac, M., Gooding, M. J., Griffiths, S., & Jones, H. E. (2012). Asynchronous flowering and within-plant flowering diversity in wheat and the implications for crop resilience to heat. *Annals of Botany*, *109*(4), 843–850.

Ma, B. L., Yan, W., Dwyer, L. M., Fregeau-Reid, J., Voldeng, H. D., Dion, Y., & Nass, H. (2004). Graphic analysis of genotype, environment, nitrogen fertilizer, and their interactions on spring wheat yield. *Agronomy Journal*, *96*(1), 169–180.

Madden, L. V., Hughes, G., & van den Bosch, F. (2007). The Study of Plant Disease Epidemics. Saint Paul: American Phytopathological Society.

Madgwick, J. W., West, J. S., White, R. P., Semenov, M., Townsend, J. A., Turner, J. A., & Fitt, B. D. (2011). Impacts of climate change in wheat anthesis and *Fusarium* ear blight in the UK. *European Journal of Plant Pathology*, *130*(1), 117–131.

Mahlein, A. K. (2010). Detection, identification, and quantification of fungal diseases of sugar beet leaves using imaging and non-imaging hyperspectral techniques. Ph.D. Dissertation, University of Bonn, Bonn, Germany. http://hss.ulb.uni-bonn.de/2011/2428/2428a.pdf. Accessed on 31 October 2016.

Mahlein, A. K., Steiner, U., Dehne, H. W., & Oerke, E. C. (2010). Spectral signatures of sugar beet leaves for the detection and differentiation of diseases. *Precision agriculture*, *11*(4), 413–431.

Mahlein, A-K., Oerke, E-C., Steiner, U., & Dehne, H-W. (2012). Recent advances in sensing plant diseases for precision crop protection. *European Journal of Plant Pathology*, *133*(1), 197–209.

Mahlein, A. K., Rumpf, T., Welke, P., Dehne, H. W., Plümer, L., Steiner, U., & Oerke, E. C. (2013). Development of spectral indices for detecting and identifying plant diseases. *Remote Sensing of Environment*, *128*, 21–30.

Mahlein, A. K. (2016). Plant Disease Detection by Imaging Sensors – Parallels and Specific Demands for Precision Agriculture and Plant Phenotyping, *Plant Disease*, *100*(2), 241–251.

Malbrán, I., Mourelos, C. A., Girotti, J. R., Aulicino, M. B., Balatti, P. A., & Lori, G. A. (2012). Aggressiveness variation of *Fusarium graminearum* isolates from Argentina following point inoculation of field grown wheat spikes. *Crop Protection*, *42*(12), 234–243.

Malbrán, I., Mourelos, C. A., Girotti, J. R., Balatti, P. A, & Lori, G. A. (2014). Toxigenic Capacity and Trichothecene Production by *Fusarium graminearum* Isolates from Argentina and Their Relationship with Aggressiveness and Fungal Expansion in the Wheat Spike. *Phytopathology*, *104*(4), 357–64.

Maldague, X. P. V. (2002). Introduction to NDT by active infrared thermography. *Materials Evaluation, 60*(9), 1060–1073.

Martin, C., Schöneberg, T., Vogelgsang, S., Vincenti, J., Bertossa, M., Mauch-Mani, B., & Mascher, F. (2017). Factors of wheat grain resistance to *Fusarium* head blight. *Phytopathologia Mediterranea*, *56*(1), 154−166.

Maxwell, K., & Johnson, G. N. (2000). Chlorophyll fluorescence--a practical guide. *Journal of experimental botany*, *51*(345), 659–668.

Meier A. (2003). Zur Bedeutung von Umweltbedingungen und pflanzenbaulichen Maßnahmen auf den *Fusarium*-Befall und die Mykotoxinbelastung von Weizen. Ph.D. Dissertation, University of Bonn, Bonn, Germany. http://hss.ulb.uni-bonn.de/2003/0316/0316.htm. Accessed on 28 January 2016.

Mentewab, A., Rezanoor, H. N., Gosman, N., Worland, A. J., & Nicholson, P. (2000). Chromosomal location of *Fusarium* head blight resistance genes and analysis of the relationship between resistance to head blight and brown foot rot. *Plant Breeding*, *119*(1), 15–20.

Meola, C., & Carlomagno, G. M. (2004). Recent advances in the use of infrared thermography. *Measurement Science and Technology*, *15*(15), 27–58.

Merzlyak, M. N., Gitelson, A. A., Chivkunova, O. B. & Rakitin, V. Y. (1999). Non-destructive optical detection of pigment changes during leaf senescence and fruit ripening. *Physiologica Plantarum*, *106*, 135–141.

Mesterhazy, A. (2002). Role of deoxynivalenol in aggressiveness of *Fusarium graminearum* and *F. culmorum* and in resistance to *Fusarium* head blight. *European Journal of Plant Pathology, 108*(7), 675–684.

Mesterhazy, A. (2003). Breeding Wheat for *Fusarium* Head Blight Resistance in Europe. In Leonard, K.J., Bushnell, W.R. (Eds.), *Fusarium* Head Blight of Wheat and Barley. Saint Paul: APS Press.

Mesterházy, Á., Bartók, T., Kászonyi, G., Varga, M., Tóth, B., & Varga, J. (2005). Common resistance to different *Fusarium* spp. causing *Fusarium* head blight in wheat. *European Journal of Plant Pathology, 112*(3), 267–281.

Mesterházy, Á., Tóth, B., Varga, M., Bartók, T., Szabó-Hevér, Á., Farády, L., & Lehoczki-Krsjak, S. (2011). Role of fungicides, application of nozzle types, and the resistance level of wheat varieties in the control of *Fusarium* Head Blight and Deoxynivalenol. *Toxins*, *3*(11), 1453–1483.

Meyer, G. H. (2006). Kornbefall durch *Fusarium* -Arten an Winterweizen in Nordrhein-Westfalen in den Jahren 2001 – 2003 unter besonderer Berücksichtigung Moniliformin-bildender Arten. Ph.D. Dissertation, University of Bonn, Bonn, Germany. http://hss.ulb.uni-bonn.de/2006/0764/0764.pdf. Accessed on 12 October 2017.

Miedaner, T., Moldovan, M., & Ittu, M. (2003). Comparison of Spray and Point Inoculation to Assess Resistance to *Fusarium* Head Blight in a Multienvironment Wheat Trial. *Phytopathology*, *93*(9), 1068–1072.

Moradi, G. M. (2008). Microbiological and Molecular Assessment of Interactions among the Major *Fusarium* Head Blight Pathogens in wheat Ear. Ph.D. Dissertation, University of Bonn, Bonn, Germany. http://hss.ulb.uni-bonn.de/2008/1395/1395.pdf. Accessed on 28 January 2016.

Moroni, M., Lupo, E., & Cenedese, A. (2013). Hyperspectral proximal sensing of Salix Alba trees in the Sacco river valley (Latium, Italy). *Sensors*, *13*(11), 14633–14649.

Moshou, D., Bravo, C., Oberti, R., West, J., Bodria, L., McCartney, a., & Ramon, H. (2005). Plant disease detection based on data fusion of hyper-spectral and multi-spectral fluorescence imaging using Kohonen maps. *Real-Time Imaging*, *11*(2), 75–83.

Muhammed, A. A., Thomas, K., Ridout, C., & Andrews, M. (2010). Effect of nitrogen on mildew and *Fusarium* infection in barley. *Aspect of Applied Biology*, *105*, 261–266.

Mutlu, A. C., Boyaci, I. H., Genis, H. E., Ozturk, R., Basaran-Akgul, N., Sanal T., & Evlice, A. K. (2011). Prediction of wheat quality parameters using near-infrared spectroscopy and artificial neural networks. *European food research and technology*, *233*(2), 267–274.

Nelson, P. E., Toussoun, T. A., & Marasas, W. D. O. (1983). *Fusarium* Species – An Illustrated Manual for Identification. University Park, Pennsylvania: The Pennsylvania State University Press.

Nicolas, H. (2004). Using remote sensing to determine of the date of a fungicide application on winter wheat. *Crop Protection*, *23*, 853–863.

O'Donnell, K., Ward, T. J., Geiser, D. M., Kistler, H. C., & Aoki, T. (2004). Genealogical concordance between the mating type locus and seven other nuclear genes supports formal recognition of nine phylogenetically distinct species within the *Fusarium graminearum* clade. *Fungal Genetics and Biology*, *41*(6), 600–623.

Oerke, E. C. & Dehne, H. W. (2004). Safeguarding production losses in major crops and the role of crop protection. *Crop Protection*, *23*(4), 275–285.

Oerke, E.-C., Steiner, U., Dehne, H.-W., & Lindenthal, M. (2006). Thermal imaging of cucumber leaves affected by downy mildew and environmental conditions. *Journal of Experimental Botany*, *57*(9), 2121–2132.

Oerke, E. C., & Steiner, U. (2010). Potential of digital thermography for disease control. In Oerke, E. C., Gerhards, R., Menz, G., & Sikora, R. A. (Ed.), Precision Crop Protection-the Challenge and Use of Heterogeneity. Dordrecht: Springer.

Oerke, E. C., Fröhling, P., & Steiner, U. (2010). Thermographic assessment of scab disease on apple leaves. *Precision Agriculture*, *12*(5), 699–715.

Oerke, E. C., Mahlein, A. K., & Steiner, U. (2014). Proximal sensing of plant diseases. In Gullino, M. L., & Bonants, P. J. M. (Ed.), Detection and Diagnostics of Plant Pathogens. Dordrecht: Springer.

Osborne, L. E., & Stein, J. M. (2007). Epidemiology of *Fusarium* head blight on small-grain cereals. *International Journal of Food Microbiology*, *119*(1-2), 103–108.

Parry, D. W., Jenkinson, P., & Mcleod, L. (1995). *Fusarium* ear blight (scab) in small grain cereals – a review. *Plant Pathology*, *44*, 207–238.

Paul, P. A., El-Allaf, S. M., Lipps, P. E., & Madden, L. V. (2005). Relationships between incidence and severity of *Fusarium* head blight on winter wheat in Ohio. *Phytopathology*, *95*(9), 1049–1060.

Paula Júnior, T. J., Jesus Junior, W. C., Morandi, M. A. B., Bettiol, W., Vieira, R. F., & Hau, B. (2010). Interactions between aerial and soil-borne pathogens: mechanisms and epidemiological considerations. *Pest Technology*, *4*(1), 19–28.

Peñuelas, J., Pinol, J., Ogaya, R., & Filella, I. (1997). Estimation of plant water concentration by the reflectance Water Index WI (R900/R970). *International Journal of Remote Sensing*, *18*(13), 2869–2875.

Pojić, M. M. & Mastilović, J. S. (2013). Near infrared spectroscopy - advanced analytical tool in wheat breeding, trade, and processing. *Food and Bioprocess Technology*, *6*(2), 330–352.

Popovski, S., & Celar, F. A. (2013). The impact of environmental factors on the infection of cereals with *Fusarium* species and mycotoxin production – a review. *Acta Agriculturae Slovenica*, *101*(1), 105–116.

Pradhan, S., Bandyopadhyay, K. K., Sahoo, R. N., Sehgal, V. K., Singh, R., Gupta, V. K., & Joshi, D. K. (2014). Predicting Wheat Grain and Biomass Yield Using Canopy Reflectance of Booting Stage. *Journal of the Indian Society of Remote Sensing*, *42*(4), 711–718.

Prandini, A., Sigolo, S., Filippi, L., Battilani, P., & Piva, G. (2009). Review of Predictive Models for *Fusarium* Head Blight and Related Mycotoxin Contamination in Wheat. *Food and Chemical Toxicology*, *47*(5), 927–931.

Prasad, B., Carver, B. F., Stone, M. L., Babar, M. A., Raun, W. R., & Klatt, A. R. (2007). Potential use of spectral reflectance indices as a selection tool for grain yield in winter wheat under great plains conditions. *Crop Science*, *47*, 1426–1440.

Reis, E. M., Boareto, C., Danelli, A. L. D., & Zoldan, S. M. (2016). Anthesis, the infectious process and disease progress curves for *Fusarium* head blight in wheat. *Summa Phytopathologica*, *42*(2), 134–139.

Rossi, V., Ravanetti, A., Pattori, E., & Giosuè. S. (2001). Influence of temperature and humidity on the infection of wheat spikes by some fungi causing *Fusarium* head blight. *Journal of Plant Pathology*, *83*(3), 189–98.

Rouse, J. W., Haas, R. H., Schell, J. A. & Deering, D. W. (1974). Monitoring vegetation systems in the Great Plains with ERTS. In: Proceedings of the 3rd Earth Resources Technology Satellite-1 Symposium, pp. 301– 317.

Schaffnit, E. (1912). Der Schneeschimmel und die übrigen durch *Fusarium nivale* Ces. Hervorgerufenen Krankheitserscheinungen des Getreide. Brlin: Paul Pary.

Schlang, N. (2010). Auftreten der partiellen Taubährigkeit in Weizenbeständen – räumliche Verteilung der *Fusarium*-Arten und assoziierter Mykotoxine. Ph.D. Dissertation, University of Bonn, Bonn, Germany. http://hss.ulb.uni-bonn.de/2010/2000/2000.pdf. Accessed on 12 October 2017.

Schmitz, A., Kiewnick, S., Schlang, J., & Sikora, R. A. (2004). Use of high resolutional digital thermography to detect *Heterodera schachtii* infestation in sugar beets. *Communications in Agriculture and Applied Biological Sciences*, *69*, 359–363.

Scholes, J., & Rolfe, S. A. (2009). Chlorophyll fluorescence imaging as tool for understanding the impact of fungal diseases on plant performance: a phenomics perspective. *Functional Plant Biology*, *36*, 880–892.

Shaner, G. E. (2003). Epidemiology of *Fusarium* head blight of small grain cereals in North America. In *Fusarium* Head Blight of Wheat and Barley. Leonard, K. J., & Bushnell, W. R. (Ed.), Saint Paul: American Phytopathological Society.

Shank, R. A., Foroud, N. A., Hazendonk, P., Eudes, F., & Blackwell, B. A. (2011). Current and future experimental strategies for structural analysis of trichothecene mycotoxins-A prospectus. *Toxins*, *3*(12), 1518–1553.

Shewry, P. R. (2009). Wheat. *Journal of Experimental Botany*, *60*(6), 1537–1553.

Simpson, D. R., Weston, G. E., Turner, J. A., Jennings, P., & Nicholson, P. (2001). Differential control of head blight pathogens of wheat by fungicides and consequences for mycotoxin contamination of grain. *European Journal of Plant Pathology*, *107*(4), 421–431.

Sims, D. A., & Gamon, J. A. (2002). Relationships between leaf pigment content and spectral reflectance across a wide range of species, leaf structures and developmental stages. *Remote Sensing of Environment*, *81*(2–3), 337–354.

Sobrova, P., Adam, V., Vasatkova, A., Beklova, M., Zeman, L., & Kizek, R. (2010). Deoxynivalenol and its toxicity. *Interdisciplinary toxicology*, *3*(3), 94–9.

Spurr, A. R. (1969). A low-viscosity epoxy resin embedding medium for electron microscopy. *Journal of Ultrastructure Research*, *26*, 31–34.

Steinrauf, L. K. (1985). Beauvericin and other enniatins. In Sigel, H. (Ed.), Metal Ions in Biological Systems. New York: Dekker.

Stenglein, S. A. (2009). *Fusarium poae*: A pathogen that needs more attention. *Journal of Plant Pathology*, *91*(1), 25–36.

Stoll, M., Schultz, H. R., Baecker, G., & Berkelmann-Loehnertz, B. (2008). Early pathogen detection under different water status and the assessment of spray application in vineyards through the use of thermal imagery. *Precision Agriculture*, *9*, 407–417.

Summerell, B. A., Laurence, M. H., Liew, E. C. Y., & Leslie, J. F. (2010). Biogeography and phylogeography of *Fusarium*: A review. *Fungal Diversity*, *44*, 3–13.

Teich, A. H., & Hamilton, J. R., (1985). Effect of cultural practices, soil phosphorus, potassium, and pH on the incidence of *Fusarium* head blight and deoxynivalenol levels in wheat.

Applied and Environmental Microbiology, *49*(6), 1429–1431.

Trail, F. (2009). For blighted waves of grain: *Fusarium graminearum* in the postgenomics era. *Plant physiology*, *149*(1), 103–110.

Ustin, S. L., Roberts, D. A., Gardner, M. & Dennison, P. (2002). Evaluation of the potential of Hyperion data to estimate wildfire hazard in the Santa Ynez Front Range, Santa Barbara, California. In: Proceedings of the 2002 IEEE IGARSS and 24th Canadian Symposium on Remote Sensing, pp. 796–798.

Vadivambal, R., & Jayas, D. S. (2011). Applications of thermal imaging in agriculture and food industry—a review. *Food and Bioprocess Technology*, *4*(2), 186–199.

Van Kooten, O., & Snell, J. F. H. (1990). The use of chlorophyll fluorescence nomenclature in plant stress physiology. *Photosynthesis Research*, *25*(3), 147–150.

Van Maanen, A., & Xu, M. (2003). Modelling plant disease epidemics. *European Journal of Plant Pathology*, *109*(7), 669–682.

Waalwijk, C., van der Heide, R., de Vries, I., van der Lee T., Schoen, C., Costrel-de Corainville, G., Häuser-Hahn, I., Kastelein, Pieter., Köhl, J., Lonnet, P., Demarquet, T., & Kema., G. H. J. (2004). Quantitative detection of *Fusarium* species in wheat using TaqMan. *European Journal of Plant Pathology*, *110*, 481–494.

Wang, J., Wieser, H., Pawelzik, E., Weinert, J., Keutgen, A. J., & Wolf, G. A. (2005). Impact of the fungal protease produced by *Fusarium culmorum* on the protein quality and breadmaking properties of winter wheat. *European Food Research and Technology, 220*(5-6), 552–559.

Wang, M., Ling, N., Dong, X., Zhu, Y., Shen, Q., & Guo, S. (2012). Thermographic visualization of leaf response in cucumber plants infected with the soil-borne pathogen *Fusarium oxysporum* f. sp. cucumerinum. *Plant Physiology and Biochemistry*, *61*, 153–161.

Wang, X., Zhang, M., Zhu, J., & Geng, S. (2008). Spectral prediction of Phytophthora infestans infection on tomatoes using artificial neural network (ANN). *International Journal of Remote Sensing*, *29*(6), 1693–1706.

Wegulo, S. N., Bockus, W. W., Nopsa, J. H., De Wolf, E. D., Eskridge, K. M., Peiris, K. H. S., & Dowell, F. E. (2011). Effects of Integrating Variety Resistance and Fungicide Application on *Fusarium* Head Blight and Deoxynivalenol in Winter Wheat. *Plant Disease*, *95*(5), 554–560.

Wegulo, S. N. (2012). Factors influencing deoxynivalenol accumulation in small grain cereals. *Toxins*, *4*(11), 1157–1180.

Xu, X. M., Parry, D. W., Edwards, S. G., Cooke, B. M., Doohan, F. M., Van Maanen, A., Brennan, J. M., Monaghan, S., Moretti, A., Tocco, G., Mule, G., Hornok L., Giczey, G., Tatnell, J., Nicholson, P., & Ritieni, A. (2004). Relationship between the incidences of ear and spikelet infection of Fusarium ear blight in wheat. *European Journal of Plant Pathology*, *110*(9), 959–971.

Xu, X. M., Monger, W., Ritieni, A., & Nicholson, P. (2007). Effect of temperature and duration of wetness during initial infection periods on disease development, fungal biomass and mycotoxin concentrations in wheat inoculated with single, or combinations of, *Fusarium* species. *Plant Pathology*, *56*, 943–956.

Xu, X., & Nicholson, P. (2009). Community ecology of fungal pathogens causing wheat head blight. *Annual review of phytopathology*, *47*(1), 83–103.

Xuan, T. N. T. (2014). Comparative studies on the infection and colonization of maize leaves by *Fusarium graminearum*. Ph.D. Dissertation, University of Bonn, Bonn, Germany. http://hss.ulb.uni-bonn.de/2014/3470/3470.pdf . Accessed on 14 September 2017.

Yang, F., Jensen, J. D., Spliid, N. H., Svensson, B., Jacobsen, S., Jørgensen, L. N., Jørgensen, H., Collinge, D. B., & Finnie, C., (2010). Investigation of the effect of nitrogen on severity of *Fusarium* head blight in barley. *Journal of Proteomics*, *73*(4), 743–752.

Yang, L., van der Lee, T., Yang, X., Yu, D., & Waalwijk, C. (2008). *Fusarium* populations on Chinese barley show a dramatic gradient in mycotoxin profiles. *Phytopathology*, *98*(6), 719–727.

Yli-Mattila T. (2010). Invited review ecology and evolution of toxigenic *Fusarium* species in cereals in northern Europe and Asia. *Journal of Plant Pathology*, *92*(1), 7–18.

Yue, J., Yang, G., Li, C., Li, Z., Wang, Y., Feng, H., & Xu, B. (2017). Estimation of winter wheat above-ground biomass using unmanned aerial vehicle-based snapshot hyperspectral sensor and crop height improved models. *Remote Sensing*, *9*(7), 708–727.

Zarco-Tejada, P. J., Berjon, A., Lopez-Lozana, R., Miller, J. R., Martin, P., Cachorro, V., Gonzalez, M.R. & de Frutos, A. (2005). Assessing vineyard conditions with hyperspectral indices: leaf canopy reflectance simulation in a row structured discontinuous canopy. *Remote Sensing of Environment*, *99*, 271–287.

Zhang, X. Y., Loyce, C., Meynard, J. M., & Savary, S. (2006). Characterization of multiple disease systems and variety susceptibilities for the analysis of yield losses in winter wheat. *Crop Protection*, *25*(9), 1013–1023.

Zhang, X., Halder, J., White, R. P., Hughes, D. J., Wang, C., & Fitt, B. (2014). Climate change increases risk of *Fusarium* ear blight in wheat in central China. *Annals of Applied Biology*, *164*(3), 384–395.

Zhao, C., Liu, L., Wang, J., Huang, W., Song, X., & Li, C. (2005). Predicting grain protein content of winter wheat using remote sensing data based on nitrogen status and water stress. *International Journal of Applied Earth Observation and Geoinformation*, *7*(1), 1–9.

Zühlke, S., Dehne, H. W., Herebian, D., & Spiteller, M. (2008). *Mykotoxinmultimethode für die Landwirtschaft*, *32*(1), 22–27.

ACKNOWLEDGEMENT

On this exceptional day, I would like to express my gratitude to **Prof. Dr Heinz Wilhelm Dehne** for providing me with the opportunity to join his incredible research team at INRES, Plant Diseases and Plant Protection. I appreciate the scientific discussion, the guidance and the encouragement especially during finalising my research. “Believe me, nature is not that simple” I liked these words that he often tells during our discussions.

I would like to express my thanks to **Prof. Dr Jens Léon,** my first co-supervisor. Also, I would like to thank **Prof. Dr Petr Karlovsky**, my second co-supervisor, for agreeing to serve in my PhD exam-committee. I am very honoured to have you on this day and your efforts and contributions are highly appreciated.

Very special thanks to **PD Dr Erich-Christian Oerke**, for his support and guidance in lab, greenhouse and in the field. I cannot forget the assistance and the support he provided during the preparation for publishing. I would like to thank **PD Dr Ulrike Steiner** for her support and guidance especially in microscopy. Many thanks to **PD Dr Joachim Hamacher**, he was always collaborative and very kind. Very special thanks to **PD Dr Anne-Katrin Mahlein**, especially during the beginning of my study, her guidance is always highly appreciated.

I will always be thankful and so much gratitude to **Prof. Dr Bernhard Hau** who decided to keep standing beside me not only during my master but also after that at the PhD. I appreciate his contributions, especially when it comes to modelling and statistics, in addition to his feedback during writing this work.

I would like to express much of gratitude to **Regina Kirchner-Bierschenk** and **Giesela Sichtermann**, since I got to know to you I have had a home in Germany.

I would like to thank my colleagues and friends who contributed to my work during different stations of this journey: **Said Dadschani, Jan Dupuis**, **Christian Rose**, **Yinfei Li**, **Laura Carlota**

Paz, **Oyiga Benedict Chijoke**, **Bobby Mathew**, **Merwas Wahabzada, Paul Schmieja** and **Maren Steinbiss**. Every one of you is a great personality. I am pleased to have you during this time.

Very special thanks to **Carolin Sichtermann**, her support in the field experiments and in the laboratory investigations is highly appreciated.

Kerstin Lange and **Jennifer Stracke**, you were always so wonderful, thank you very much for your efforts to support the group and bring them together, you were amazing especially in the social activities.

I would like to thank **Inge Neukirchen** and **Ellen Laurenze**n, your presence made me easily integrated into the group.

The current PhD. students: **Marlene Leucker**, **Matheus Kuska, Lisa Hallau**, **Stefan Thomas**, **Thi Thu Vo**, **Sandra Weißbrodt**, **Bianca Boehnke**, **David Bohnenkamp**, **Anna Brugger,** and **Elias Alisaac** also the former: **Zhiqing Guo**, **Carlos Berdugo**, **Sandra Gomez** and **Nguyen Thi Thanh Xuan,** I thank you so much for the beautiful time we spend together, I have learned a lot from every one. My gratitude is extended to all of you, we have had a beautiful memory together.

From the Arabic community in Bonn, I would like to thank **Hosam Al Hassan**, **Souhaib Aldabbagh** and **Mohammad Rajaai Mahli** for your support and the beautiful time we had.

My mother **Walaa** and father **Anwar**, my sisters and brothers especially **Bilal** and **Ismail**, I love you so much, and I promise, I will keep on loving you. Despite the distances and the war, you were always the source of my power.

Finally, I would also like to acknowledge funding from these sources: European Union Seventh Framework Programme (FP7/2007-2013) by "PlantFoodSec - Plant and Food Biosecurity" Project, Damascus University and DAAD.

Declaration

I, the undersigned, declare that this dissertation, to the best of my knowledge does not incorporate without acknowledgement any material previously published or written by another person except where reference is made. It is an original piece of work conducted by myself and has never been submitted elsewhere.

Bonn, 24.10.2017

Ali Al Masri